LEVEL II

AD

12

TECHNICAL REPORT

NATICK/TR-80/021

PENETRATION MECHANICS OF TEXTILE STRUCTURES

BY

DAVID ROYLANCE

SU-SU WANG

MIT

CONTRACT NO. DAAG 17-76-C-0013

Approved for public release;
distribution unlimited.

JUNE 1979

UNITED STATES ARMY
NATICK RESEARCH and DEVELOPMENT COMMAND
NATICK, MASSACHUSETTS 01760

Clothing, Equipment and Materials Engineering Laboratory

CEMEL-218

UNCLASSIFIED

SECURITY CLASSIFICATION OF THIS PAGE (When Data Entered)

REPORT DOCUMENTATION PAGE

READ INSTRUCTIONS BEFORE COMPLETING FORM

1. REPORT NUMBER: NATICK/TR-80/021
2. GOVT ACCESSION NO.: AD-A089445
3. RECIPIENT'S CATALOG NUMBER:

4. TITLE (and Subtitle): PENETRATION MECHANICS OF TEXTILE STRUCTURES

5. TYPE OF REPORT & PERIOD COVERED: NATICK/CEMEL

6. PERFORMING ORG. REPORT NUMBER: CEMEL #218

7. AUTHOR(s): David Roylance and Su-Su Wang

8. CONTRACT OR GRANT NUMBER(s): DAAG 17-76-C-0013

9. PERFORMING ORGANIZATION NAME AND ADDRESS: Massachusetts Institute of Technology, Cambridge, MA 02139

10. PROGRAM ELEMENT, PROJECT, TASK AREA & WORK UNIT NUMBERS: 62723A, 1Y762723AH98CC006

11. CONTROLLING OFFICE NAME AND ADDRESS: U.S. Army Natick R&D Command (DRDNA-VMP), Natick, MA 01760

12. REPORT DATE: June 1979

13. NUMBER OF PAGES: 154

14. MONITORING AGENCY NAME & ADDRESS (if different from Controlling Office): NATICK, NATICK/CEMEL

15. SECURITY CLASS. (of this report): Unclassified

15a. DECLASSIFICATION/DOWNGRADING SCHEDULE:

16. DISTRIBUTION STATEMENT (of this Report)

Approved for public release; distribution unlimited.

17. DISTRIBUTION STATEMENT (of the abstract entered in Block 20, if different from Report)

18. SUPPLEMENTARY NOTES

19. KEY WORDS (Continue on reverse side if necessary and identify by block number)

TEXTILES	BODY ARMOR	TEXTILE STRUCTURES
FIBERS	BALLISTIC PROTECTION	PENETRATION
BALLISTICS	STRESS	
KEVLAR	STRAIN	

20. ABSTRACT (Continue on reverse side if necessary and identify by block number)

This report reviews those aspects of wave propagation and dynamic fracture relevant to the penetration mechanics of textile structures intended for use in personnel ballistic protection, and then describes the development and implementation of numerical analyses for use in instances for which closed-form analyses are intractable. These numerical treatments are used to assess the manner in which fiber material properties influence ballistic resistance, and this is done by performing simulations of missile impact on four fabrics of actual interest: ballistic nylon, Kevlar 29*, Kevlar 49*, and graphite. Following this parametric

DD FORM 1473 EDITION OF 1 NOV 65 IS OBSOLETE

UNCLASSIFIED

SECURITY CLASSIFICATION OF THIS PAGE (When Data Entered)

22000

materials study, the numerical treatment is extended to include the effect of linear and non-linear viscoelastic relaxation on fabric response to impact. Finally, a special purpose computer code is described which was developed to study stress wave effects occurring at fiber crossovers.

---

*Trademark of E.I. du Pont Co. for its aramid fiber material. Use of this trademark does not imply government endorsement of a commercial product.

FOREWORD

This work was carried out for the U.S. Army Natick Research and Development Command DAAG-17-76-C-0013, with Dr. R.C. Laible acting as technical monitor. The authors gratefully acknowledge the considerable assistance of Dr. Laible, as well as that of Dr. W.D. Claus, Dr. G.C. DeSantis, and Ms. M.A. Wall.

TABLE OF CONTENTS

TABLE OF CONTENTS (continued)

LIST OF FIGURES

12 Illustration that the numerical scheme converges to accurate values with time, as indicated by the energy discrepancy ratio. Note that nonoptimum values of the stability ratio (η in this figure) lead to divergence at longer times.

13 Illustration that the numerical scheme predicts values of final projectile velocity after penetration in agreement with experimental observation.

14 Computed and experimentally observed values of cone deformation cone size at time of projectile penetration. The V_{50} is that value of impact velocity at which penetration occurs nearly instantaneously.

15 Distribution of strain along orthogonal fibers passing through the impact point. Curves are drawn for various fabric types, at various times after a 400 m/sec impact.

16 Effect of initial projectile velocity on the development of strain at the point of impact for nylon fabric.

17 Relative ability of the various fabric types to slow the projectile during impact. Ordinal values represent the ratio of current to initial projectile velocity.

18 Energy absorbed by a Kevlar 29 panel after a 400 m/sec impact, illustrating the partition of impact energy into kinetic and strain energy in the panel.

19 Illustration of the relative ability of the four fabric types to absorb impact energy. The curves are terminated at the right by projectile penetration, as indicated by a maximum-breaking strain failure criterion.

20 Development of strain at the point of impact in the various fabric types after a 400 m/sec impact.

21 "Master" curve for impact-induced strain at the point of impact. Ordinal values represent strain normalized on the basis of the strain which would be generated in a single fiber by impact at the same velocity, while abscissal values are adjusted by a factor equal to the fourth root of the fiber modulus.

22 Wiechert spring-dashpot model for linear viscoelastic fiber response.

23 Normalized strain plotted against Lagrangian fiber coordinate for various times after impact.

24 Normalized tension distribution along fiber.

25 Numerical values for tension distribution for t = 41.08 microsec after impact.

26 Stress distributions along orthogonal fibers running through impact point for linear elastic and viscoelastic fabrics (t = 30.4 microsec).

27 Distribution of strain along orthogonal fibers running through impact point.

28 Stress histories at impact point for linear elastic and viscoelastic materials.

29 Stress relaxation at impact point for various impact velocities.

30 Stress distributions along orthogonal fibers running through impact point for linear elastic and nonlinear viscoelastic fabrics.

31 Comparison of stress relaxation in linear and nonlinear viscoelastic fabrics.

32 Stress histories at impact point for linear elastic, linear viscoelastic, and nonlinear viscoelastic fabrics.

33 Schematic of model for numerical analysis of two crossed fibers.

34 Discrete element of fiber.

35 Strain distributions in two crossed fibers of Kevlar 29, 28.7 microsec after impact at 400 m/sec.

36 Influence of the fiber modulus on the fraction of stress wave intensity which is transmitted through a fiber crossover, in the absence of fiber-fiber sliding.

37 A comparison of the reflection-only bounce model for wave propagation in an impacted fabric, in comparison with the fabric model of this report.

38 The influence of fiber-fiber sliding on the fraction of stress wave intensity which is reflected at fiber crossovers, as indicated by computer experiments on Kevlar 29 fibers.

39 The influence of fiber-fiber sliding on the extent to which a portion of the propagating stress wave is diverted from the primary fiber to begin propagating along the transverse secondary fiber.

40. The influence of sliding on the extent of stress wave intensity propagated beyond fiber crossovers.

PENETRATION MECHANICS OF TEXTILE STRUCTURES

I. BALLISTICS OF TRANSVERSELY IMPACTED FIBERS*

Introduction

Although impact of single fibers or fiber assemblies is an important subject in its own right, being relevant to climbing ropes, aircraft carrier arrest cables, high-speed weaving, etc., the principal developments in this area have been made by workers whose major interests have been in the impact resistance of woven or non-woven textile structures. The most notable of these structures have been the lightweight armor vests used by police and military personnel, but among other important applications can be listed aircraft engine containment shrouds, flak blankets, and vehicle seat belts. Ballistic nylon has been used successfully for these vests since the Second World War, although current developments have emphasized the du Pont aramid fiber marketed as Kevlar**. Although, as will be shown below, excellent single-fiber ballistic response does not necessarily guarantee a superior vest, any understanding of textile structure ballistics must be pre-

* From Reference 1 (see Page 109). Used by permission of Textile Research Journal

**Trademark of E.I. du Pont de Nemours & Co., Inc.

ceeded by an understanding of single-fiber response.

A strong motive for discussing fibers is that single fiber tests are often used as screening tests for ballistic protection materials. As an example, one often encounters tabulations of "transverse critical velocity", that ballistic velocity at which a transversely impacted yarn experiences nearly instantaneous failure. Typical data is shown below.

Transverse critical velocities of textile fibers.[2]*

	V_{cr}, m/sec
Nylon	616
Polyester	472
Nomex	442
Fiberglass	274
Kevlar 29	570

Such tests are often indicative of relative ballistic resistance, but perfect correlations cannot be guaranteed. In the above tabulation Kevlar 29 proves to be the best ballistic material when put into a panel, in spite of its having a lower transverse critical

* Numbers in brackets refer to references listed on pages 109-110.

velocity than nylon.

Longitudinal Wave Propagation

Wave propagation phenomena in fibers and thin rods are considerably less complicated than in a general medium, since the possibility of unrestrained transverse contraction in fibers eliminates (to a good approximation) the simultaneous propagation of independent dilatational and distortional waves which are present in general. The equation of motion for fibers or rods is simply [3]:

$$\frac{\partial^2 u}{\partial t^2} = \frac{E}{\rho} \frac{\partial^2 u}{\partial x^2} \tag{1}$$

where u is the longitudinal particle displacement, ρ is the material density, E is the longitudinal Young's modulus, and x and t are the space and time coordinates. This is the well-known wave equation, whose solution represents a disturbance traveling at a velocity

$$c = \sqrt{E/\rho} \tag{2}$$

Conventional textile units employing stiffness per unit linear density are very convenient in wave propagation analyses, since the factor ρ is included implicitly in the modulus. For modulus expressed in grams per denier and wavespeed in meters per second, Equation 3 becomes:

$$c = \sqrt{kE} \tag{3}$$

where k = 88,260 is the necessary units-conversion factor. In these equations, as well as those to follow, the modulus is taken to be the "dynamic" stiffness relevant to the high strain rates corresponding to wave propagation tests. The development of such dynamic constitutive relations from experimental fiber-impact data has been described elsewhere [4,5].

Consider a fiber fixed at one end whose free end is suddenly subjected to a constant outward velocity V in the longitudinal (fiber) direction. After a time it, the strain wave, will have propagated into the fiber a distance ct, while the free end will have displaced outward an amount Vt. The strain resulting from the impact is then the displacement Vt divided by the

affected length ct:

$$\epsilon = \frac{Vt}{ct} = \frac{V}{c} = \frac{V}{\sqrt{kE}} \tag{4}$$

The corresponding stress is

$$\sigma = E\epsilon = V\sqrt{E/k} \tag{5}$$

The above relations have assumed a linear elastic material whose stiffness E is independent of the strain. In this case the wavefront will propagate as a sharp discontinuity (a shock wave) at which the strain rises instantaneously from zero to the value given by Equation 4. Many ballistic fibers are nonlinear, however, and the effect of material nonlinearity leads to some complication of the above description. A nonlinear fiber can be characterized as having a strain-dependent modulus $E = E(\epsilon)$, so that Equation 3 becomes:

$$c = c(\epsilon) = \sqrt{kE(\epsilon)} \tag{6}$$

The shape of the wavefront is now dependent on the shape of the dynamic stress-strain curve. If the curve is concave toward the strain axis, so that the modulus decreases monotonically with strain, each suceeding increment of strain in the propagating wave travels more slowly than the previous increment. The wave is then dispersive, and broadens as it travels. If on the other hand portions of the stress-strain curve are away from the strain axis, then portions of the strain wave will overtake more slowly propagating increments of lesser strain, and the wave will contain shock components. In general, a wave may contain both dispersive and shock components.

In the region behind the wave, material flows in the direction of the imposed velocity with a "particle velocity" w. This motion is fed by the strain developed in the propagating wave, and the particle velocity is related to the wave to the wave speed by:

$$w = \int_0^{\epsilon_0} c(\epsilon)\, d\epsilon = \int_0^{\epsilon_0} \sqrt{kE(\epsilon)}\, d\epsilon \qquad (7)$$

where ϵ_0 is the ultimate value of strain generated by the impact. Since the particle velocity must match the imposed velocity, we have

$$V = \int_0^{\epsilon_0} \sqrt{kE(\epsilon)}\, d\epsilon \qquad (8)$$

The strain ϵ_0 developed by longitudinal impact is found by solving Equation 8, perhaps numerically.

Transverse Impact of Fibers

As the transverse impact of fibers seems intuitively germane to impact of woven textile panels, the technical community interested in lightweight ballistic protection has devoted intensive effort to this problem since World War II. Following the pioneering works of Taylor [6] and von Karman [7] during the war, valuable contributions have been made by Peterson et al. [8], Shultz et al. [9], Wilde et al. [5], among others, but by far the most prolific of these efforts has been that of Jack C. Smith and his colleages at the National Bureau of Standards. Reference [10] provides a review of most of this work, which contains a wealth of

experimental and theoretical contributions ranging over a period of approximately ten years in the fifties and sixties.

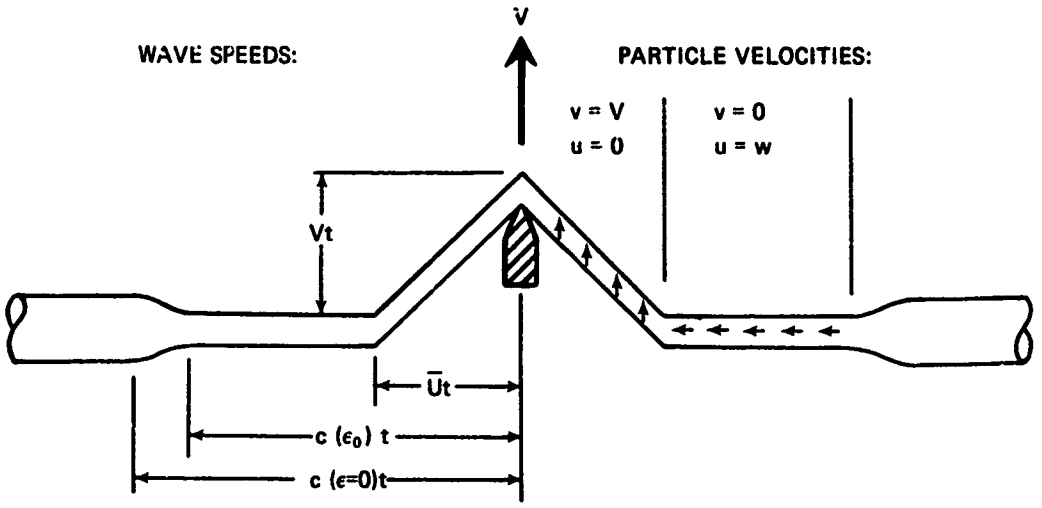

Figure 1. Wave Propagation in a transversely impacted fiber.

The rate-independent theory of transverse fiber impact as developed by Smith can be stated with reference to Figure 1. This illustrates a fiber, originally straight in the horizontal direction, which has been impacted by a projectile traveling vertically upward. Upon impact, longitudinal waves of the type described in the previous section are propagated outward from the point of impact. Behind these waves material flows inward toward the point of impact at a constant velocity w, strain ϵ_0, and stress σ_0. In

addition to the longitudinal waves, transverse "kink" waves are also propagated outward from the impact point. At the transverse wavefront the inward material flow ceases abruptly and is replaced by a transverse particle velocity equal in magnitude and direction to that of the projectile. The strain and tension are unchanged across the transverse wavefront, but both the longitudinal and transverse particle velocities experience discontinuities there; in this sense the transverse wave is a geometrical shock. The apprently unbalanced tensions on either side of the transverse wavefront are compensated by the change in particle momentum as the wave propagates. Behind the transverse wavefront all particle velocities are equal in magnitude and direction to the projectile velocity, and the fiber configuration is a straight line at a constant inclination θ from the longitudinal direction.

The inward particle velocity is found, as in the longitudinal case, as

$$w = \int_0^{\epsilon_0} c(\epsilon)\, d\epsilon = \int^{\epsilon_0} \sqrt{k E(\epsilon)}\, d\epsilon \qquad (9)$$

The final strain ϵ_0 is unknown as yet, but $E(\epsilon)$ is known as the slope of the dynamic stress-strain

curve. The outward velocity U of the transverse kink wave, measured relative to a Lagrangian frame attached to and extending with the fiber, is:

$$U = \sqrt{\sigma_0 k / (1+\epsilon_0)} \tag{10}$$

To a fixed observer the transverse wave appears to propagate in a "laboratory" frame of reference at

$$\bar{U} = (1+\epsilon_0) U - w \tag{11}$$

Finally, the above variables are related to the impact velocity V through the relation:

$$V = \sqrt{(1+\epsilon_0)^2 U^2 - \bar{U}^2} \tag{12}$$

Equations 9-12 constitute four relations between, V, w, ϵ_0, σ_0, U, and $\bar{U}$. The material dynamic stress-strain curve relates σ_0 and ϵ_0, so that once one of the parameters (say V) is specified, the other four independent parameters (w, ϵ_0, U, $\bar{U}$) can be found. For nonlinear stress-strain curves, numerical solutions will likely be more convenient.

Certain limitations to the Smith analysis described above must be mentioned. First, it is

rate-independent. Most polymeric fibers exhibit strong rate dependencies, and these effects are beyond the capacity of this analysis to describe. Perhaps a more severe limitation is that the Smith analysis is not applicable to late-time effects in the wave propagation process. In real situations the outgoing longitudinal wave soon collides with an obstacle: a clamp, in the case of single-fiber tests, or a fiber crossover, in the case of impact in woven textile panels. Upon such a collision a reflected wave is propagated from the collision point in the direction opposite that of the original wave. This reflected wave in turn soon collides with the outward-traveling transverse wave, and this collision generates another two waves which travel away from the collision point. These waves in turn eventually collide with the clamps, or the projectile, or other waves. The result of these wave reflections and interactions is a situation which becomes intractable by closed-form mathematical methods, and this late-time intractability is a principal reason for the development of numerical computer solutions.

Use of the Rate-Independent Theory in Preliminary Design

In spite of the limitations of the Smith theory outlined above, the rate-independent analysis provides

a highly useful means of assessing approximate relations between fiber material properties and ballistic response. These relations are of considerable value in performing preliminary design steps in development of textile ballistic-protection devices.

Assuming the material to be linear in stress-strain response (E = constant), the Smith analysis can be cast in the simple form:

$$V = \sqrt{\epsilon_0 kE\left[2\sqrt{\epsilon_0(1+\epsilon_0)} - \epsilon_0\right]} \qquad (13)$$

which provides a relation for the strain ϵ_0 developed by impact at a velocity V in terms of the fiber modulus. The relation can be solved numerically if one wishes to compute ϵ_0 for a given V, or it can be used directly to plot ϵ_0 versus V for the purpose of developing design curves (see Fig. 2). Once ϵ_0 is known, then σ_0, U, $\bar{U}$, and w can be found from either the stress-strain relation or Equations 9 - 12. Figure 3 shows such a plot of tension, σ_0 versus V, with modulus as a parameter.

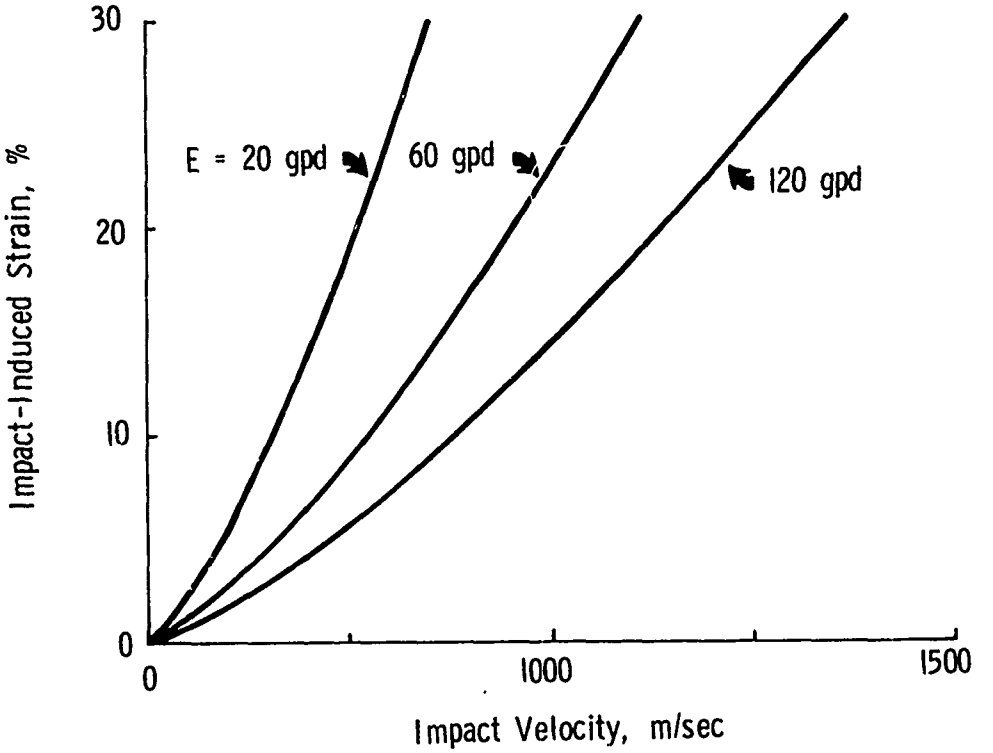

Figure 2. Predicted impact strain for linear rate-independent fibers.

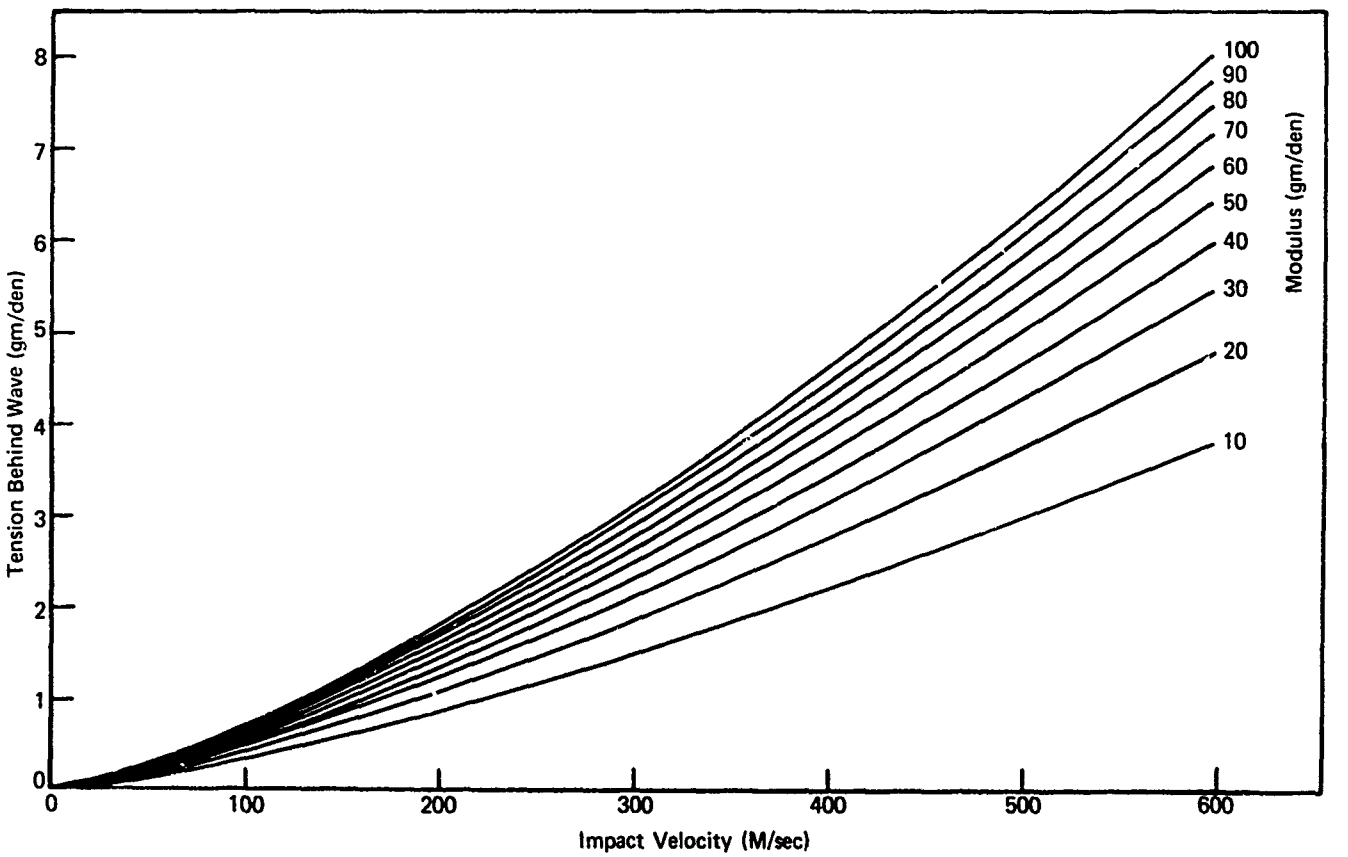

Figure 3. Predicted impact tension for linear rate-independent fibers.

Since the above curves rise monotonically with velocity, one can observe the influence of modulus more easily by plotting ballistic response at a constant velocity, and Figure 4 shows such a plot at V = 400 m/sec. Here are plotted the strain and tension from the above methods, along with the strain energy $\mathcal{U} = \frac{1}{2} \sigma_0 \epsilon_0$ developed behind the wave and the rate of energy absorption $\dot{\mathcal{U}}_c$ of the fiber. (The term, $\dot{\mathcal{U}}_c$, is shown in mixed units, but it could be converted to joules/sec once the density and denier of the fiber are specified.) The rate of energy absorption at the wavefront must equal the rate at which the fiber extracts kinetic energy from the projectile, and it is a reasonable measure of ballistic efficiency. Note that this energy absorption rate rises monotonically with fiber modulus, although with less dramatic improvements after approximately 500 g/den.

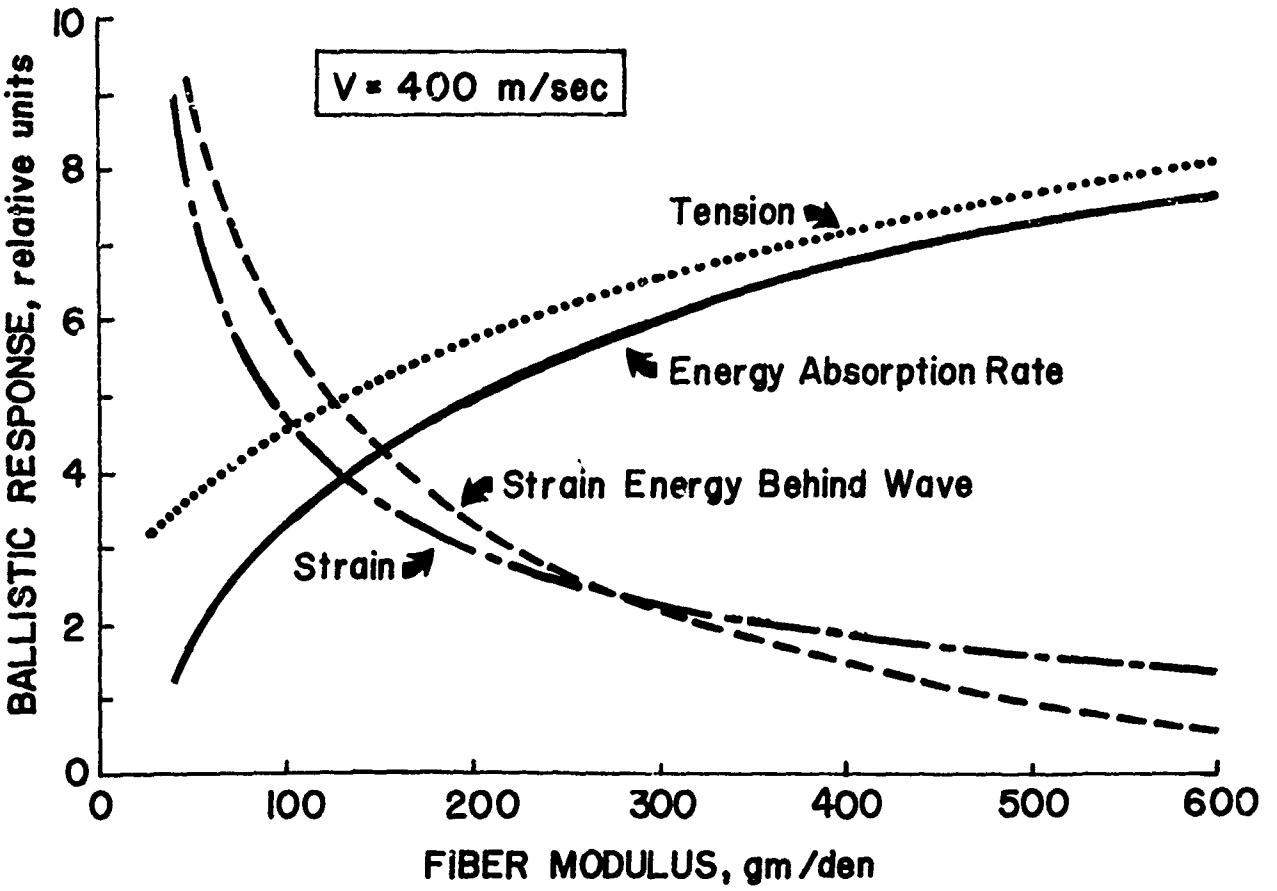

Figure 4. Effect of fiber stiffness on ballistic response; 10 = 10 g/den for tension, 10% for strain, 0.03 g/den for strain energy, and 900 g/den sec for energy absorption rate.

Of course, one cannot improve ballistic efficiency indefinitely by continuing to seek stiffer fibers. In general, increases in stiffeness are accompanied by decreases in breaking strain, and a point may well be reached where this reduced ductility overshadows the beneficial reduction in impact-generated strain shown in Figure 2. This effect may be quantified by means of Equation 13, where one may calculate the critical transverse velocity by determining the velocity which just generates the dynamic breaking strain on impact. If one

knows the variation of breaking strain with stiffness, these calculations may be used to select approximately an optimum fiber stiffness for ballistic efficiency. This process is carried through for illustrative purposes in Figure 5.

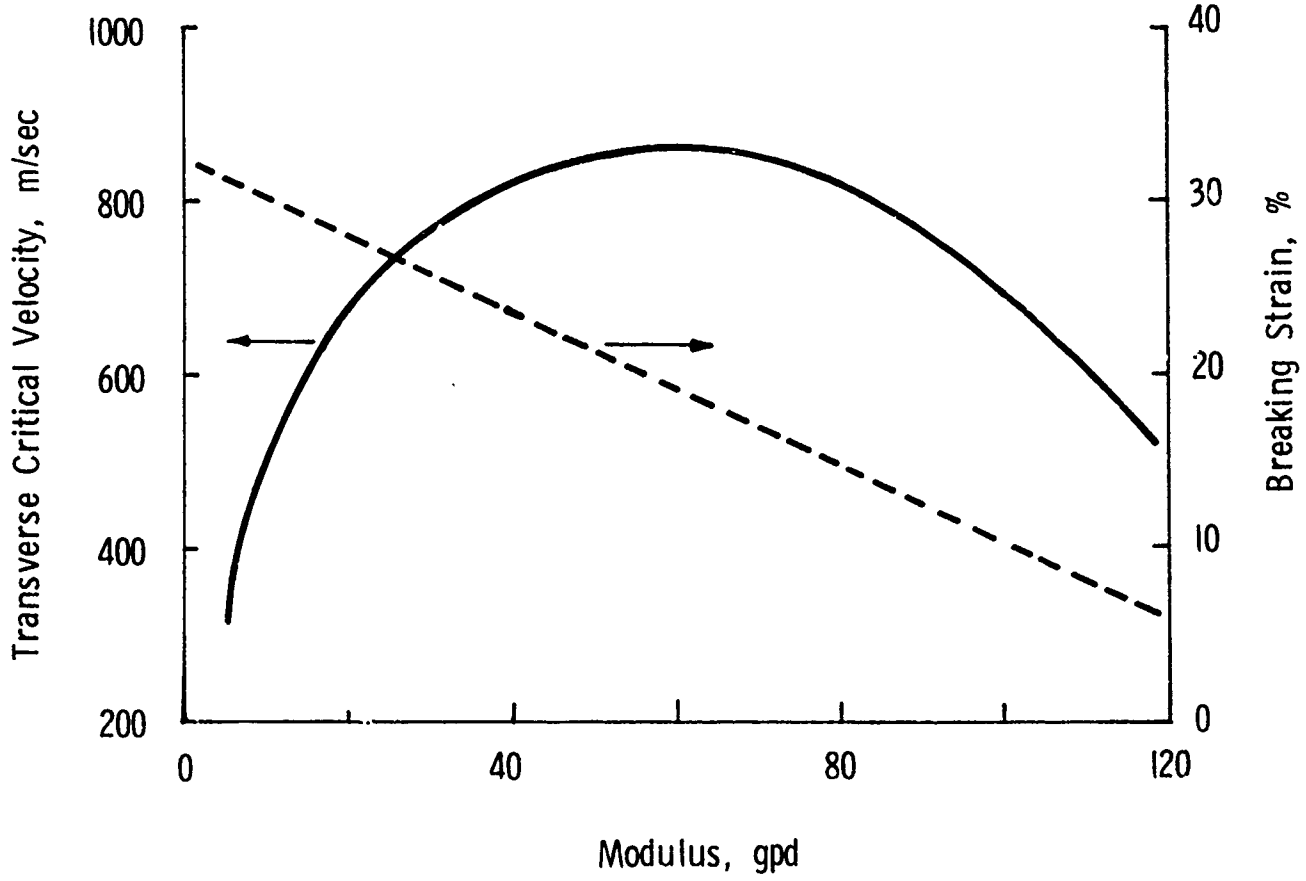

Figure 5. Prediction of optimum stiffness for nylon fibers.

The dashed line in this Figure is the relation between dynamic stiffness and breaking strain as determined from fiber-impact tests on a series of nylon yarns that had been subjected to various

drawing treatments by the manufacturer [5]. The solid line is the the calculated transverse critical velocity, considering the effect of stiffness on both impact-induced strain and on breaking strain. An optimum is observed near 60 g/den, which is in fair agreement with experimental observation. All this is a quantification of the often-quoted guideline in armor design that one seeks the highest possible modulus in order to spread the impact over a wide area via increased wavespeed, but that the process must not be carried so far as to induce excessive brittleness. In hard armor this reasoning has led to the use of ceramic faceplates to give high wavespeed, backed by a fiberglass laminate to provide the needed toughness.

Selection of a Failure Criterion

The use of simple ultimate breaking strain as a failure criterion in the above example is overly simplistic, since it does not incorporate the strong temperature and rate dependencies that are known to exist in polymeric material. A versatile fracture model which does incorporate these dependencies and is still computationally convenient is that due to Zhurkov [11], which states that the lifetime τ of a solid subjected to a uniaxial stress σ is of the form

$$\tau = \tau_0 \exp\left\{ (U^* - \gamma^* \sigma)/RT \right\} \qquad (14)$$

where τ_0 is a pre-exponential factor with units of time, U* is an apparent activation energy for the fracture process, γ^* is a factor with units of volume, R is the gas constant (8.314 J/mole °K), and T is the absolute temperature. For constant temperature, Equation 14 reduces to

$$\tau = \alpha \exp(-\beta\sigma) \qquad (15)$$

where

$$\alpha = \tau_0 \exp(U^*/RT) \qquad (16)$$
$$\beta = \gamma^*/RT$$

When stress and temperature vary during the loading process, one can assume linear superposition and write the Zhurkov criterion in the form:

$$\int_0^{\tau} dt \Big/ \left\{ \tau_0 \exp\left[(U^* - \gamma^* \sigma)/RT \right] \right\} = 1 \qquad (17)$$

In a constant-stress-rate experiment at constant temperature, for instance,

$$\sigma(t) = Ct$$

$$\int_0^{\tau} dt / \{\alpha \exp(-\beta C t)\} = 1 \qquad (18)$$

$$[\exp(\beta C t)] / (\alpha \beta C) = 1$$

$$\tau = \ln(1 + \alpha \beta C) / \beta C$$

To illustrate the order of rate dependency provided by Zhurkov's model, Figure 6 shows a plot of Equation 18 for the case of drawn nylon fibers. In this figure $\alpha = 2.20 \times 10^{19}$ sec, and $\beta = 5.13$ $(g/den)^{-1}$; these are the values obtained by Zhurkov [11] by fitting Equation 15 to creep-rupture data. Such a plot can be used to depict the time-to-break for a fiber, and the tenacity-at-break, as a function of the loading rate.

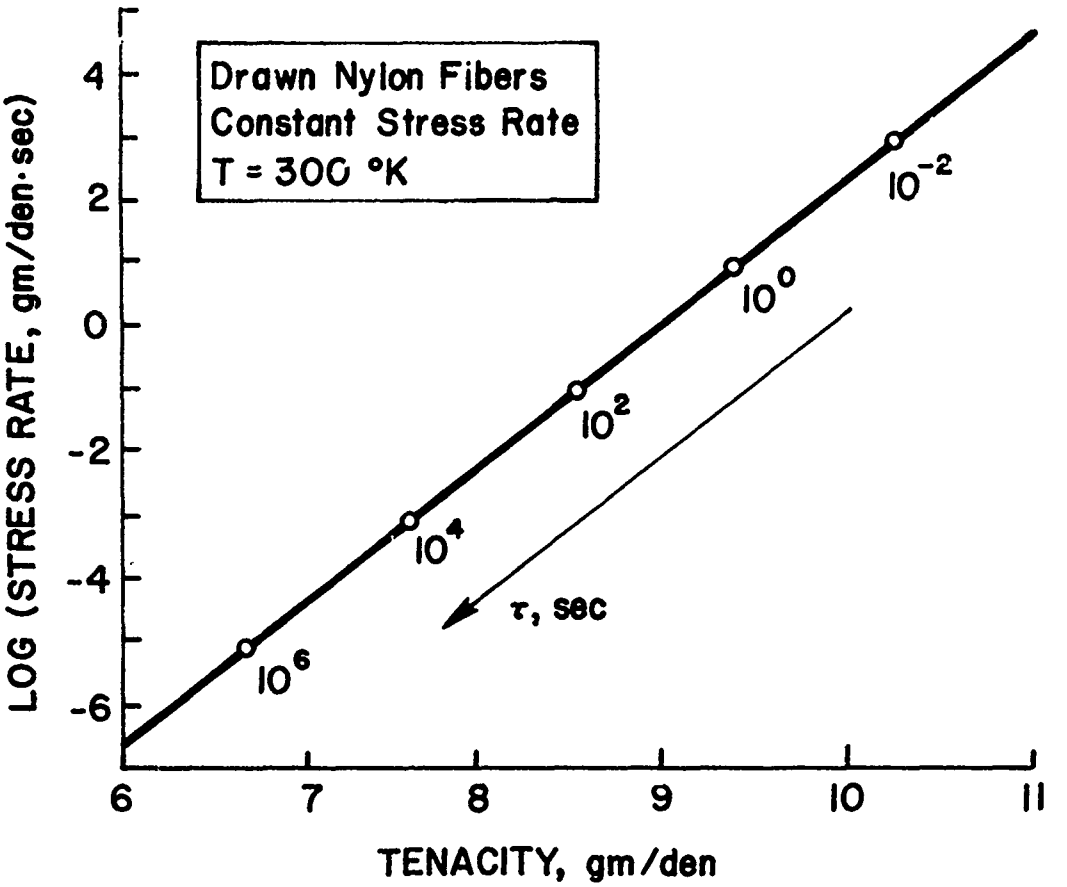

Figure 6. Variation of breaking tenacity with loading rate - Khurkov model.

As a more direct example of the utilization of Zhurkov's model in fiber ballistics, the stress predicted by the Smith theory for a given impact velocity and fiber modulus can be used in Equation 14 to predict the time after impact at which the fiber will rupture. This analysis predicts that there is no unique critical transverse velocity, but rather a range of velocities over which the fiber will fail in experimentally observable times. Figure 7 shows the predicted results for drawn nylon fibers, using an assumed dynamic modulus of 80 g/den with the same values of α and β used in Figure 6. This figure

shows that at velocities above approximately 775 m/sec, rupture occurs in less than fifty microseconds and would be counted in most high-speed photographic records as having occurred instantaneously upon impact. The times-to-break become exponentially longer at lower velocities, and failure will occur at the clamp due to wave reflection at times dependent on the wavespeed and fiber length. This variation in what may be termed critical velocity for impact may make up a large part of the scatter observed experimentally in determining critical transverse velocities.

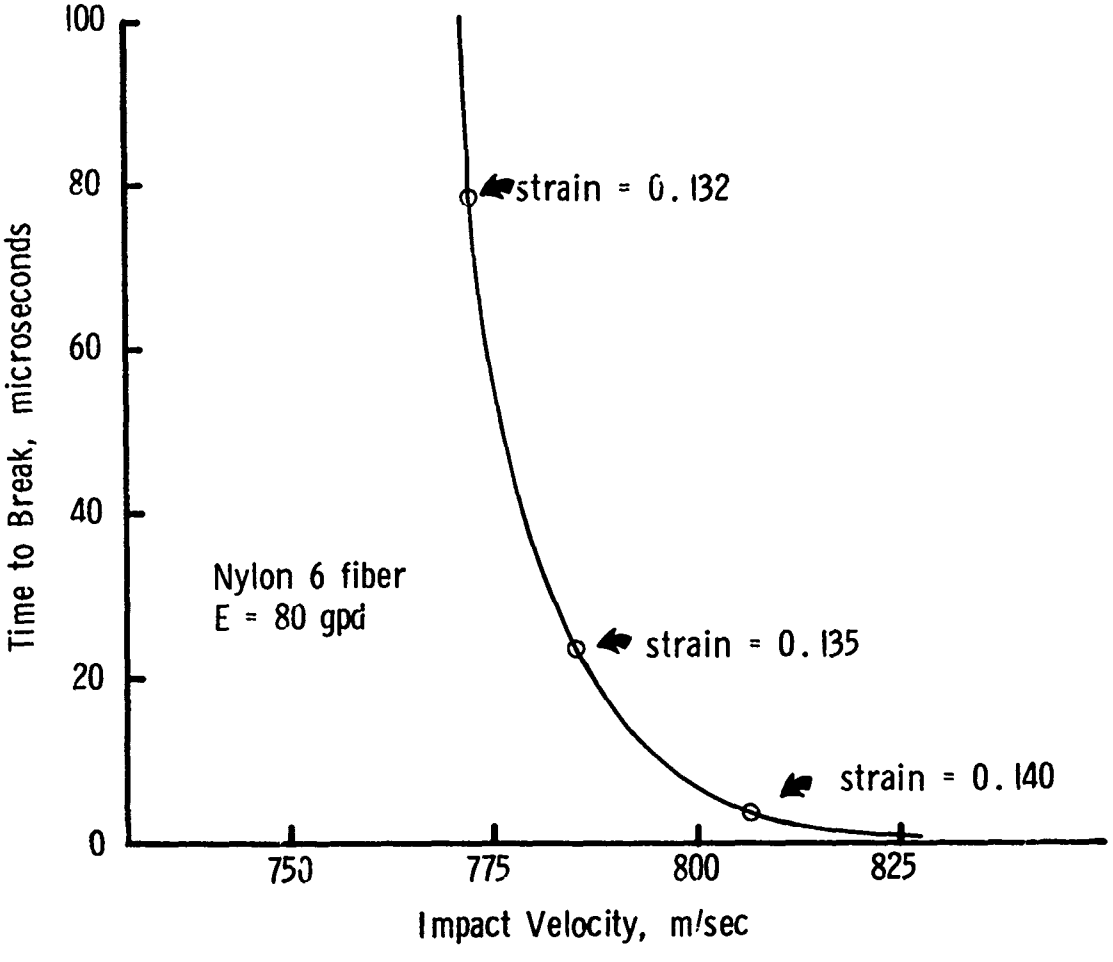

Figure 7. Variation in transverse critical velocity due to fracture rate effects.

An important advantage to Zhurkov's model is that it is derivable in terms of basic reaction-rate fracture analysis. As such, it provides a means whereby the materials scientist can predict materials and processing modifications so as to manipulate the fracture parameters and improve ballistic performance. A recent review [12] describes the basic implications of reaction rate models such as Zhurkov's, as well as their limitations and experimental corroboration. The development of these models is somewhat controversial, with several quite divergent approaches having strong advocates. Zhurkov's model in particular is often criticized as being simplistic, but is convenient for use in impact by virtue of its computational convenience and its ability to model a wide range of materials behavior, if only phenomenologically. Finally, it should be cautioned that the experiments Zhurkov used in corroborating his model were no faster than the millisecond time scale, some three orders of magnitude slower than ballistic impact fractures. Such an extrapolation is clearly dangerous and should be verified by additional experimentation. The plot given in Figure 7 is in reasonable but not excellent agreement with experimental data given in Smith's papers, indicating that the approach is promising but needing of further corroboration.

II. NUMERICAL ANALYSIS OF IMPACT ON WOVEN PANELS

Method of Analysis

The method of analysis used in this study is a direct numerical approach which attacks the governing dynamic equations of the problem through a computer-aided iterative scheme. It may be considered as a hybrid of the finite element method in selecting control volumes and the finite difference in establishing recurrence formulas.

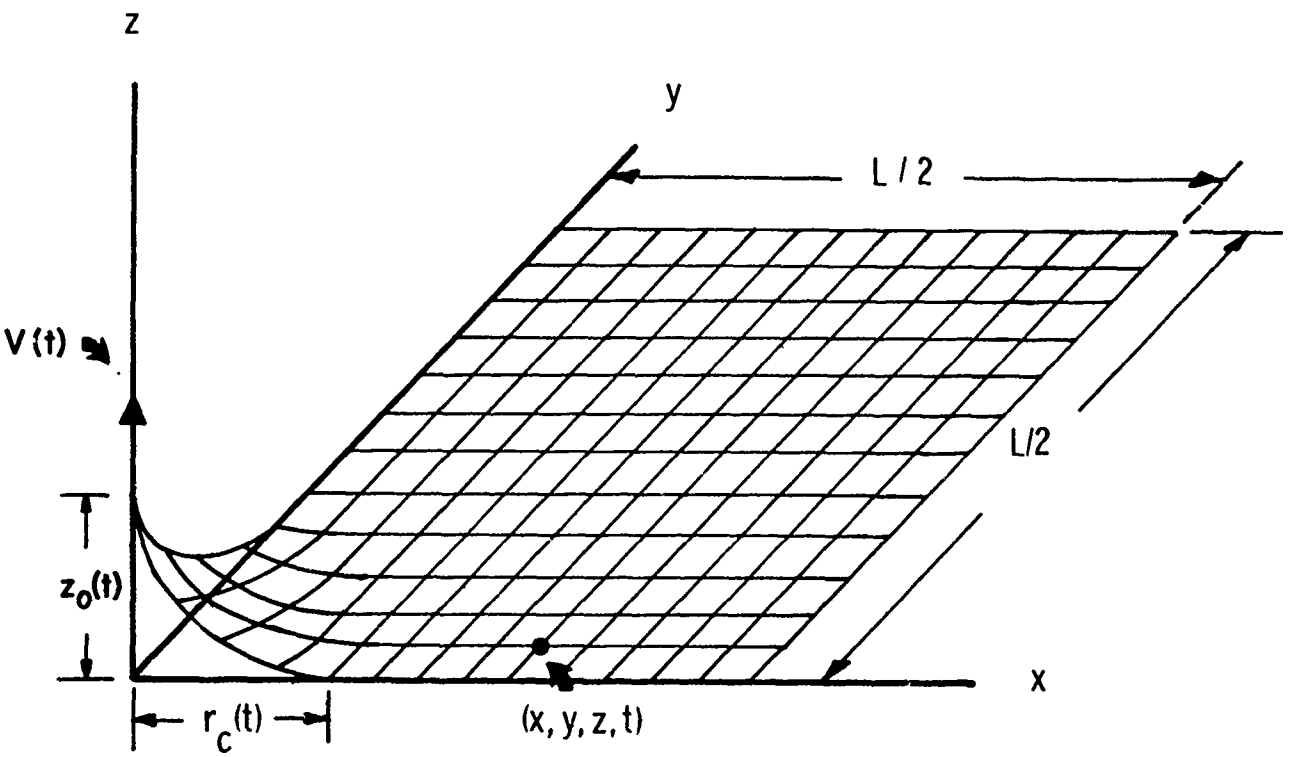

Figure 8. Idealization of impacted fabric panel as an essemblage of pin-jointed tension members.

The fabric of dimension L by L shown in Figure 8 is modeled as a network of interconnected fiber elements impacted at zero obliquity by a rigid missile of mass M_p with an initial striking velocity V_p. The network model rather than a continuous membrane is employed here, for it is not only more consistent with the discrete fabric structure but also leads to better agreement with the physical deformation configuration (pyramidal cone rather than hemisphere) as observed by Wilde [13] in high speed photographs. The elastic continuum supporting the fabric deformation is generally very flexible in transverse direction: bending effects are neglected. The constituent fibers are considered to have a slender and uniform cross section that only plane waves propagate uniaxially. Furthermore, crossovers are modeled as hinged connections; then, slippage is assumed to be negligible.

Mathematical Formulation

Considering a typical crossover in the panel, as shown in Figure 9, the impulse-momentum balance

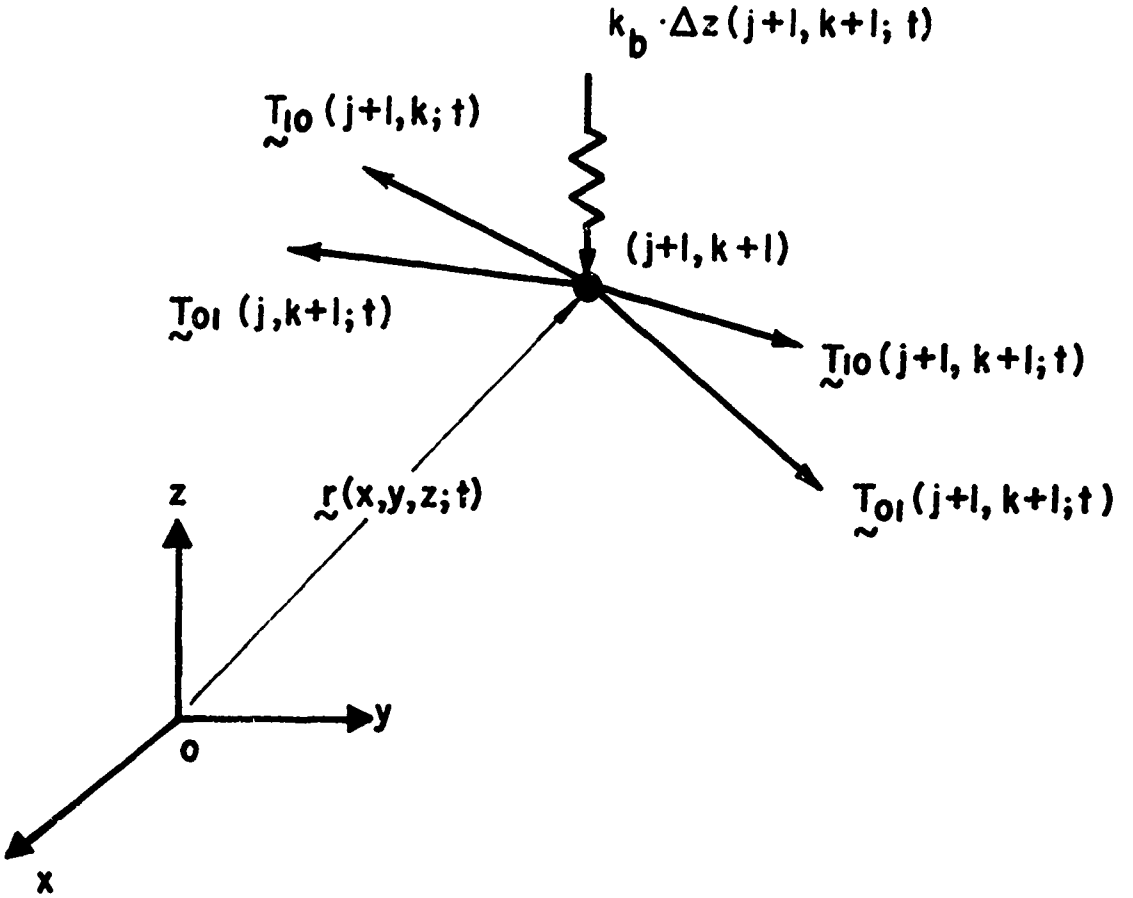

Figure 9. Free-body diagram of forces acting at a fabric crossover point, showing the influence of the four fiber elements meeting there and the elastic resistive force provided by the fabric backing.

during time dt may be written as

$$\Delta m \cdot d\underset{\sim}{v} = \underset{\sim}{T} \cdot dt \qquad (19)$$

where $d\underset{\sim}{v}$ is an incremental velocity, $\underset{\sim}{T}$ is the resultant tensile force, and Δm is the lumped mass of a

fabric element. This relation provides a means of calculating current velocity from field variables in previous time increment. For instance, at node (j+1, k+1), the velocity at time t_{m+1} may be expressed in a finite difference form as

$$\underset{\sim}{v}^{m+1}_{j+1,k+1} = \underset{\sim}{v}^{m}_{j+1,k+1} + \underset{\sim}{T}^{m}_{j+1,k+1} \cdot \frac{\Delta t}{2 s \rho \Delta l} \tag{20}$$

where ρ is the linear fiber density, Δl, the length of an orthogonal fiber element, s, a numerical factor associated with the crimping and wave of the fabric structure, and the tensile force $\underset{\sim}{T}$ is given as

$$\begin{aligned} \underset{\sim}{T}^{m}_{j+1,k+1} = {} & \underset{\sim}{T10}^{m}_{j+1,k+1} - \underset{\sim}{T10}^{m}_{j,k+1} \\ & + \underset{\sim}{T01}^{m}_{j+1,k+1} - \underset{\sim}{T01}^{m}_{j+1,k} \\ & - k_b \underset{\sim}{u}^{m}_{j+1,k+1} \end{aligned} \tag{21}$$

in which k_b is a backup spring constant and $\underset{\sim}{u}$ is the displacement vector. T_{10} and T_{01} are tensile vectors in the deformed orthogonal fibers running through the crossover as shown in Figure 9. The Lagrangian

* The $\sim$ underline is used to denote a vector quantity.

coordinates of the node are then evaluated by

$$\underset{\sim}{r}^{m+1}_{j+1,k+1} = \underset{\sim}{r}^{m}_{j+1,k+1} + \underset{\sim}{v}^{m+1}_{j+1,k+1} \cdot \Delta t \qquad (22)$$

The up-to-date strain defined as e(j+1, k+1; m+1) = $\{e_{10}, e_{01}\}$ may now be determined from a continuity condition;

$$\underset{\sim}{e}_{10}{}^{m+1}_{j+1,k+1} = \underset{\sim}{e}_{10}{}^{m}_{j+1,k+1} + \left\{ \left[\underset{\sim}{r}^{m+1}_{j+2,k+1} - \underset{\sim}{r}^{m+1}_{j+1,k+1} \right] / \left[\underset{\sim}{r}^{m}_{j+2,k+1} - \underset{\sim}{r}^{m}_{j+1,k+1} \right] - 1 \right\} \qquad (23)$$

and

$$\underset{\sim}{e}_{01}{}^{m+1}_{j+1,k+1} = \underset{\sim}{e}_{01}{}^{m}_{j+1,k+1} + \left\{ \left[\underset{\sim}{r}^{m+1}_{j+1,k+2} - \underset{\sim}{r}^{m+1}_{j+1,k+1} \right] / \left[\underset{\sim}{r}^{m}_{j+1,k+2} - \underset{\sim}{r}^{m}_{j+1,k+1} \right] - 1 \right\} \qquad (24)$$

Tensile stresses for the fibers at the crossover may be computed from material's dynamic constitutive relationship. For the case of a simple elastic fabric, T may be calculated by

$$\underset{\sim}{T}^{m+1}_{j+1,k+1} = E \underset{\sim}{e}^{m+1}_{j+1,k+1} \tag{25}$$

Current missile velocity $V_p(t)$ may be obtained by

$$V_p^{m+1} = V_p^m + \{4(T_{10_z})^{m+1}_{0,0} \times \sin\theta_p + k_b(M_z)^{m+1}_{0,0}\} \cdot \Delta t/M_p \tag{26}$$

where the fabric inclination θ_p at the impact point may be evaluated from

$$\theta_p = \tan^{-1}\{[(M_z)^{m+1}_{0,0} - (M_z)^{m+1}_{1,0}]/\Delta l\} \tag{27}$$

The total kinetic energy loss of the missile

during penetration can be computed from

$$\Delta E_p = \frac{1}{2} M_p (V_p^2 - V_r^2) \tag{28}$$

where V_r is the residual velocity of the missile upon penetration. The fabric energy absorption and partition are of great interest, since they provide a means of evaluating the performance of the material. The kinetic and strain energy, $\Delta E^k(t)$ and $\Delta E_f^s(t)$, obtained by the panel during impact may be calculated by

$$\Delta E_f^k(t) = \int_0^t \int_A \frac{1}{2} \cdot \Delta m \left| \underset{\sim}{v}_{x,y}^t \right|^2 dA\, dt \tag{29}$$

$$\Delta E_f^s(t) = \int_0^t \int_A \left| \underset{\sim}{T} \right|^2 \cdot (1/2E)\, dA\, dt \tag{30}$$

Where A is the area of the fabric. The above formulations have been coded in FORTRAN, and the computation algorithm proceeds from one node to the next along a wave front propagating through the fabric. Due to geometric symmetry, only half of one quadrant is con-

sidered. At each time increment, the code begins at the origin (the impact point) and works outward until the wavefront is reached. The space progression consists of a series of passes along lines diagonal to the orthogonal fibers, indicated by dashes in Figure 10. The algorithm begins at the x-axis (a subroutine is employed to handle the slightly different conditions along this symmetry boundary), and progresses along the diagonal until reaching the end of the octant. For reasons of stability, the rate at which the code progresses outward from the impact point is related to the fabric wavespeed; these stability considerations will be discussed in a later section.

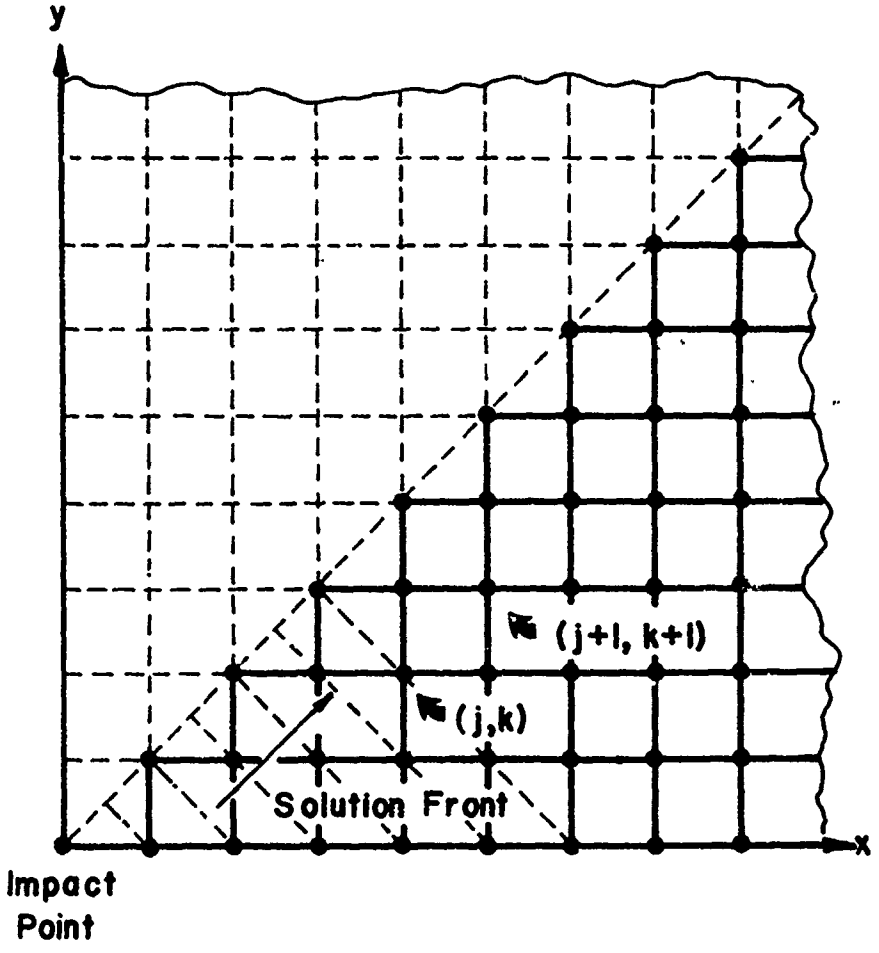

Figure 10. Propagation scheme for the iterative wave propagation algorithm.

The numerical method requires appropriate initial and boundary conditions in order to proceed with the computation. The initial condition is that all nodal points are at rest except that the initial projectile velocity is imposed at the center of the panel, i.e.

$$\underset{\sim}{v}^{0}_{0,0} = \{0, 0, V_p\} \tag{31}$$

The boundaries of the fabric are assumed to be rigidly clamped during impact, thus

$$\underset{\sim}{v}^{t}_{\pm L/2, y} = \underset{\sim}{0}$$
$$\underset{\sim}{v}^{t}_{x, \pm L/2} = \underset{\sim}{0} \tag{32}$$

Solution Stability, Convergence and Accuracy

Solution stability and convergence are directly related to the theory of characteristics for the hyperbolic system. The Von Neumann stability criterion [14] for the probem may be written as

$$c_r (\Delta t / \Delta \ell) < 1 \tag{33}$$

where c_r is the wave velocity in the fabric. Hence the selection of Δt and $\Delta \ell$ cannot be arbitrary.

The value of c_r is not known prior to the analysis, but a preliminary study by Roylance [15] indicates that it is a fixed fraction of the wave velocity ir a single fiber, c_f, i.e.

$$c_r = c_f / \alpha \tag{34}$$

where α is a numerical factor. It generally has value greater than unity, which may be attributed to the effective increase on lineal density caused by fiber crossovers. In a square-woven fabric, the lineal density of a fiber along which a wave is propagating is effectively doubled. This retards the wave velocity according to Equation 2 by a factor of $\alpha = \sqrt{2}$. The stability condition is then of the form

$$c_f \Delta t / (\alpha \Delta \ell) < 1 \tag{35}$$

In the current analysis, $\Delta \ell$ is obtained by physical considerations; therefore Δt is constrained by Equation (35). The parameter α has its optimum value obtained from stable solutions and is defined as

$$\bar{\alpha} = (\Delta \ell / c_f) / \Delta t \tag{36}$$

In the absence of a complete theory for finding the exact value of this parameter, it is a common practice in the use of numerical methods to have the computer determine it. The optimum $\bar{\alpha}$ may be obtained by changing its value continuously in test cases until a known solution is matched and a variation of the quantity will not yield any appreciable difference in the results. Unfortunately, there is no existing solution for this problem and one must resort to numerical tests of smoothness or of conservation laws for this purpose. A convenient measurement of stability and convergence is to study the rate of energy conservation of the system. In this study, an energy discrepancy parameter η is introduced for the purpose, and is defined as

$$\eta = \left| (E_p - E_f)/E_p \right| \tag{37}$$

where E_f is the total energy absorption by the fabric, and E_p is the projectile energy loss defined previously. Figures 11 and 12 give illustrations of the dependence of solution stability and convergence on the values of α parameter. An optimum value $\alpha = \sqrt{2}$ is obtained from these results, in agreement with physical reasoning.

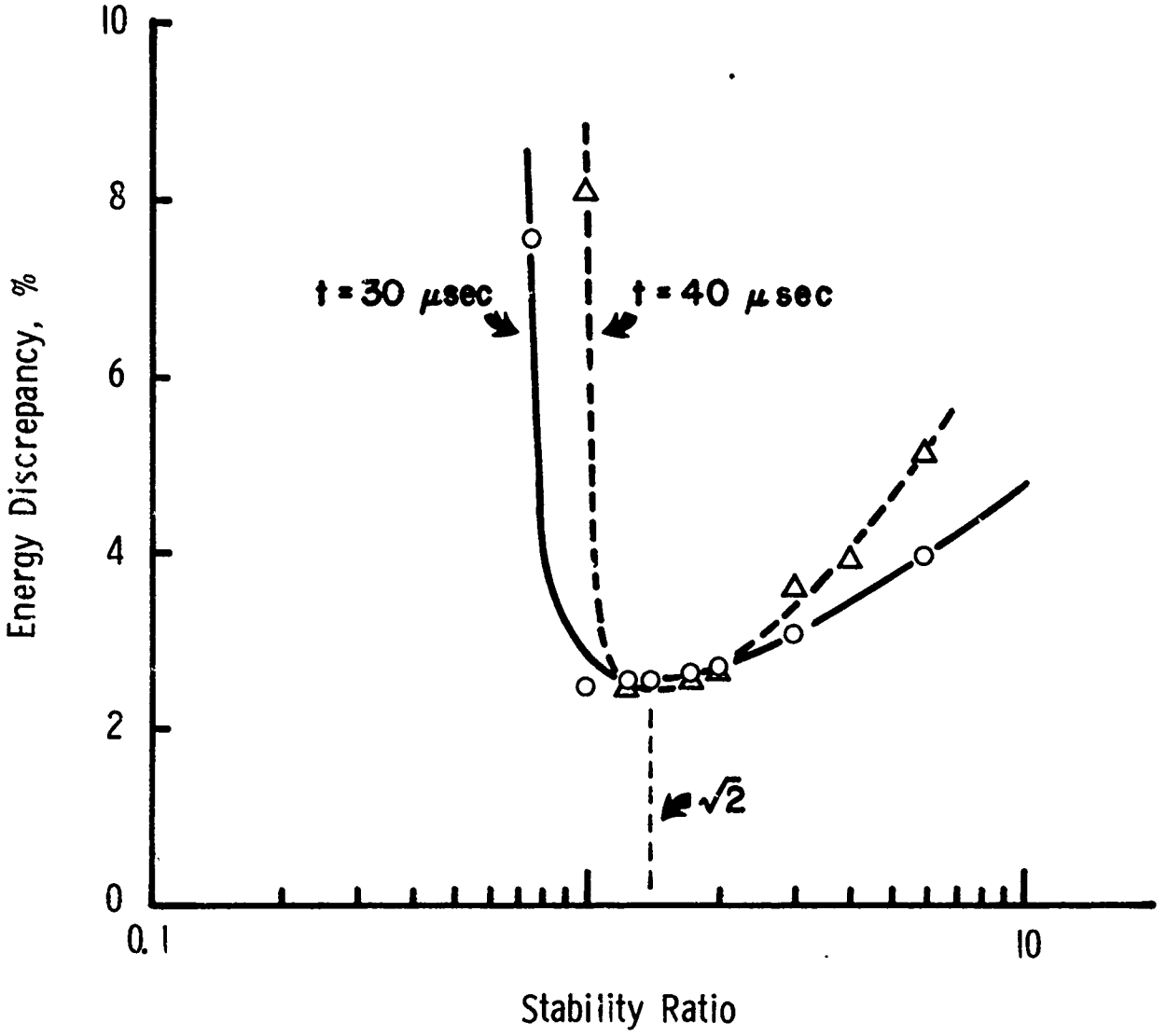

Figure 11. Stability of the numerical scheme as indicated by a minimum in the discrepancy between energy lost by the projectile and energy absorbed by the fabric. These data were obtained from a simulation of a 400 m/sec impact on Kevlar 29 fabric at times after impact as shown, and for various values of the stability ratio α defined by Equation 36.

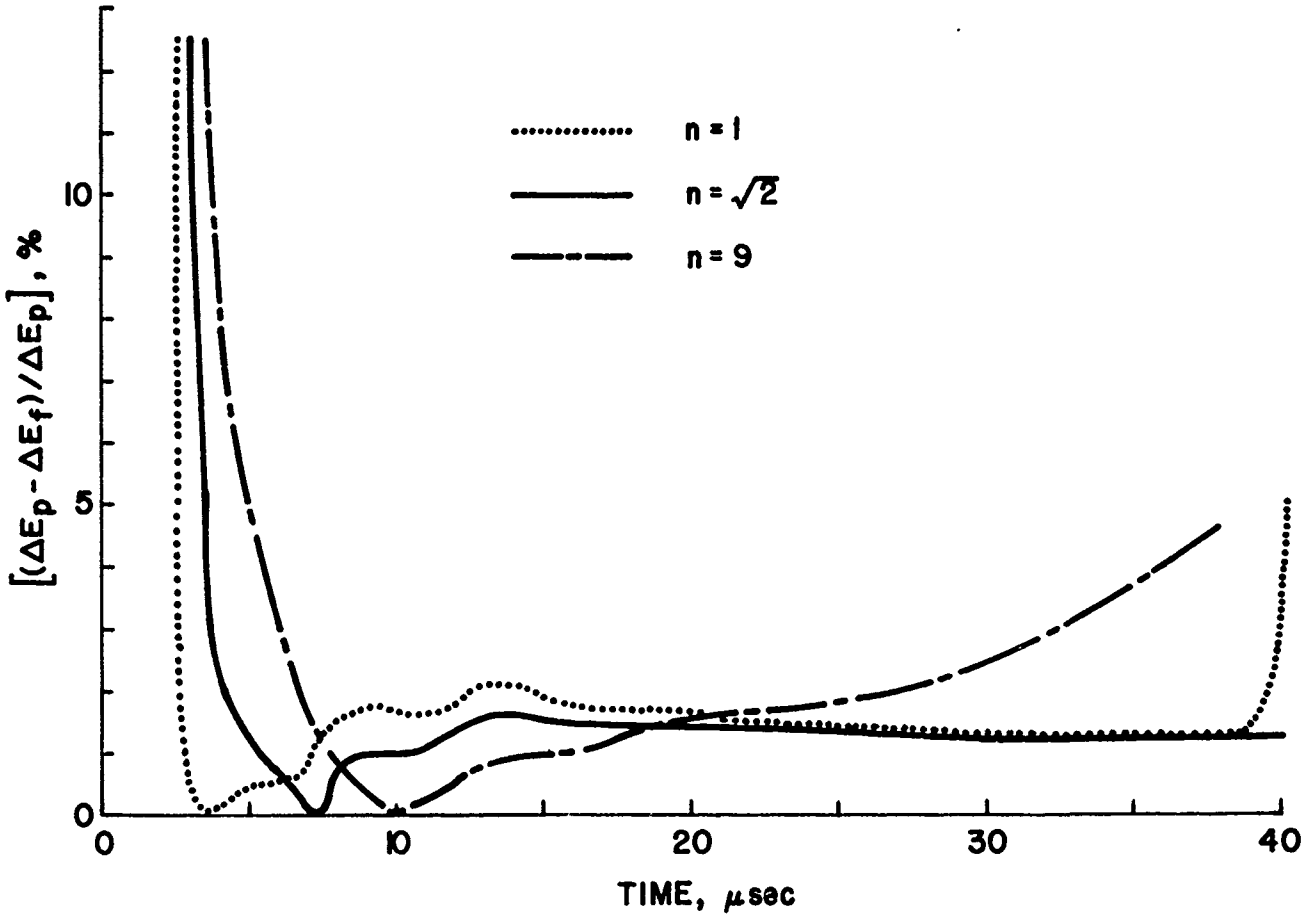

Figure 12. Illustration that the numerical scheme converges to accurate values with time, as indicated by the energy discrepancy ratio. Note that nonoptimum values of the stability ratio (η in this figure) lead to divergence at longer times.

Assessment of accuracy of the numerical analysis is somewhat problematical, as no closed-form mathematical analyses are available against which to check the code results. Certain experimental observations are available, however, one of which is shown in Figure 13. This figure is a plot of residual projectile velocity

Figure 13. Illustration that the numerical scheme predicts values of final projectile velocity after penetration in agreement with experimental observation.

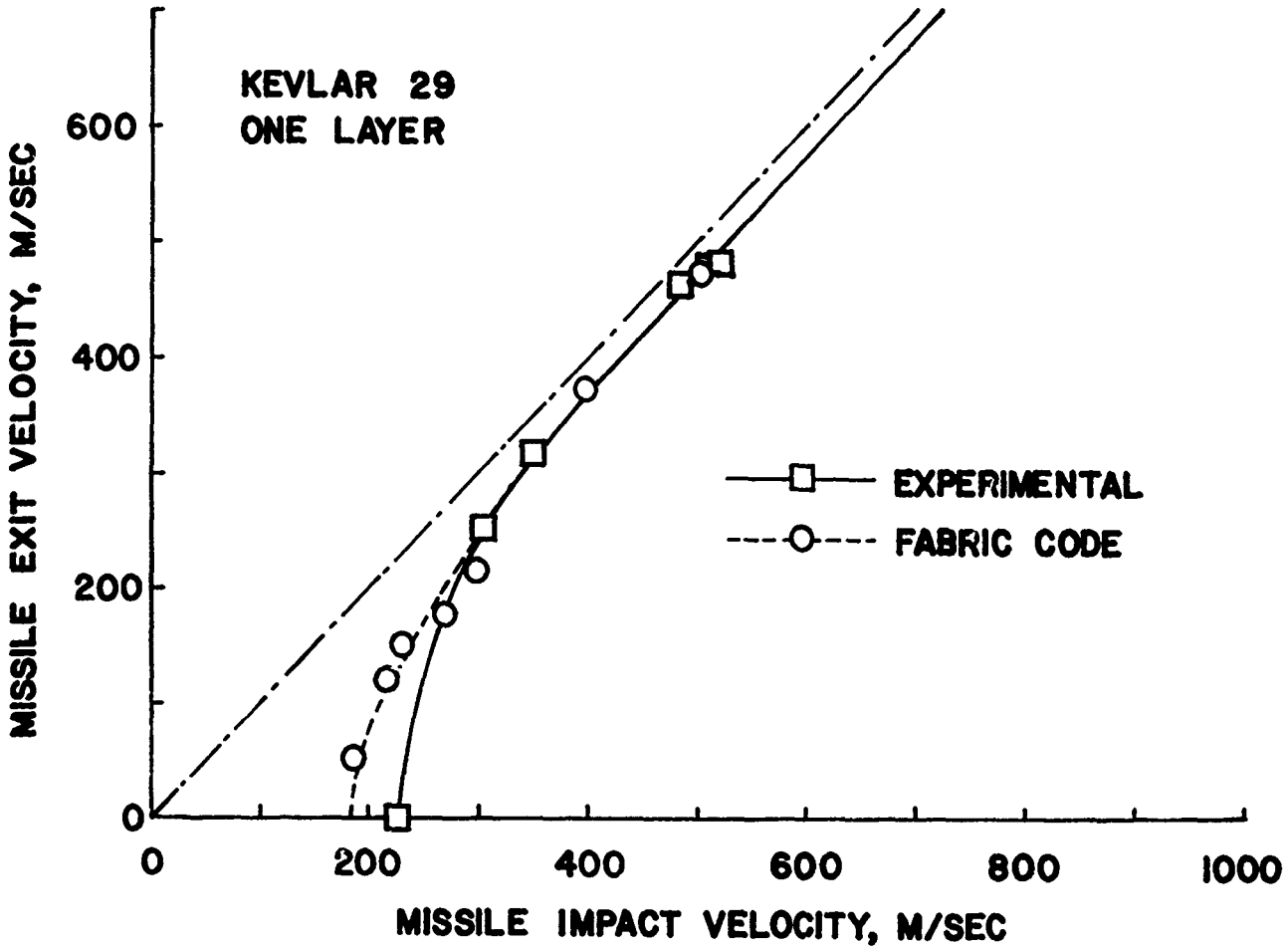

after penetration of a Kevlar panel, as a function of initial velocity. The good agreement of the predicted and observed results is important, since it provides some assurance that both the transient response and the final fracture processes are being modeled reasonably. It might also be mentioned that this particular plot is one which plays an important role in the design process, so that the ability to generate it numerically without prior ballistic data or any idealizing assumptions is of considerable practical importance.

Another result of the numerical calculations which may be checked against experiment has to do with the shape of the transverse deformation cone, since the cone may be followed by high-speed photography during the impact event. It should be mentioned that this photgraphic evidence provided the initial impetus to the development of the present pin-jointed fiber model, as opposed to various membrane approaches which have been attempted in the past. The photographs clearly show a pyramidal deformation cone which reflects the orthogonal nature of the woven structure, as opposed to the circular cones which would be predicted by axy-symmetric membrane analyses. The present numerical treatment predicts this pyramidal shape correctly. A convenient indicator of deformation is the size of the cone at the time of projectile penetration, as this parameter also reflects both transient and fracture properties of the panel. Figure 14 shows the predicted and observed cone size at penetration for a Kevlar panel, and again it is seen that agreement is satisfactory.

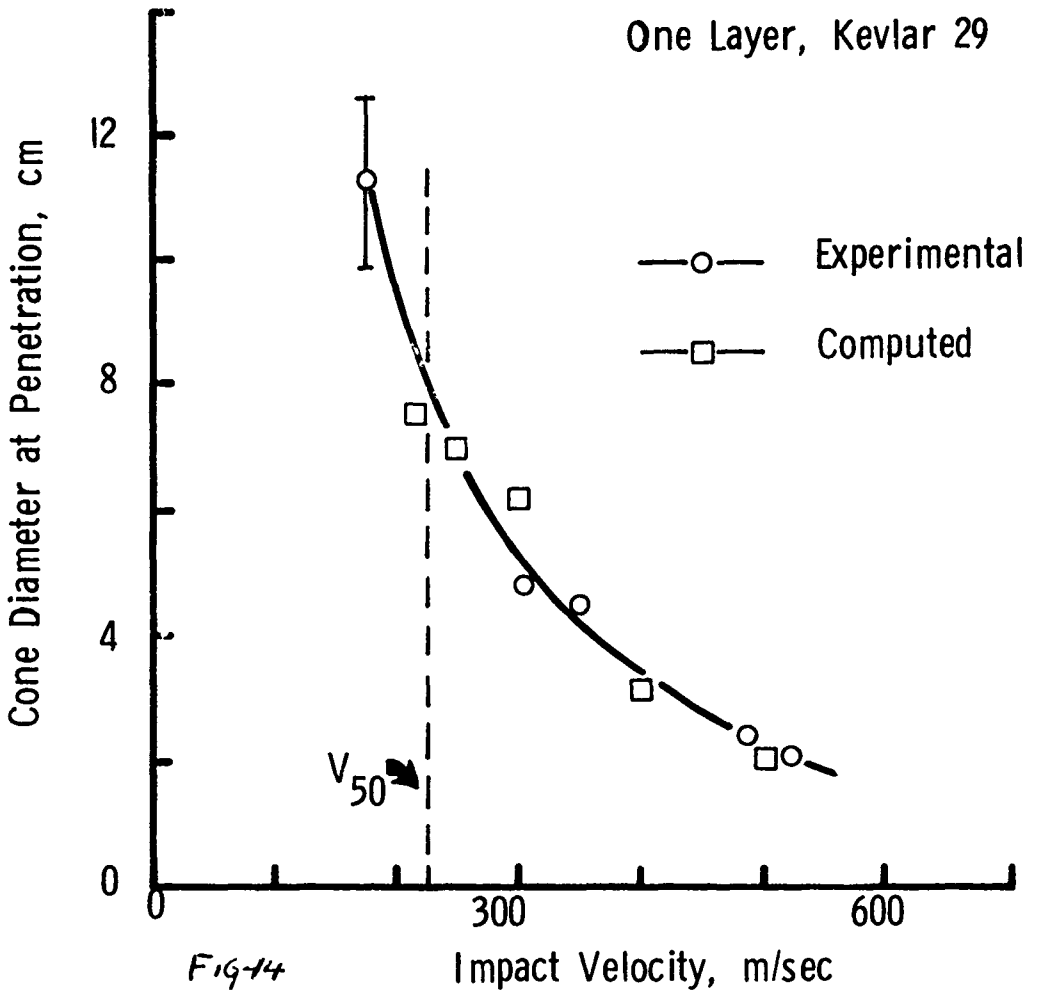

Figure 14. Computed and experimentally observed values of cone deformation cone size at time of projectile penetration. The V_{50} is that value of impact velocity at which penetration occurs nearly instantaneously.

Parametric Materials Study

The utility of the numerical model will be illustrated by means of a number of computer experiments in which the influence of fabric materials properties on ballistic resistance is assessed. These results help validate the reliability of the model in that it can be shown to generate data in agreement with experimental observations. It also provides a means of illustrating certain phenomena, such as transient wave propagation, which are not generally observable experimentally; in this regard one's intuitive understanding of the impact even is improved considerably.

Numerical results have been obtained for a series of four simulated orthogonally-woven square panels 203 mm on a side, impacted at zero obliquity by a 0.22-caliber projectile weighing 1.10 gram. Such a projectile is commonly used in experimental work to simulate the effect of fragment impact. The edges of the panels were assumed to be clamped, although penetration generally occurred before the arrival of stress waves at the clamps; the nature of the edge boundary conditions is therefore relatively unimportant. Rather than perform straightforward parametric tests in which one variable, such as fiber modulus, is varied while others are held constant, it was decided to simulate

a series of actual fabrics for which input data was available either from the weaver or from laboratory measurement. The computer results can thus be compared directly with laboratory ballistic tests, although in general, more than one variable is changed in each simulation. In particular, the fabric panel weight varies slightly for each material type, although this effect was expected to be small relative to the large change resulting from the markedly different fiber moduli.

For the purpose of these parametric tests, only very simple constitutive and fracture models were employed. Although more realistic models are available as described elsewhere in this report, the numerical data necessary for input into these models are generally not available. For this reason the fiber stiffness was set to a constant value obtained from handbook quasi-static stress-strain data, and the failure criterion was a simple maximum-breaking-strain check, where the maximum allowed was also taken from quasistatic tensile test results. In spite of these questionable choices, the results of the computer simulations are of considerable interest.

The data for the four fabric types are shown below:

GEOMETRIC AND MATERIALS PROPERTIES USED IN FABRIC STUDIES

Fiber	Nylon	Kevlar 29™	Kevlar 49™	Graphite
Tensile modulus, gpd	80	550	990	2650
Fracture Strain, %	14.0	4.0	2.2	1.1
Fabric Mass, gm	19.53	17.38	25.75	27.09
Yarn denier	1050	1167	1485	1500
Yarn/cm	17	16	16	16

Figure 15 shows typical computer predictions of strain wave profiles obtained at various times after a 400 m/sec impact on the various fabrics. Unlike impact on a single fiber, in which a constant level of strain is propagated outward from the impact point, the array of fiber crossover junctions around the impact point in a fabric serves to reflect a portion of the outward-propagating wave back toward the impact point. As a result, the strain is always greatest at the point of impact, and grows continuously with time (unless the projectile is slowed appreciably by the panel). Both the level of strain and the rate of propagation

are governed by the fiber modulus and density. As shown in the figure, graphite fibers have the highest modulus of the four materials, and thus propagate the lowest level of strain at the highest rate. As the modulus is decreased, the strain level is increased and the wavespeed is decreased.

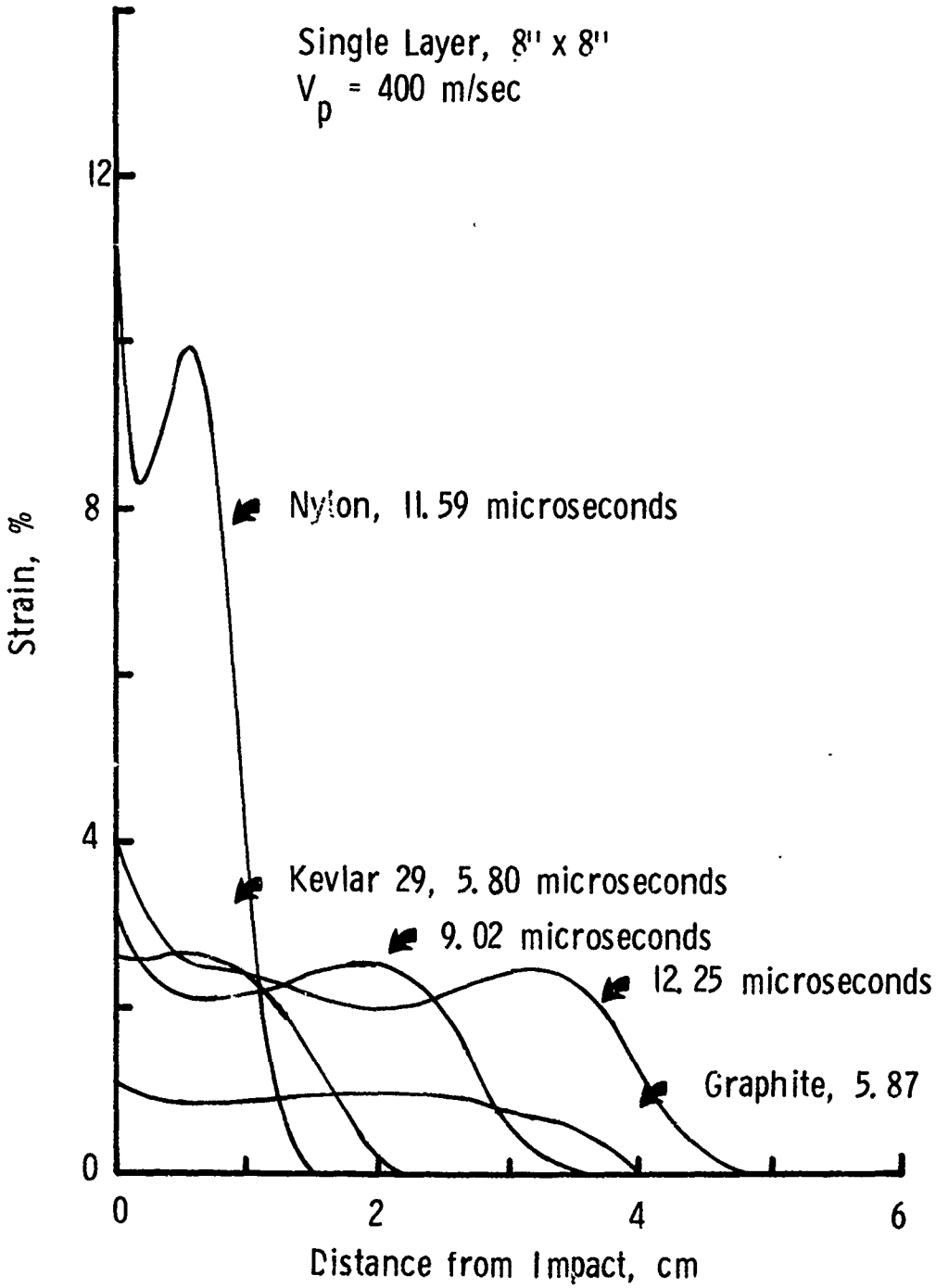

Figure 15. Distribution of strain along orthogonal fibers passing through the impact point. Curves are drawn for various fabric types, at various times after a 400 m/sec impact.

The strain history in the fabric is directly related to missile striking velocity as indicated in Figure 16. When the velocity is greater than a critical impact velocity V_{cr}, strain at the impact point continuously rises until penetration, due to the continual arrival of wavelets reflected from crossovers and boundaries. In contrast, if the velocity is smaller than V_{cr}, the impact strain develops to a level below the breaking strain and remains relatively constant for the rest of the dynamic process. Here the effect of unloading due to projectile deceleration is able to balance the increase of strain due to wave reflection. The wavy strain history in the figure may be caused by the dispersion and interaction of the traveling and reflected wavelets, and perhaps, some numerical fluctuation.

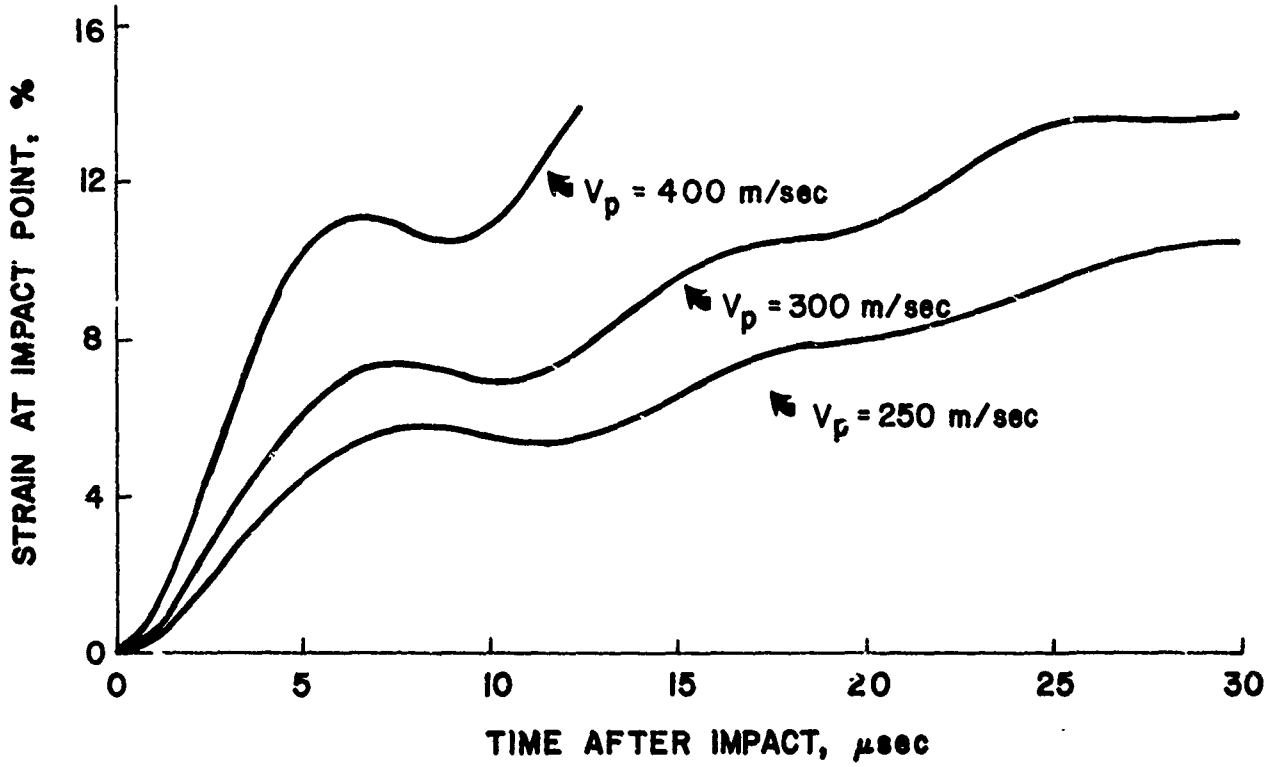

Figure 16. Effect of initial projectile velocity on the development of strain at the point of impact for nylon fabric.

Penetration dynamics can also be illustrated by the missile deceleration as shown in Figure 17, where reductions of missile velocity by various fabric materials are given. Note that the ability of the various fabrics to decelerate the projectile increases monotonically with the fiber modulus.

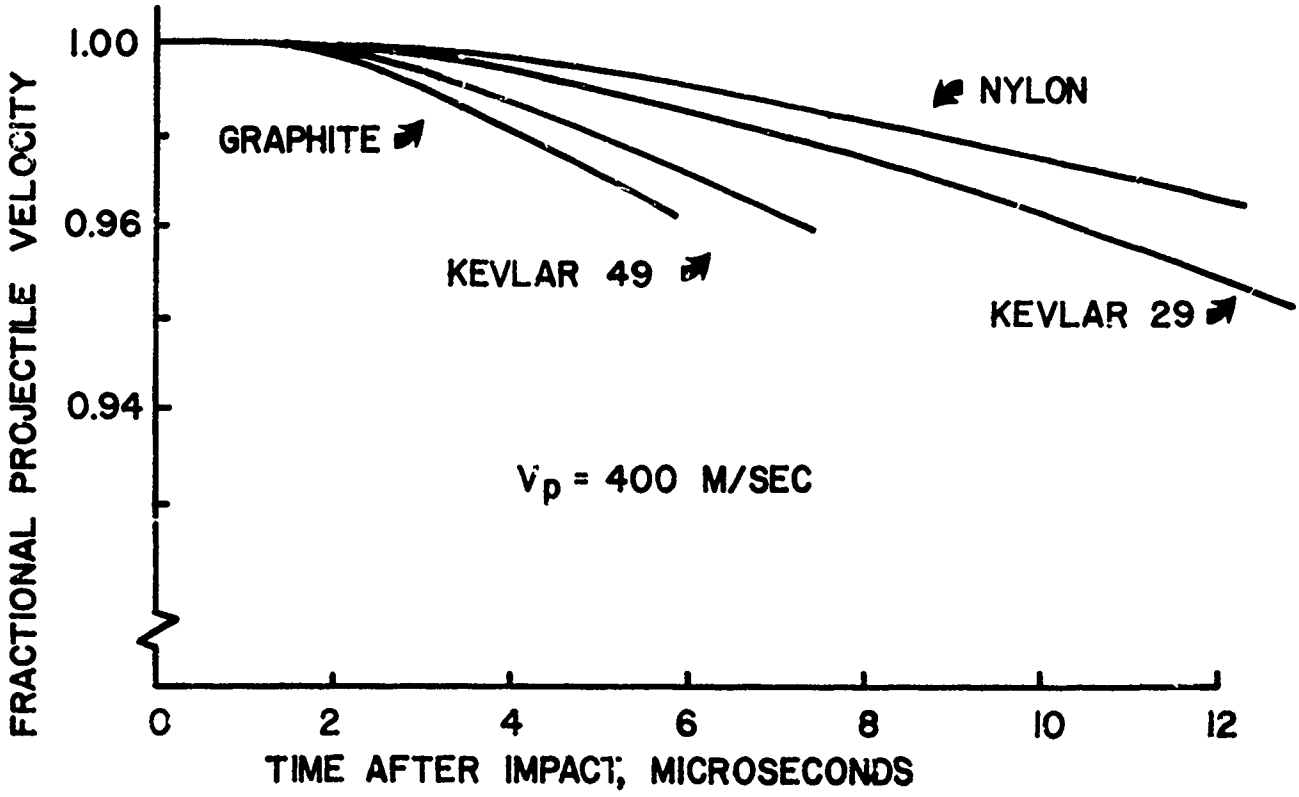

Figure 17. Relative ability of the various fabric types of slow the projectile during impact. Ordinal values represent the ratio of current to initial projectile velocity.

The energy extracted from the projectile is partitioned into strain and kinetic energy in the panel. This energy partition is easily computed, and Figure 18 indicates that approximately half the total fabric energy absorption is stored in the form of strain energy. The kinetic energy associated with transverse velocity is approximately equal to that associated with in-plane velocity components. Energy absorption is a

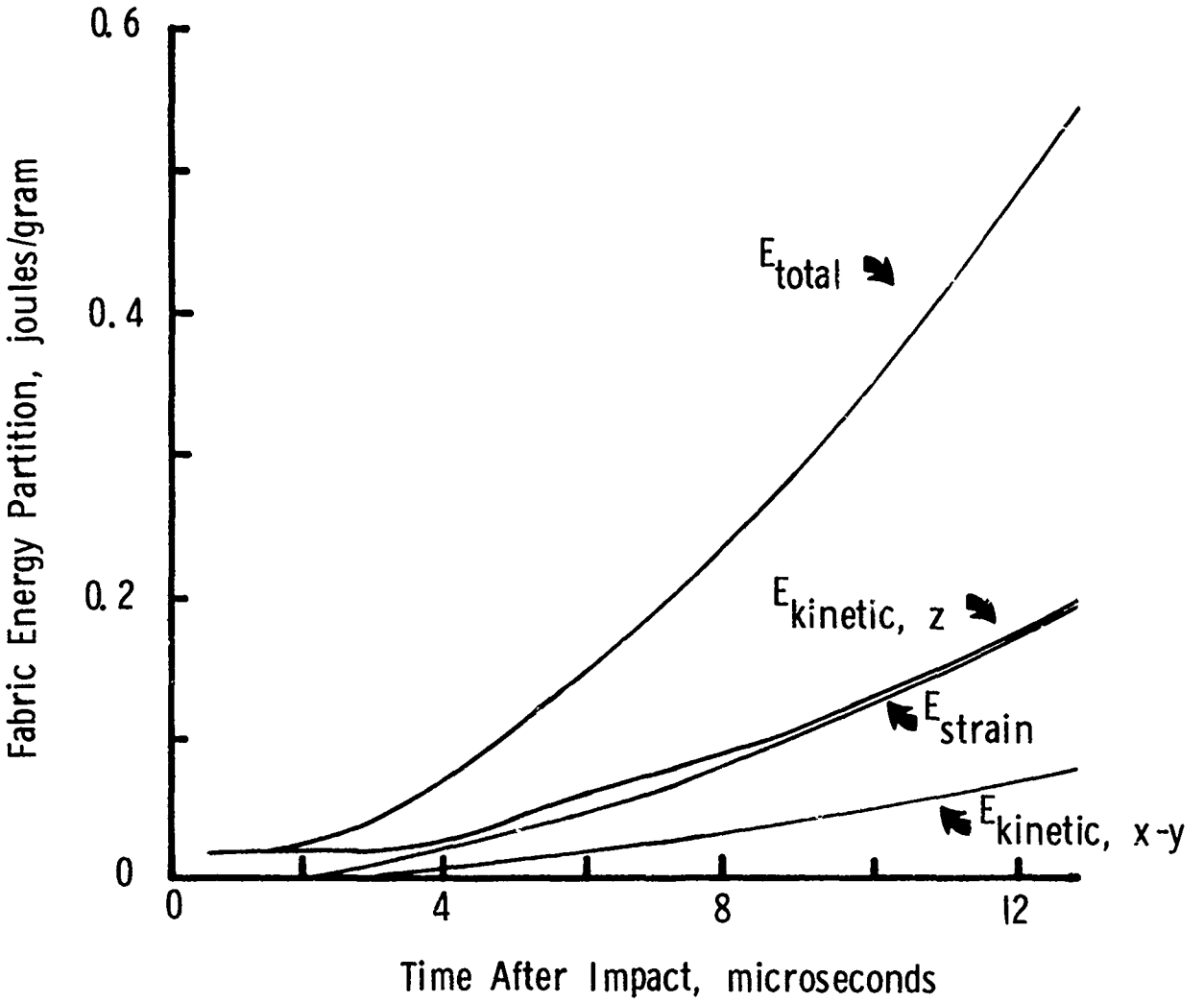

Figure 18. Energy absorbed by a Kevlar 29 panel after a 400 m/sec impact, illustrating the partition of impact energy into kinetic and strain energy in the panel.

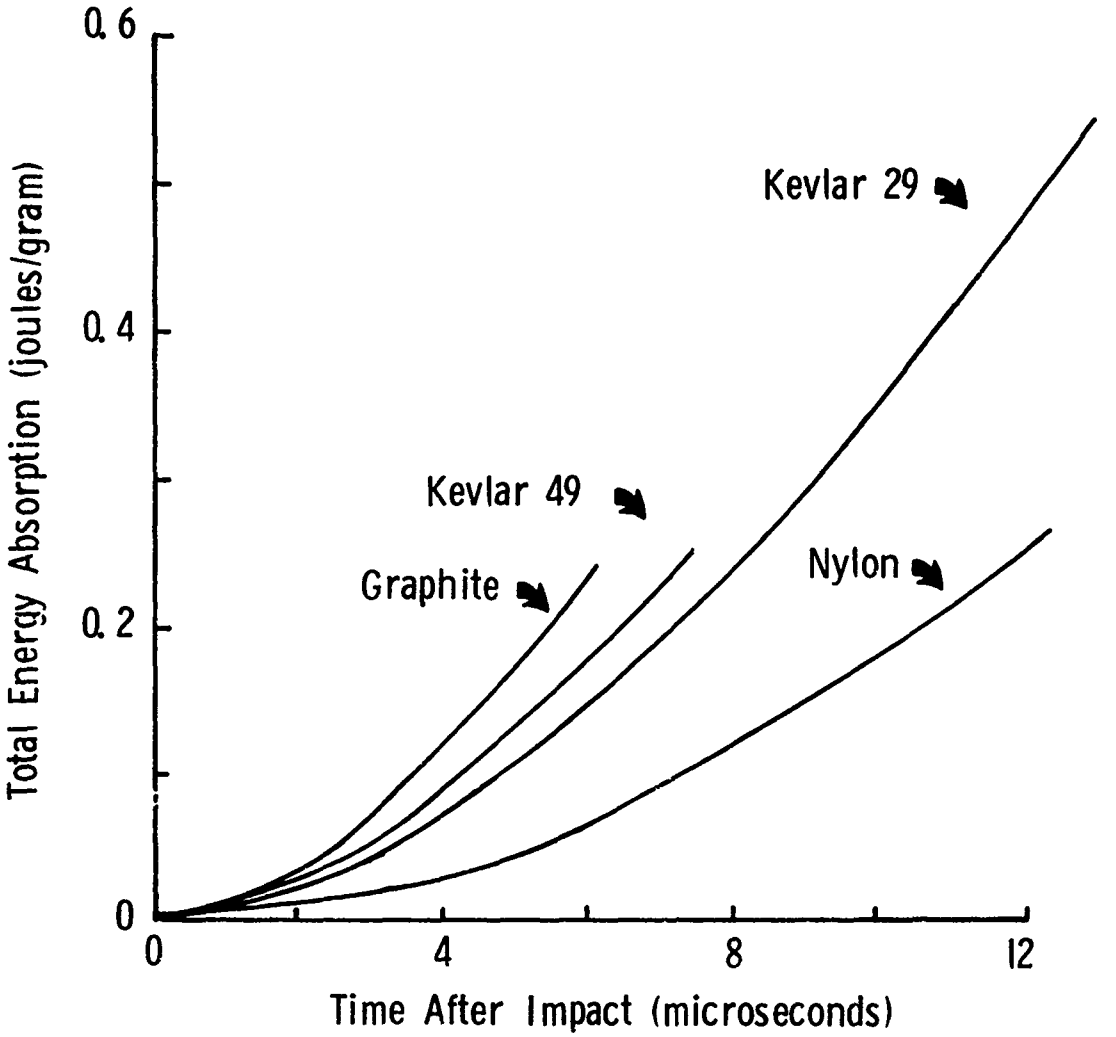

Figure 19. Illustration of the relative ability of the four fabric types of absorb impact energy. The curves are terminated at the right by projectile penetration, as indicated by a maximum-breaking strain failure criterion.

convenient indicator of panel ballistic performance, and Figure 19 illustrates the relative energy absorption capabilities of the four panel materials studied. It is seen that the high fiber modulus of the graphite panel leads to a rapid rate of energy absorption, but that fracture occurs before the panel has been able to extract as much of the projectile's impact energy as the lower-modulus fabrics. Conversely, nylon requires a long time to penetration, but the energy absorption rate is too slow to lead to a large total energy absorption. The Kevlar 29 panel exhibits the best combination of energy absorption rate and long time to penetration, and is thus predicted to be the superior ballistic material of the four types studied.

It should be mentioned that the accuracy of these results is limited by the questionable assumptions which had to be made due to the present lack of knowledge as to dynamic fiber properties which could be used as input data for the code. For these rather stiff fibers, the use of a linear elastic constitutive law is probably not a serious error; however, the use of maximum-breaking-strain failure critrion is almost certainly to blame for some inconsistencies in the results. In particular, Kevlar 49 is known to be essentially as good as, if not superior to Kevlar 29 as a ballistic material. The authors feel the shape of the energy absorption curves in Figure 19 is accurate, but that the location of the failure point is poor in the case of Kevlar 49. This points out the need for more complete dynamic fracture data on these fibers, so that more realistic models such as that described by Equation 17 may be employed.

It is natural to seek some simple relationship between fiber material properties and fabric ballistic resistance. The preceeding results lead one to expect that the most important parameter governing the stress history in the fabric before fracture is the fiber modulus. The modulus controls wavespeed through the relation $c=\sqrt{kE}$, and thus the distance the impact disturbance will have traveled in a given time. The

modulus also controls the level of strain which will be generated by impact at a given velocity. The relation is not known explicitly for fabrics, but can be determined by performing computer experiments using the numerical code.

Figure 20 depicts the computed strain history at the point of impact for 400 m/sec impacts upon the four model fabrics. It is clearly seen that an increase in fiber modulus decreases the strain for a given time, in correlation with the same result for single fibers. The fabric impact is considerably more complex than single-fiber impact, however; the point of impact feels not only the continuing influence of the projectile, but is also continually bombarded by wavelets reflected and diverted from adjacent fiber crossovers. The situation is too complex to permit simple generalizations, but the nonlinear form of the strain histories for the various fabrics can be taken to reflect the influence of wave interactions occurring in a region whose size increases quadratically with time. Note also that the shape of the strain histories varies consistently with fiber modulus: the time for arrival of the first peak, for instance, decreases monotonically with modulus.

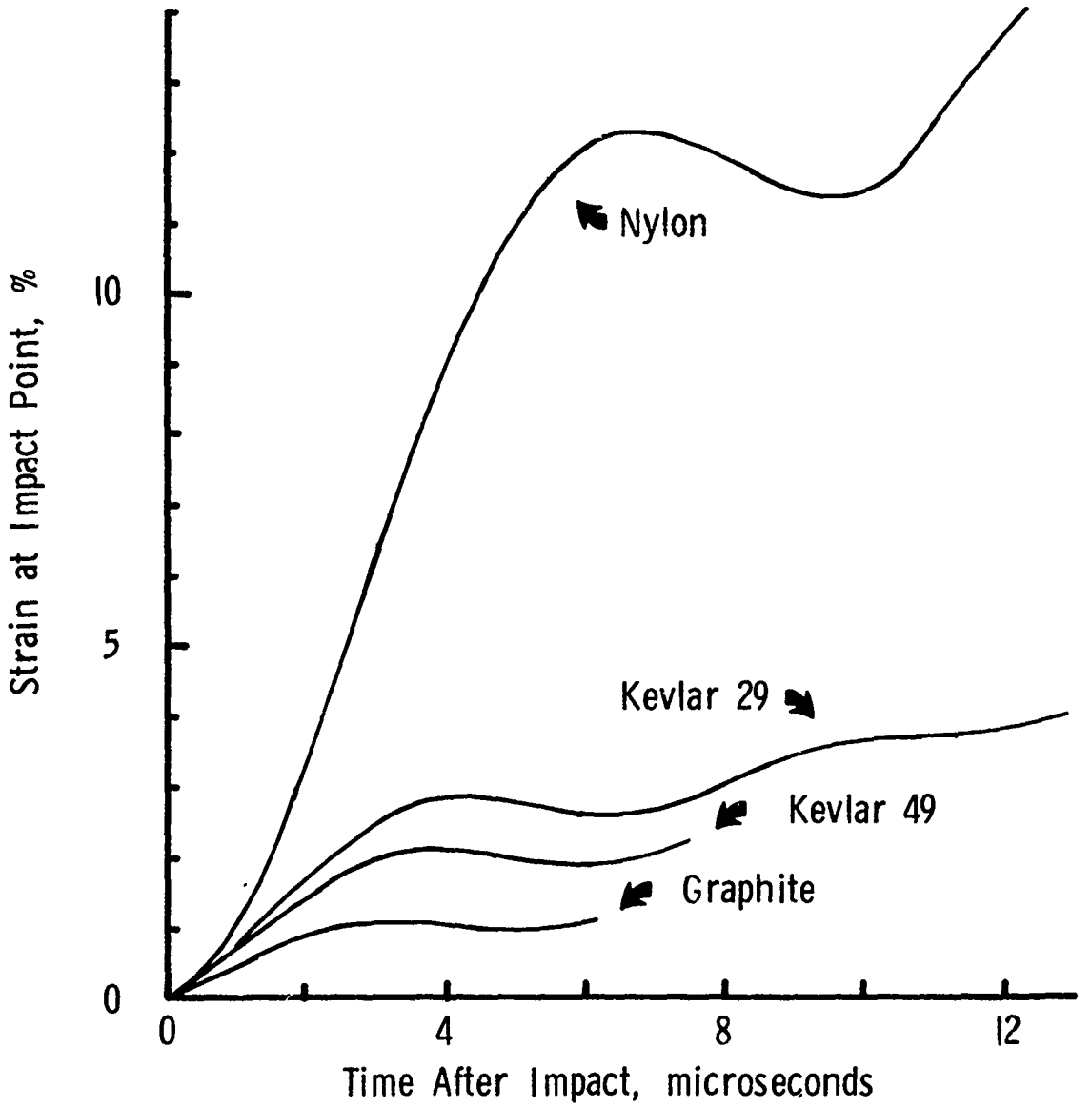

Figure 20. Development of strain at the point of impact in the various fabric types after a 400 m/sec impact.

If one normalizes the magnitudes of the ordinal values in Figure 20 by the value of strain which would be developed in a single fiber by transverse impact at the same projectile velocity, the strain magnitudes of the four curves achieve comparable values. This procedure essentially compensates the curves for the effect of the fiber modulus on the impact-induced strain.

The shift of the curves along the abscissa, however, is less clear. The rate at which the strain increases at the impact point is governed by the complex interactions of waves traveling about within the constantly expanding region of influence, and is beyond simple visualization. On average, the time necessary for a wave to reflect and return eventually to the impact point should decrease inversely with the wavespeed, i.e. inversely with the root of the modulus. However, the size of the region in which stress waves are traveling at any given time also depends on the wavespeed, and one would expect that a larger region of influence would decrease the rate at which reflected and diverted wavelets are able to return to the impact point.

It is found that the time after impact at which the first peak in the strain occurs varies linearly, with good correlation, with the fourth root of the fiber modulus (or the square root of the wavespeed). Using this observation, which is likely related to the geometry of the region of influence, one can compensate the abscissal values of Figure 20 by the factor $E^{0.25}$. The result of the ordinal and abscissal normalization is shown in Figure 21, where a curve valid for all four fabrics is developed.

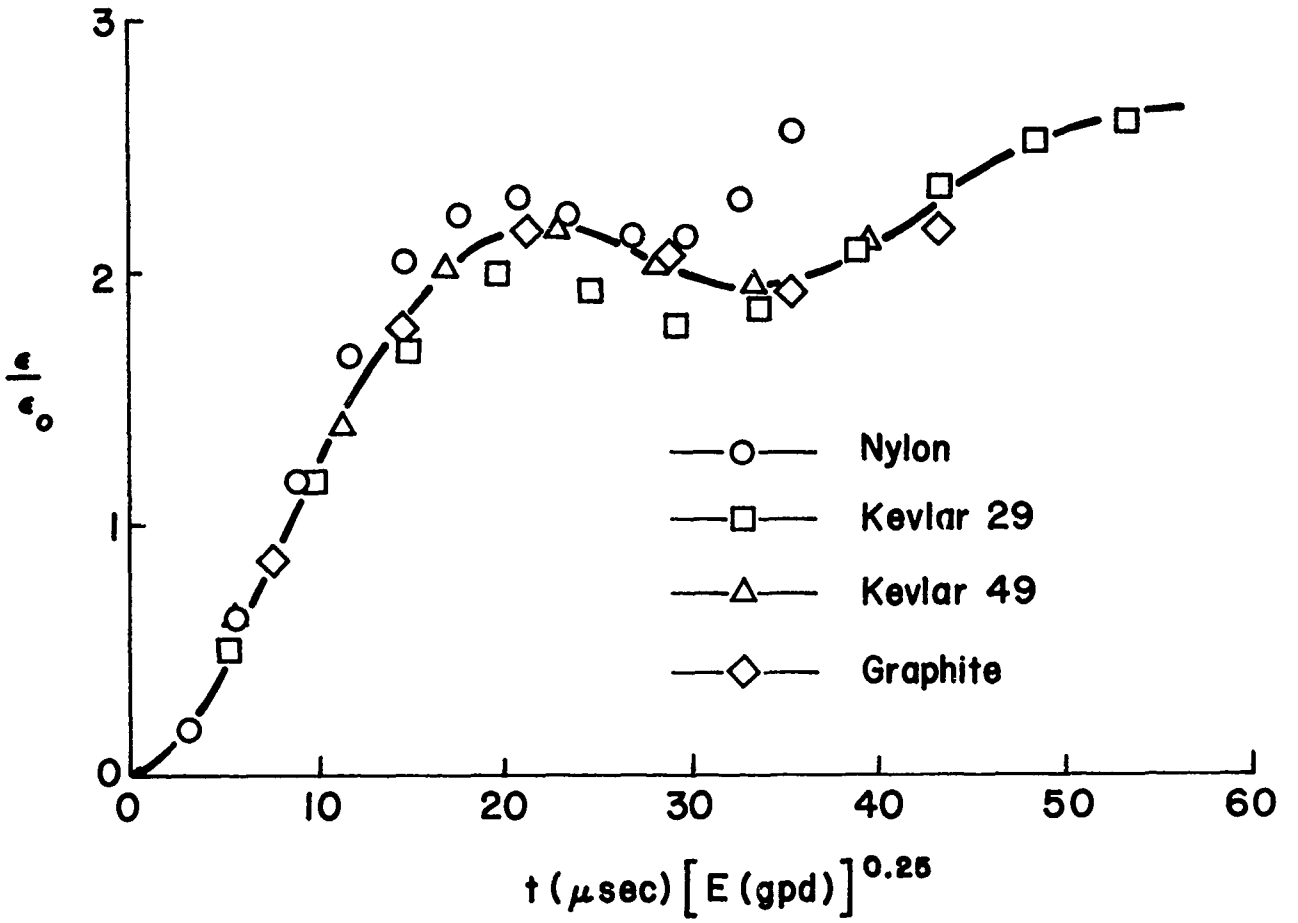

Figure 21. "Master" curve for impact-induced strain at the point of impact. Ordinal values represent strain normalized on the basis of the strain which would be generated in a single fiber by impact at the same velocity, while abscissal values are adjusted by a factor equal to the fourth root of the fiber modulus.

This master curve represents an improved means of performing preliminary armor design. Since the normalizing factors are known once the dynamic modulus of the fiber is specified, one can generate a strain vs. time curve from Figure 21 applicable for a particular fabric and impact velocity. The time for rupture is the time at which the impact-induced strain exceeds

the fiber's dynamic breaking strain. As in the fiber case, we then see that ballistic resistance is a balance between high fiber modulus leading to high wavespeeds and lower strains, and fiber breaking strain.

This approach is approximate in several respects, however, and is thus limited to preliminary design. First, it is seen in Figure 21 that perfect correlation among all four test fabrics is not attained, the nylon showing a deviation at high strain. Similar deviations in other fabrics might be observed as well. Second, the curve of Figure 21 was generated from computer experiments at relatively high velocity, so that projectile slowdown was not an appreciable factor. At low impact velocities, the fabric is able to decelerate the projectile and even bring it to rest. The effect of projectile slowdown is to generate unloading waves in the fabric which travel simultaneously with those previously described. This unloading would have a strong influence on the curves such as that in Figure 21, causing the curve to pass through a maximum and decrease thereafter in those cases in which the fabric is able to defeat the projectile. For these cases, complete treatment using the numerical code would be necessary.

III. EFFECT OF VISCOELASTIC MATERIALS RESPONSE

Viscoelastic Constitutive Relations

In the course of the iterative calculations described earlier, a constitutive material law must be evoked at each element in order to compute the element tension from its strain (or strain history). One would expect that a model incorporating viscoelastic effects would be necessary for proper simulation of polymeric materials, and in fact there is considerable direct evidence [16] that relaxation does indeed occur in the ballistic time frame. This is also to be expected in light of the dynamic mechanical spectrum of nylon, for instance, in which a beta relaxation is observed having an apparent activation energy of approximately 60 kJ/mole [17]; this relaxation is calculated to occur in approximately five microseconds at room temperature.

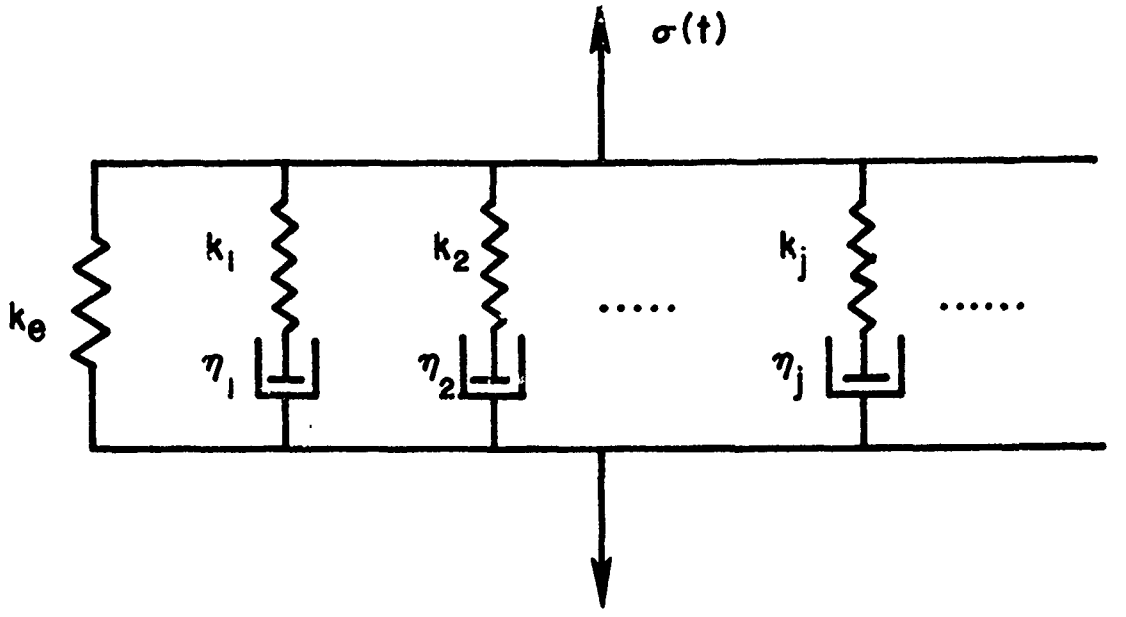

Figure 22. Wiechert spring-dashpot model for linear visco-elastic fiber response.

A general viscoelastic model well suited for computing tensions from prescribed strains is the Wiechert model, depicted schematically in Figure 22. This model takes the polymer response to be analogous to that of an array of Newtonian dashpots and Hookean springs. The differential tension-strain law for the jth arm of the model is

$$\dot{\epsilon} = \frac{1}{k_j} \dot{\sigma}_j + \frac{1}{\eta_j} \sigma_j \qquad (38)$$

where the dots indicate time differentiation, σ is the tensile stress and ϵ is the strain. Casting this equation in finite difference form relative to a discrete time increment Δt and solving:

$$\sigma_j^t = \frac{1}{[1+(\Delta t/\tau_j)]}\left[k_j(\epsilon^t - \epsilon^{t-1}) - \sigma_j^{t-1}\right] \quad (39)$$

where the superscripts t and t-1 indicate values at the current and previous times, respectively, and $\tau_j = \eta_j/k_j$ is a relaxation time for the jth arm. The total tension at time t is the sum of all the σ_j^t plus the tension in the equilibrium spring k_e:

$$\sigma^t = k_e\epsilon^t + \sum_j \frac{k_j(\epsilon^t - \epsilon^{t-1}) + \sigma_j^{t-1}}{1+(\Delta t/\tau_j)} \quad (40)$$

This tension-strain calculation is performed at each element node. In addition to storing all the k_j and τ_j, the computer must also store the previous strain and tension values at each node.

The choice of the k_j and τ_j should be such as to model the polymer viscoelastic response in a time

scale comparable to the ballistic event, which takes place on a microsecond time scale. It is of course difficult to conduct such conventional tests as creep or stress relaxation on this time scale, but guidance as to proper model parameter selection can be obtained from dynamic mechanical spectra, using the activation energies of the appropriate low-temperature relaxations to effect a temperature-rate conversion. For nylon fibers, for instance, one would fit the Wiechert model to the beta relaxation, ignoring the alpha and gamma relaxations as not being appropriate to the ballistic time scale at room temperature.

Results for Single Fibers

As a means of developing a proper context for the study of viscoelastic response of a woven textile panel, some results obtained in an earlier study [18] which used a direct numerical simulation of viscoelastic relaxation in a transversely impacted single fiber will be reviewed briefly. The numerical approach for this study was identical to that described for fabric structures, except that it considered a single fiber discretized as a series-connected assemblage of pin-jointed finite elements. As in the fabric case,

this treatment produced numerical values for the position, veloci y, strain, and tension of each finite element of fiber as a function of time after impact. A variation of this treatment will be described in some detail in Chapter IV of this report.

Figures 23 and 24 show the distribution of nondimensionalized strain and tension along the fiber at various times after impact, plotted against the Lagrangian fiber coordinate. These distributions were obtained from the Wiechert model using only a single spring-dashpot arm in parallel with the equilibrium spring; this three-element model is commonly known as the "standard linear solid", or the "Zener solid" The distributions for these two figures are for a choice of model parameters k_e = 80 gm/den, k_1 = 20 gm/den, and τ_1 = 50 μsec. The values of the ordinates have been normalized by the strain or tension which the rate-independent Smith theory predicts for a linear elastic material at the same impact velocity.

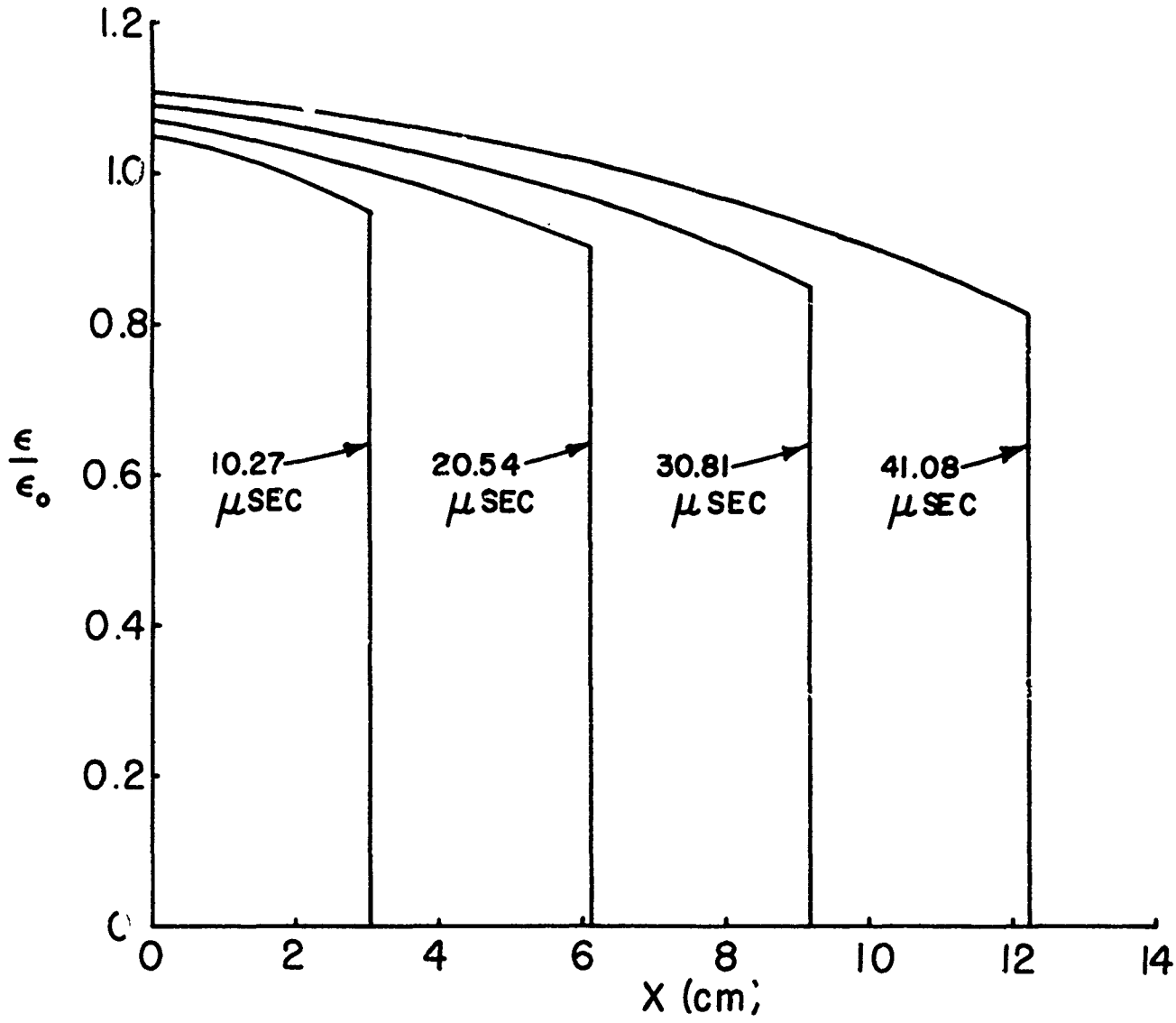

Figure 23. Normalized strain plotted against Lagrangian fiber coordinate for various times after impact.

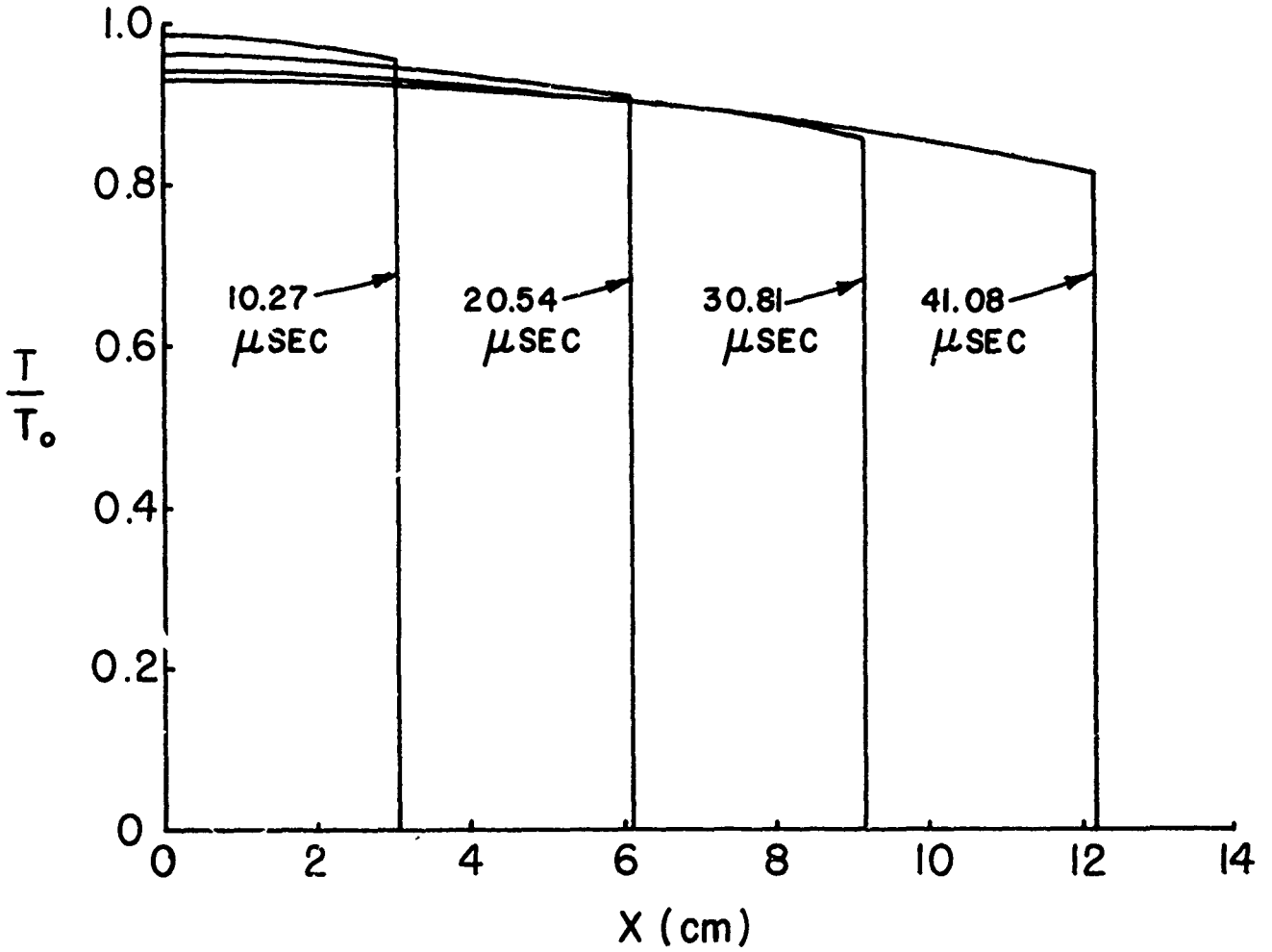

Figure 24. Normalized tension distribution along fiber.

The distributions in figures 23 and 24 demonstrate several features typical of viscoelastic wave propagation: the magnitude of the wavefront attenuates as it propagates along the fiber, the strain at a given position increases with time from its original value, and the tension decays with time. Smith [19] used the method of characteristics to show that the wavefront attenuation is given by:

$$T(ct,t) = T_o \exp(-\lambda t/2\tau) \quad (41)$$

$$\epsilon(ct,t) = \epsilon_o \exp(-\lambda t/2\tau) \quad (42)$$

where $\lambda = k_1/(k_1 + k_e)$ is the relative strength of the viscoelastic relaxation. The wavefront tension magnitude predicted by Equation 41 is shown in Figure 25, which also serves to illustrate the numerical accuracy of the direct analysis. (Here a 0.15 m fiber was divided into 200 finite elements). Some numerical overshoot is evident at the discontinuous wavefront, but the distribution extrapolates to the analytically-predicted value.

By means of Laplace transforms, Smith [20] also obtained approximate expressions for the strain and tension distributions in a longitudinally impacted fiber. These expressions predict that the tension and strain at the point of impact will approach the limiting values

$$T(0,\infty) = T_o\sqrt{(1-\lambda)} = 0.894\,T_o \quad (43)$$

$$\epsilon(0,\infty) = \epsilon_0 / \sqrt{(1-\lambda)} = 1.118\,\epsilon_0 \quad (44)$$

Where the numerical coefficients are for $\lambda = 0.2$. At x = 0, the distributions in Figures 25 and 23 approach limiting values greater than Equation 43 for tension and greater than Equation 44 for strain. Thus stress relaxation is slightly less and creep slightly greater for transverse impact than for longitudinal impact; Smith [19] reached this same conclusion in his work on transverse impact.

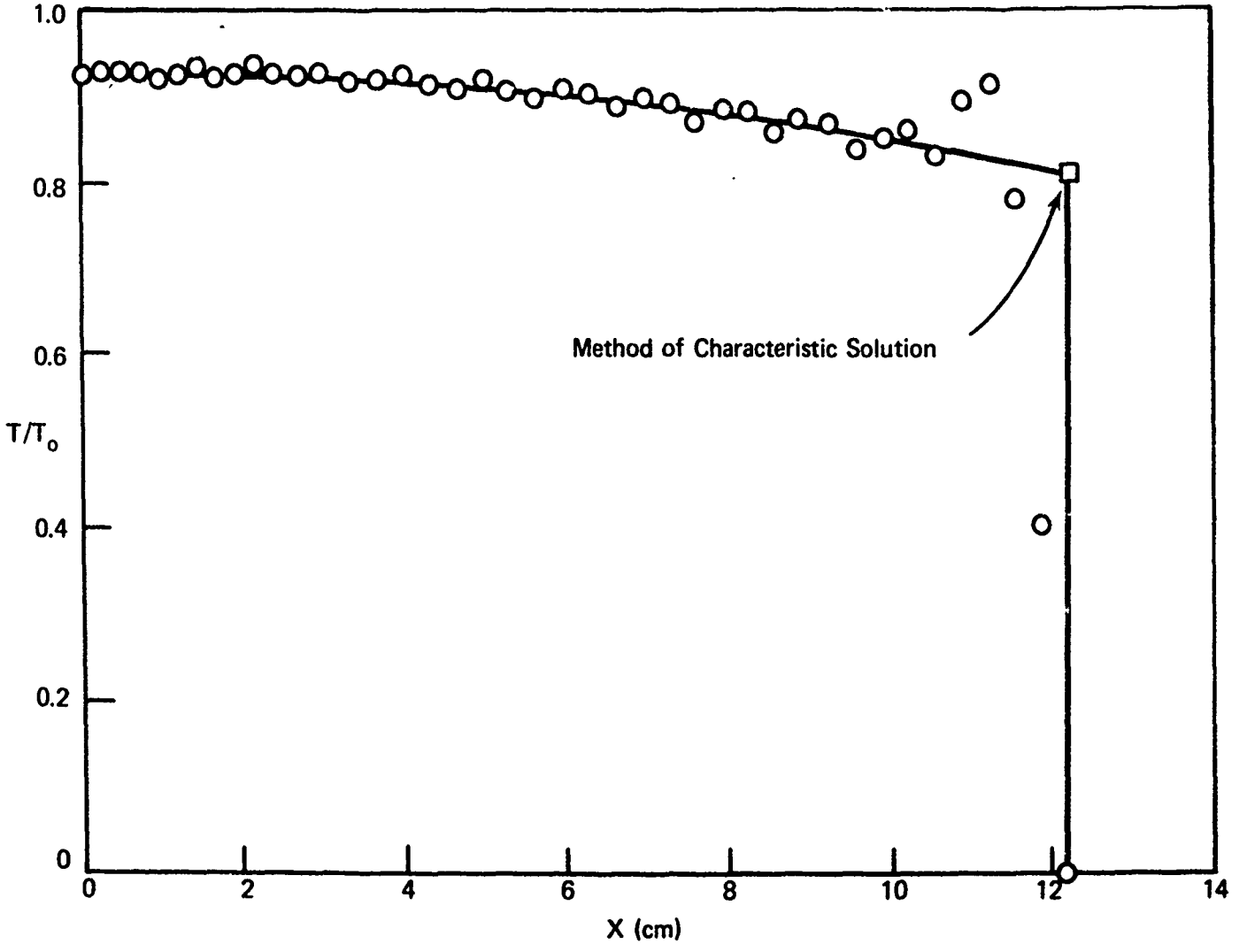

Figure 25. Numerical values for tension distribution for t = 41.08 microsec after impact.

Results for Woven Panels

The three-element Wiechert model (the standard linear solid) used in the previous section was also employed to examine the influence of viscoelastic relaxation during ballistic impact of woven panels. The model parameters were chosen to simulate ballistic nylon: k_1 = 20 gm/den, k_e = 80 gm/den, τ_1 = 5 μsec. Results have been obtained for a simulated 0.2 m x 0.2-m panel weighing 19.5 gm, impacted with a 0.22-caliber fragment simulating projectile weighing 1.10 gms at various impact velocities.

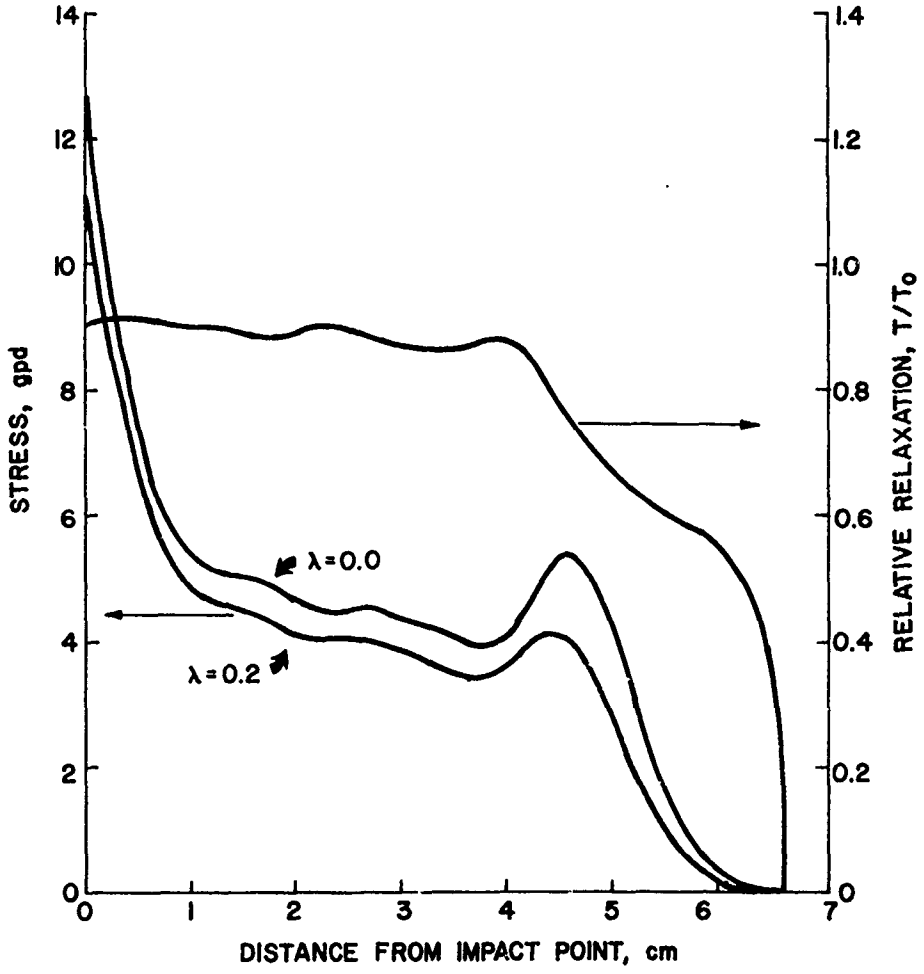

Figure 26. Stress distributions along orthogonal fibers running through impact point for linear elastic and viscoelastic fabrics (t = 30.4 microsec).

Figure 26 shows the distribution of stress along the orthogonal fibers running through the point of impact at t = 30.4 μsec after an impact at V_p = 300 m/sec. The results for the viscoelastic fabric are compared with those of an ideally elastic fabric having a stiffness equal to that of the unrelaxed viscoelastic material (100 gm/den). The nonuniform distributions along the fiber are due as described earlier to the continual reflection of wave components from fiber crossovers, resulting in a maximum in stress at the impact point. An appreciable difference in stress levels between the linear elastic and viscoelastic cases is observed, especially near the wavefront. Relaxation of the stress due to the rate-dependent material behavior may be expressed by the ratio of the viscoelastic and the elastic and the elastic stress, T/T_o, as shown in the figure. It is found that a large amount of relaxation occurs near the wave front while an equlibrium state of relaxation is reached in the region away from the disturbance front.

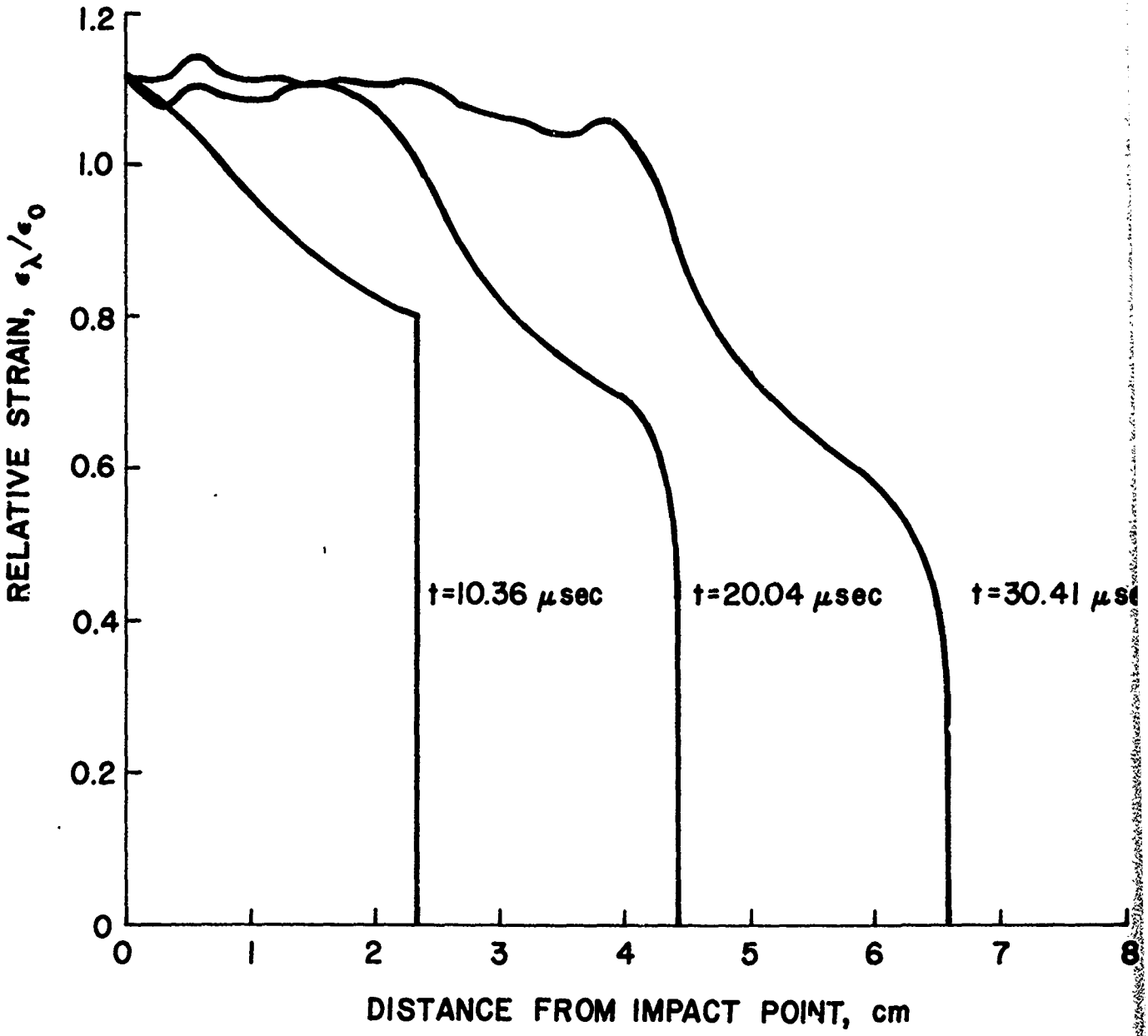

Figure 27. Distribution of strain along orthogonal fibers running through impact point.

The wave attenuation during this 300 m/sec impact is also demonstrated in Figure 27, where relative strain distributions ϵ/ϵ_0 are given for various times after impact. As illustrated in this figure, the magnitude of the wavefront attenuates significantly as it propagates along the orthogonal fibers, and the strain at a given position increases with time after impact from its original values.

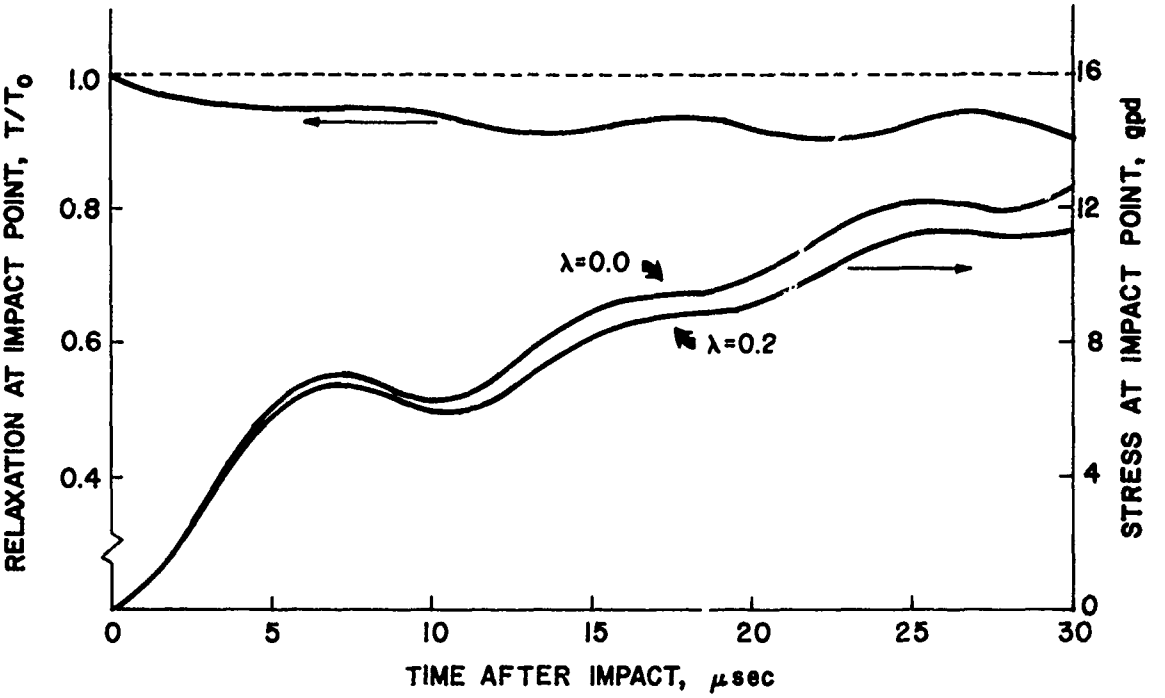

Figure 28. Stress histories at impact point for linear elastic and viscoelastic materials.

The stress and strain histories at the point of impact shown in Figure 28 give another indication of viscoelastic dissipation in the response of the panel. They increase continuously with time due to the reflection of wavelets from crossovers; however, stress relaxation and strain creep of the viscoelastic material occur simultaneously with this general increase. The viscoelastic stress at a given time is smaller than the elastic case as shown in the figure. The relative relaxation at the point of impact, denoted by the ratio of the viscoelastic and elastic case, develops gradually and reaches a steady state at long times. The relaxation histories for different missile striking velocities

are given in Figure 29. The similarity of their magnitudes is a manifestation of the linear material response. Again, these stresses approach an asymptotic equilibrium state at times longer than the characteristic material relaxation time.

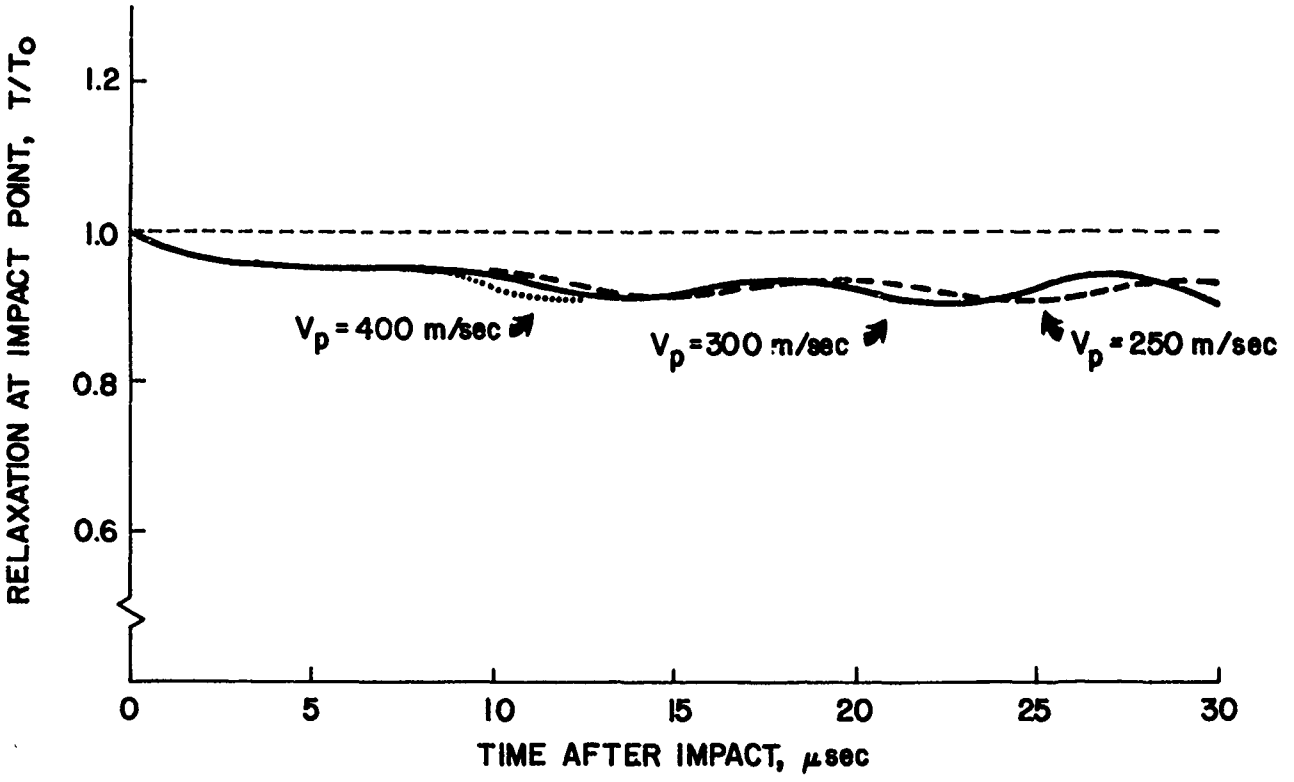

Figure 29. Stress relaxation at impact point for various impact velocities.

Nonlinear Viscoelastic Response

The use of the Wiechert model as described in the previous sections is sufficient to illustrate the most important features of rate-dependent ballistic materials. However, most materials do not meet the

rigid requirements of linearity necessary for a truly rigorous application of concepts of linear viscoelasticity. For more detailed simulations of fabric and fiber response, one must turn to general constitutive relationships which more accurately model the behavior of these materials. Unfortunately, there does not exist a general concensus of the most realistic means of achieving this goal. At present, the subject of nonlinear viscoelasticity is being pursued actively by several groups, several of which are employing highly divergent approaches to this problem. It is not possible here to select any single approach as having significantly greater merit than certain others.

However, the ease with which various constitutive laws may be incorporated into the direct analysis scheme makes it possible to assess relatively easily the influence of various assumed material models. As an illustration of this capability, some results using Eyring's model of thermally-activated nonlinear viscoelasticity will be presented.

The computationally-convenient Wiechert model can be extended to include the effect of material nonlinearity by rendering the springs and/or the dashpots nonlinear. If, for instance, one uses a power-law spring and a nonlinear Eyring dashpot [21], defined as

$$\sigma_{spring} = k\epsilon^b \quad , \quad \sigma_{dashpot} = A \sinh(\alpha\sigma) \tag{45}$$

then the finite-difference equation relating tensions and strains in the jth arm of the model is:

$$\frac{\epsilon^t - \epsilon^{t-1}}{\Delta t} = \frac{1}{b_j k_j}\left(\frac{\sigma_j^t}{k_j}\right)^{\frac{1}{b}-1}\left(\frac{\sigma_j^t - \sigma_j^{t-1}}{\Delta t}\right) + A_j \sinh(\alpha_j \sigma_j^t) \tag{46}$$

A relation such as this requires an iterative numerical solution for σ_j^t at each element and at each time step; the computer effort is increased but the principles of the impact algorithm are straightforward. The principal obstacle to the use of nonlinear models in the direct analysis is not the incorporation of the models into the computational scheme, but rather the determination of the material parameters (the b's, k's, A's, and α's in Equation 46) applicable to the microsecond time scale of polymer relaxations.

To illustrate the effect of nonlinear constitutive models on panel ballistic response, a series of computer experiments was performed on three different simulations of nylon fabric: one using only linear elastic response

(only the equlibrium spring in the Wiechert model), one using the standard linear solid model for linear viscoelastic response (the equilibrium spring plus one spring-dashpot arm), and the last being a standard linear solid but with the dashpot made a nonlinear Eyring element. The intial modulus was taken as 100 gm/den, the relaxed modulus as 80 gm/den, and the relaxation time for the standard linear solid as five μsec (the same as in the previous section). The concept of relaxation time (the time to complete 63.2% of the total relaxation) has no meaning for the nonlinear element, since the rate of relaxation changes nonlinearly with the stress. Lacking any experimental data in this time scale, the A and α were arbitrarily chosen so as to cause relaxation in approximately the same time scale as the standard linear solid. A and α were set at 10^3 sec $^{-1}$ and 0.7 den/gm,respectively. The nonlinear constitutive equation was solved at each element using Muller's method [22], which increased the computation time relative to that of the standard linear solid by roughly one-third.

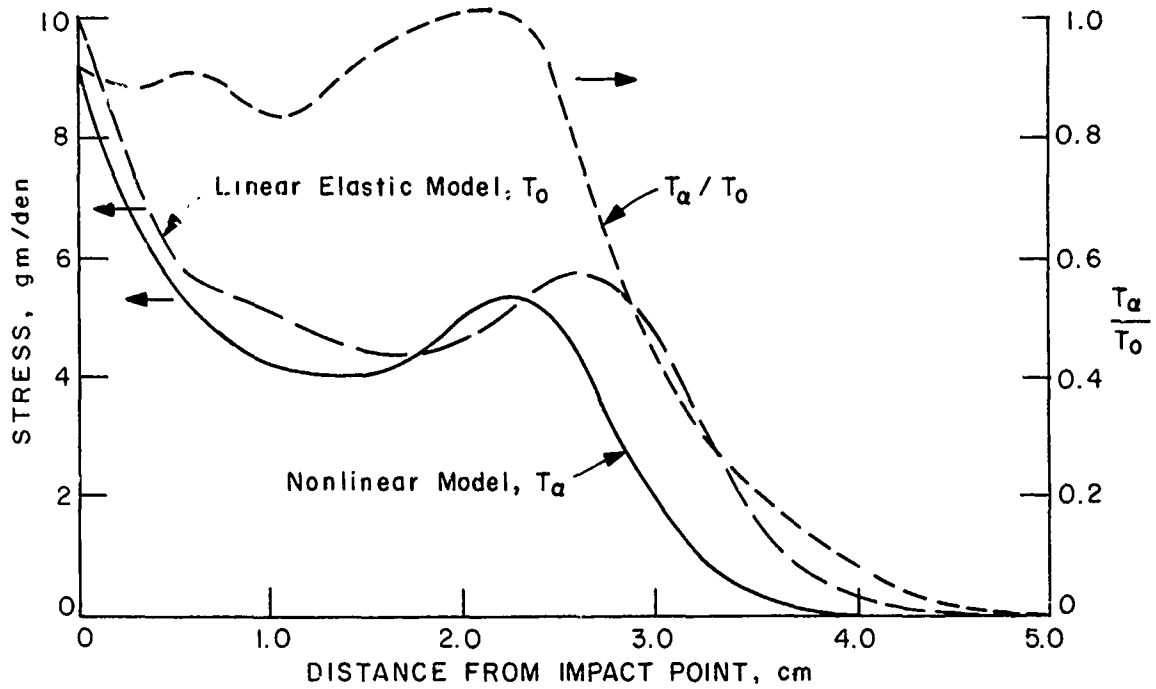

Figure 30. Stress distributions along orthogonal fibers running through impact point for linear elastic and nonlinear viscoelastic fabrics.

One means of comparing the various constitutive models is in terms of the distributions of strain along the orthogonal fibers running through the impact point, at various times after impact. Figure 30 shows the distributions for the elastic and nonlinear viscoelastic materials 20 μsec after a 300-m/sec impact. Also shown is the ratio between the nonlinear and the elastic cases. This ratio is a measure of the stress relaxation in the fabric; it is greatest at the wave-front, as the large gradient of strain there produces a similarly large rate of relaxation.

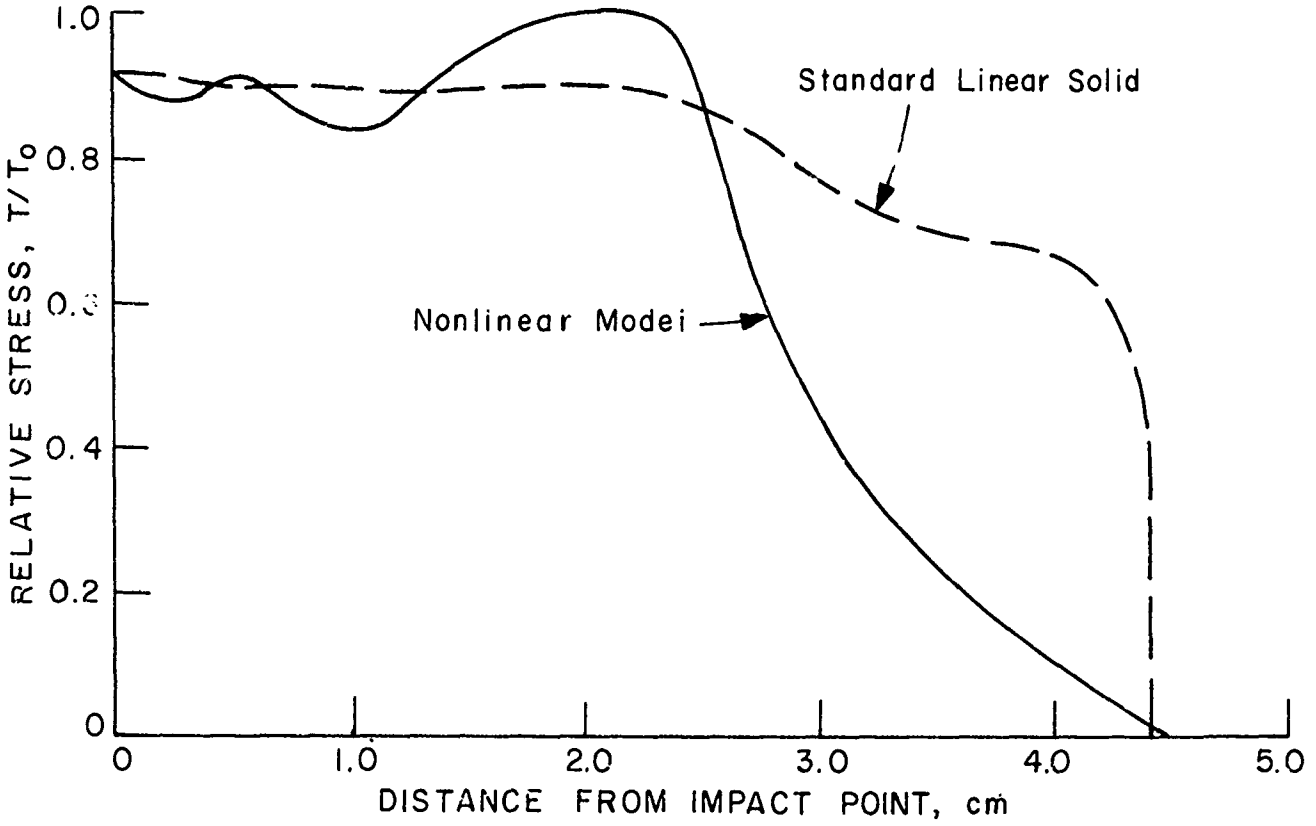

Figure 31. Comparison of stress relaxation in linear and nonlinear viscoelastic fabrics.

The nonlinear stress relaxation is compared in Figures 31 to that produced by the standard linear solid. Although the equilibrium value far from the wavefront is approximately the same in both cases, strong differences are evident near the wavefront. These are due to the relatively more rapid response to higher strain gradients in the nonlinear material. Another indicator of viscoelastic fabric response is the stress at the point of impact. The stress and strain at the impact point increase with time due to the continual arrival there of wavelets reflected from fiber cross-overs, but in viscoelastic materials both stress relax-

ation and creep strain are superimposed on this overall increase. In Figure 32 the point-of-impact stress histories for the three materials are plotted, as well as the stress relaxation ratio defined as before as the ratio between the viscoelastic and elastic stress. As in the earlier two figures, the linear and nonlinear viscoelastic models approach essentially identical equlibirum values at long times, but are markedly different near the wavefront due to the more rapid response of the nonlinear material to large gradients.

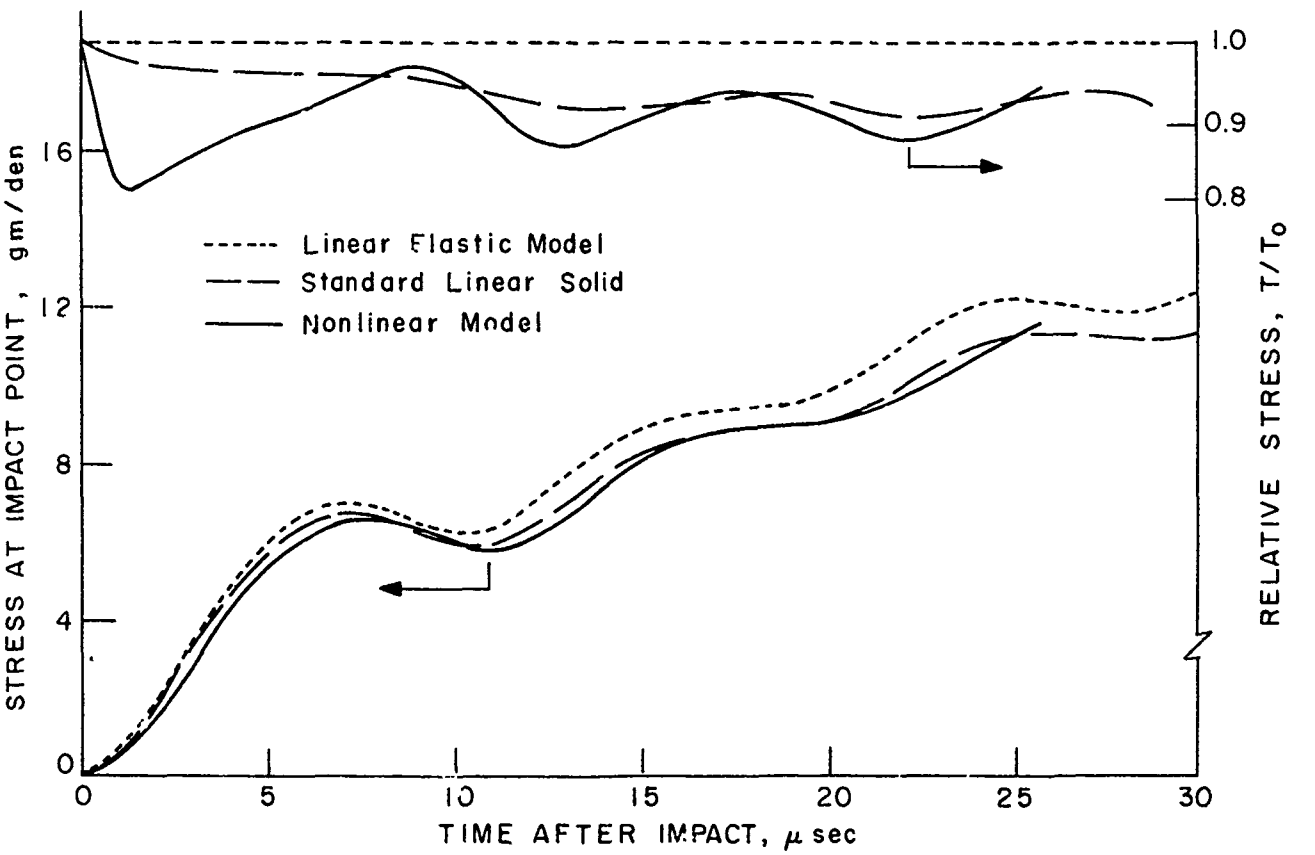

Figure 32. Stress histories at impact point for linear elastic, linear viscoelastic, and nonlinear viscoelastic fabrics.

IV. NUMERICAL ANALYSIS OF WAVE PROPAGATION IN TWO CROSSED FIBERS

Introduction

This chapter describes study of the dynamics of a special but highly important physical system: that of two fibers, one having been transversely impacted at zero obliquity by a high-speed projectile, and the other crossing the first perpendicularly at some distance from the impact point. This system is germane to the understanding of impact and wave propagation phenomena in woven textile panels used for ballistic protection. The wave propagation phenomena occurring at the fiber crossover have a strong influence on the response of a woven panel to impact, since these panels typically have on the order of forty crossovers per inch. The nature of these crossover interactions may be one of the factors causing what appears to be an excellent fiber in single-fiber ballistic tests to exhibit less ballistic protection when woven into a textile panel structure than a nominally inferior fiber. As mentioned earlier, this situation obtains in the case of the Kevlar ballistic protection vests now being used by military and police personnel: the Kevlar vest outperforms the older nylon vest, in spite of

nylon's having a higher transverse critical velocity. The inability to predict vest performance from single-fiber test data is a matter of considerable concern to the armor design community, and this study of fiber crossover dynamics was begun to clarify this situation.

Method of Solution

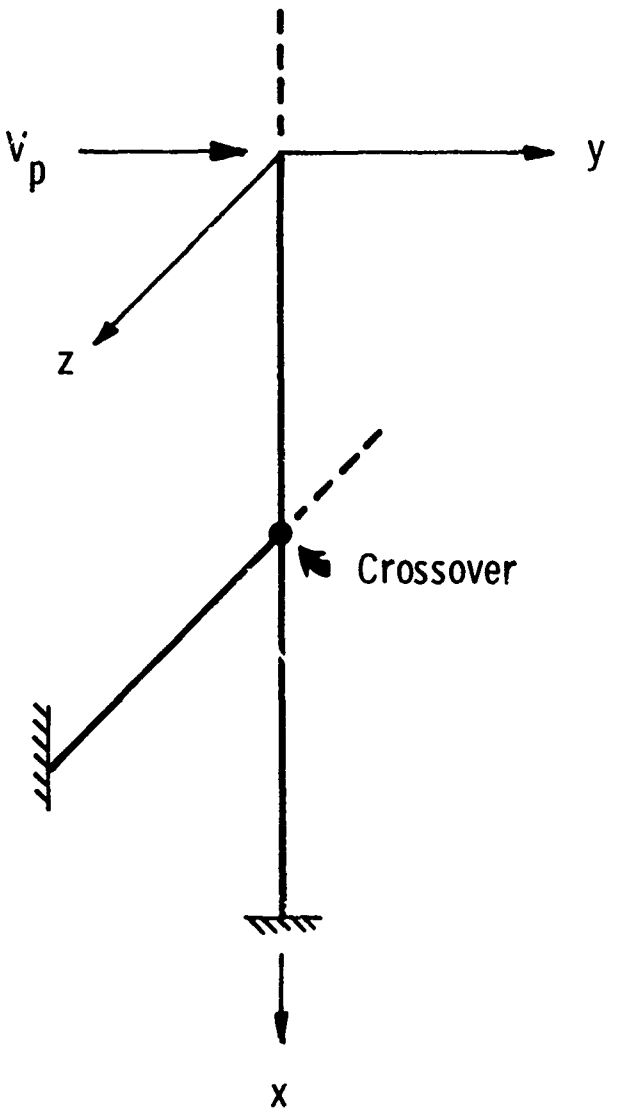

Figure 33. Schematic of model for numerical analysis of two crossed fibers.

System Idealization. The system of two crossed fibers is modeled as in Figure 33, where the origin of coordinates is placed at the midpoint of the clamped primary fiber, which extends along the x-axis. The projectile moves along the y-axis only, and impacts the primary fiber at the origin. From symmetry, only half the primary fiber need be considered. The secondary fiber extends along the z-axis and intersects the primary fiber at some arbitrary distance from the origin. At the crossover point, the secondary fiber is assumed to follow the motion of the primary fiber in the direction perpendicular to the primary fiber (in the x-y plane), but is allowed some measure of slip in the direction parallel to the primary fiber. Motion of the primary fiber is assumed to occur in the x-y plane only, while the secondary fiber may move in all three directions.

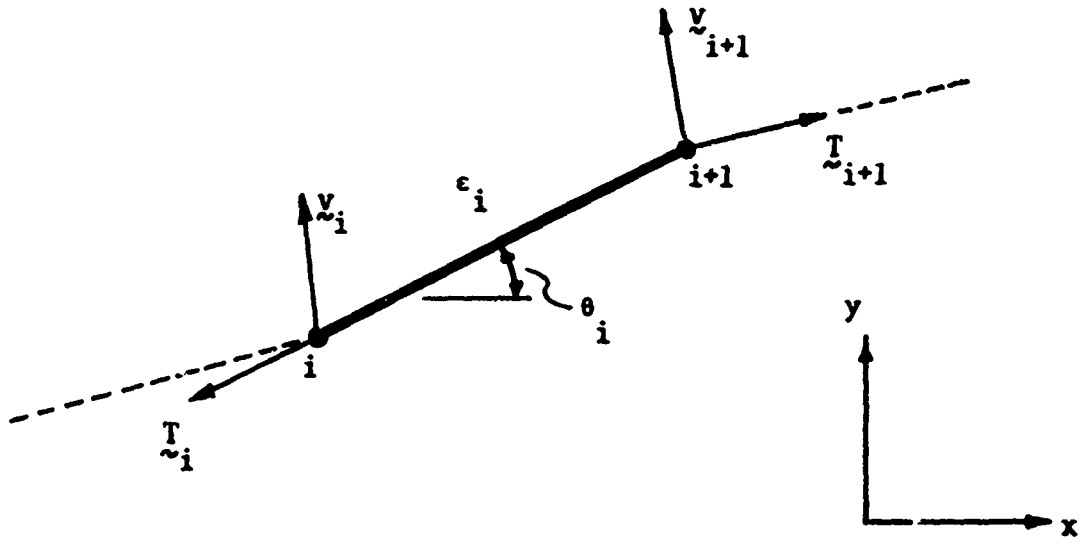

Figure 34. Discrete element of fiber.

To proceed, the fibers are discretized as a series of n pin-jointed finite elements of equal length as shown in Figure 34. The masses of the elements are taken to be lumped at the nodal end points of these elements, and at these nodes are defined vector coordinates $\underset{\sim}{x}_i$, velocity $\underset{\sim}{v}_i$, and tension $\underset{\sim}{T}_i$. The scalar strain ϵ_i at each element will be computed from the coordinates of the nodes at either end of the element. The tension $\underset{\sim}{T}_i$ has the same direction as the element itself (approximating the element's assumed inability to support a bending moment), while $\underset{\sim}{v}_i$ is not constrained in direction. These elements are now described as in the fabric analysis by simple governing equations: impulse-momentum balance, strain-displacement relation, constitutive relation, etc. These relations are cast as a recursive algorithm for proceeding from one element to the next along the fiber length, and then repeating the process at a new increment of time. The computer solution thus is referenced to a Lagrangian frame of reference attached to and extending with the fiber, which effectively reduces the problem to one dimension.

Momentum Balance. A consideration of impulse-momentum balance at the $i + 1^{st}$ node provides a means of computing the current velocity at that node in terms

of its velocity in the previous time increment and the tensions acting on it during that time increment. (In the follc ing, subscripts on a variable refer to the node at which it is defined ,while superscripts t and t-1 refer to values at the current and previous times respectively). The impulse-momentum balance can be written in finite difference form as

$$\Sigma \underset{\sim}{T} = \Delta m \, \frac{\Delta \underset{\sim}{v}}{\Delta t} \tag{47}$$

$$\underset{\sim}{T}^{t-1}_{i+1} - \underset{\sim}{T}^{t-1}_{i} = \frac{\Delta m}{\Delta t} \left(\underset{\sim}{v}^{t}_{i+1} - \underset{\sim}{v}^{t-1}_{i+1} \right) \tag{48}$$

Letting $A = \Delta m / \Delta t$, a fixed parameter, equation 48 may be solved for $\underset{\sim}{v}^{t}_{i+1}$:

$$\underset{\sim}{v}^{t}_{i+1} = \underset{\sim}{v}^{t-1}_{i+1} + A \left(\underset{\sim}{T}^{t-1}_{i+1} - \underset{\sim}{T}^{t-1}_{i} \right) \tag{49}$$

This vector expression can be written in scalar form by reference to the inclination angles θ_i and θ_{i+1} of the $\underset{\sim}{T}_i$ and $\underset{\sim}{T}_{i+1}$ vectors respectively:

$$\theta^{t-1}_{i} = \mathrm{Tan}^{-1} \frac{y^{t-1}_{i+1} - y^{t-1}_{i}}{x^{t-1}_{i+1} - x^{t-1}_{i}} \tag{50}$$

$$\Theta_{i+1}^{t-1} = \tan^{-1} \frac{y_{i+2}^{t-1} - y_{i+1}^{t-1}}{x_{i+2}^{t-1} - x_{i+1}^{t-1}} \tag{51}$$

Then the x and y components of velocity are:

$$u_{i+1}^{t} = u_{i+1}^{t-1} + A\left(T_{i+1}^{t-1}\cos\theta_{i+1}^{t-1} - T_{i}^{t-1}\cos\theta_{i}^{t-1}\right) \tag{52}$$

$$v_{i+1}^{t} = v_{i+1}^{t-1} + A\left(T_{i+1}^{t-1}\sin\theta_{i+1}^{t-1} - T_{i}^{t-1}\sin\theta_{i}^{t-1}\right) \tag{53}$$

where $T = |\underset{\sim}{T}|$ is the tension magnitude. The boundary conditions are easily incorporated into the impulse-momentum balance: at the first mode, the velocity is set equal to the current projectile velocity ($\underset{\sim}{v}_1^t = V^t$), and at the clamp the velocity is set to zero ($\underset{\sim}{v}_n^t = 0$).

Strain-displacement Relation. Having computed the velocities at the i^{th} and $i+1^{st}$ nodes, the strain in the element between these nodes is computed as

$$\Delta\epsilon_i = \frac{L_i^t - L_i^{t-1}}{L_i^{t-1}} \tag{54}$$

where L_i is the element length. Continuing:

$$\epsilon_i^t = \epsilon_i^{t-1} + \frac{L_i^t}{L_i^{t-1}} - 1 \tag{55}$$

where

$$L_i^{t-1} = \left| \underset{\sim}{x}_{i+1}^{t-1} - \underset{\sim}{x}_i^{t-1} \right| \tag{56}$$

and

$$L_i^t = \left| \underset{\sim}{x}_{i+1}^t - \underset{\sim}{x}_i^t \right| \tag{57}$$

$$= \left| \left(\underset{\sim}{x}_{i+1}^{t-1} + \underset{\sim}{v}_{i+1}^t \Delta t \right) - \left(\underset{\sim}{x}_i^{t-1} + \underset{\sim}{v}_i^t \Delta t \right) \right|$$

Constitutive Relation. Knowing the strain ϵ_i^t, the tension magnitude T_i^t is computed from the material's dynamic stress-strain law. These relations are as described earlier, and currently available constitutive models include linear elastic, nonlinear elastic (cubic

polynomial and exponential strain hardening), linear viscoelasticity (Wiechert model), and nonlinear viscoelasticity (Eyring model).

Computation of New Projectile Velocity. The algorithm described above proceeds from one element to the next along the length of fiber, and is started by imposing the initial projectile velocity on the first node. At the end of the first time increment, a strain will have developed in the first element due to the velocity difference between the first and second nodes. (Initially, all velocities, tensions, and strains are set to zero.) This strain produces a tension as calculated from the constitutive relation, and this tension produces a velocity in the second node beginning at the next time increment.

After each time increment, at the completion of the lengthwise recursive calculations, a new projectile velocity v_p^t can be computed by means of a momentum balance using the tension at the first node:

$$-zT_y = M_p \frac{\Delta v_p}{\Delta t} = M_p \frac{v_p^t - v_p^{t-1}}{\Delta t} \qquad (58)$$

where M_p is the projectile mass, T_y is the component of fiber tension in the projectile travel direction, and the factor 2 accounts for the other half of the primary fiber extending in the -x direction. T_y is:

$$T_y = T_1^t \cos\theta_1^t = T_1^t \cos\left\{\tan^{-1}\frac{y_{s1}^t - y_{s2}^t}{x_1^t - x_2^t}\right\} \quad (59)$$

Crossover Fiber Calculations. Computation of field variables along the secondary fiber proceeds in a lengthwise manner exactly as described above, although the vector resolutions become slightly more complicated due to the motion in three rather than two dimensions. The secondary algorithm is started by imposing on the first node of the crossover fiber the velocity imparted to it by the primary fiber. As stated earlier, the secondary fiber is allowed a measure of slip along the primary fiber but is constrained to follow it in the direction normal to the primary fiber. Denoting the node on the primary fiber nearest the crossover point as ix, the velocity of this node resolved in directions parallel and perpendicular to the primary fiber there

are:

$$v^t_{para} = u^t_{ix} \cos\theta^t_{ix} + v^t_{ix} \sin\theta^t_{ix} \tag{60}$$

$$v^t_{perp} = v^t_{ix} \cos\theta^t_{ix} - u^t_{ix} \sin\theta^t_{ix} \tag{61}$$

$$\theta^t_{ix} = \tan^{-1} \frac{y1^t_{ix} - y1^t_{ix-1}}{x1^t_{ix} - x1^t_{ix-1}} \tag{62}$$

In equation 62, the notation of the form y1 or y2 indicates field variables for the primary and secondary fibers, respectively. The velocity imposed on the first (crossover) node of the secondary fiber is:

$$u2^t_1 = \alpha_s v^t_{para} \cos\theta^t_{ix} - v^t_{perp} \sin\theta^t_{ix} \tag{63}$$

$$v2^t_1 = \alpha_s v^t_{para} \sin\theta^t_{ix} + v^t_{perp} \cos\theta^t_{ix} \tag{64}$$

$$w2^t_1 = 0 \tag{65}$$

where α_s is a slide factor which permits no sliding when set to 1 and unrestrained sliding when set to zero.

The crossover node ix will change with time if the tangential slip along the primary fiber is sufficient. After each time increment, a new position of the first node on the secondary fiber is computed, and ix is assigned to the nearest node on the primary fiber.

The momentum-balance calculation of $\underset{\sim}{v}^t_{i+1}$ in the primary fiber must be modified when the $i+1^{st}$ node is also the crossover node ix, since the secondary fiber applies its own tension to that node. Denote the direction angles of the primary and secondary fibers at that node as $\phi 1_x, \phi 1_y, \phi 1_z$ and $\phi 2_x, \phi 2_y, \phi 2_z$, respectively, ($\phi 1_z = 0$). Then the components of tension applied by the secondary fiber, resolved along directions parallel and perpendicular to the primary fiber, are:

$$Tz^t_{para} = Tz^t_1 \left[\cos \phi 2_x \cos \phi 1_x + \cos \phi 2_y \cos \phi 1_y\right] \quad (66)$$

$$Tz^t_{perp} = Tz^t_1 \left[\cos \phi 2_y \cos \phi 1_x - \cos \phi 2_x \cos \phi 1_y\right] \quad (67)$$

where the direction cosines are computed from the current nodal coordinates. The primary fiber is allowed to feel the impulse of the perpendicular component fully, but the parallel component is reduced by the slide variable α_s. The usual computation of $\underset{\sim}{v}^t_{i+1}$ is the adjusted as

$$u1^t_{i+1} \leftarrow u1^t_{i+1} + ZA\left[TZ^t_{perp}\cos\phi 1_y + \alpha_s TZ^t_{para}\cos\phi 1_x\right] \quad (68)$$

$$v1^t_{i+1} \leftarrow v^t_{i+1} + ZA\left[TZ^t_{perp}\cos\phi 1_x + \alpha_s TZ^t_{para}\cos\phi 1_y\right] \quad (69)$$

where the $\leftarrow$ symbol indicates a computer replacement operation; i.e. the additional impulse from the secondary fiber is added to that already computed from equations 63 and 64.

Stability, Accuracy, and Efficiency. Criteria for stability and accuracy of the above method are related as in the fabric case to the theory of characteristics for hyperbolic systems of partial differential equations and are similar to those for finite-difference solutions of wave propagation problems [14]. Given a wave equation of the form

$$\partial^2 u / \partial t^2 = c^2 \left(\partial^2 u / \partial x^2 \right) \tag{70}$$

which is to be solved by approximating ∂t and ∂x by finite differences Δt and Δx, a stability ratio α can be defined as

$$\alpha = c \Big/ \left(\frac{\Delta x}{\Delta t} \right) \tag{71}$$

The finite difference scheme is stable and accurate for $\alpha = 1$, stable but increasingly inaccurate for $\alpha < 1$, and unstable for $\alpha > 1$. The choices for Δx and Δt are thus not independent, but are related by the wavespeed for the choice of $\alpha = 1$.

In the direct analysis of the fibers described above, this stability criterion is equivalent to adjusting the rate of march of the computer solution along the fiber to match the rate of propagation of the strain wave. Conceptually, this requirement is related to the necessity of programming the finite governing equations so as to model the actual continuous dynamic process as accurately as possible. If a major disturb-

ance - such as the passage of a strain wave with its accompanying energy input - takes place in a finite element which is not considered explicitly in the computational scheme, divergent numerical results are very likely.

Once a stable computational scheme has been developed, one usually attempts to increase its accuracy to whatever limit is desired by decreasing the size of the elements; i.e. by increasing the number of nodes. Since for $\alpha = 1$ a decrease in Δx requires a corresponding decrease in Δt, the computation time - and therefore the expense - required for analysis of a given impact event increases as the square of the number of nodes. The element size is therefore chosen so as to balance the conflicting requirements of economy and accuracy. As an example of computation time, the CPU requirement for the IBM 370/168 system was 0.168 minutes for a problem in which the strain wave propagated 0.2 m along the primary fiber and 0.1 along the secondary fiber, with a length increment of 2.0 mm. As a means of improving code efficiency, the program employs logical flags which terminate the length loop computation when the computer passes the point along the fiber length corresponding to the wavefront.

Accuracy assessment for the case of two crossed fibers is difficult, since no experimental or closed-form mathematical analysis of this problem is available, but some assurance of accuracy is derived from computer runs in which the secondary fiber is placed at the origin (the impact point). In this case, response of both the primary and secondary fibers is found to be that predicted by independent analyses. Data such as that previously presented in Figure 23 is obtained along the primary and secondary fibers. In certain cases to be discussed below, the numerical overshoot and oscillation observed near wavefronts cause problems in interpretation of results. These oscillations are a result of the inability of the discrete difference equations to model discontinuities accurately. Although the method is conditionally stable and the oscillations are damped out away from the discontinuity, problems of interpretation remain near the discontinuity. The oscillation at the wavefront is diminished by the material viscosity, and in some cases an "artificial" viscosity may be included solely for the purpose of smoothing the numerical results.

Results and Discussion

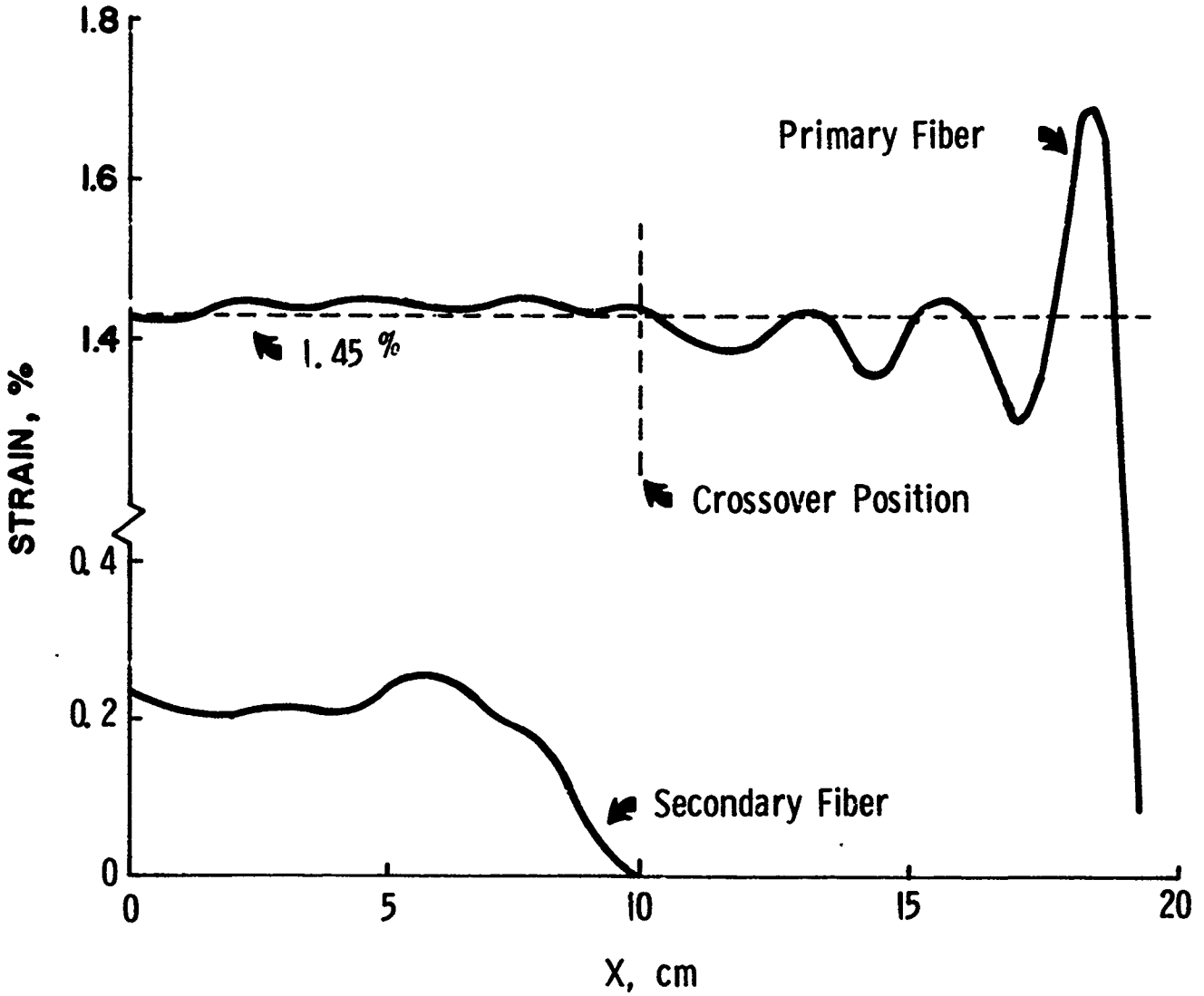

Figure 35. Strain distributions in two crossed fibers of Kevlar 29, 28.7 microsec after impact at 400 m/sec.

Figure 35 shows typical results obtained from the above described computer treatment, in this case for two crossed fibers of Kevlar 29, the crossover point being 10 cm along the primary fiber from the impact point. The fibers were assumed to respond elastically, and no sliding was permitted at the crossover (α_s=1).

The figure shows the distribution of strain in each fiber 28.7 μsec after impact at 400 m/sec, where the abscissa measures the distance along the secondary fiber from the crossover point. The dotted line at strain = 1.45% depicts the level of strain which would be generated in a single fiber at this impact velocity. In this example no viscosity has been included, and the large overshoot at the wavefront causes problems in interpretation of results. In spite of this oscillatory behavior, however, an increase in strain in the primary fiber behind the crossover due to the wavelet reflected from the crossover is evident, as is a reduction in the strain intensity in the region of the primary fiber beyond the crossover. More easily measured is the level of strain intensity propagated along the secondary fiber.

Computer experiments were conducted on the crossover system for a range of fiber moduli and slide factors, and graphical output similar to Figure 35 used to determine coefficients of wave reflection, transmittance, and diversion. These coefficients are defined as that fraction of the outward-propagating strain wave which is reflected backwards by the crossover, the fraction which passes through the crossover and continues its outward propagation, and the fraction which is diverted and begins propagating along the fiber passing

transversely through the crossover. As a means of obtaining these coefficients in spite of the uncertainties caused by the numerical fluctuations near the wavefronts, the computer was asked to determine the average strain level over a portion of the fiber length away from the oscillation region. In order to guarantee conservation of energy, the sum of the squares of the above three coefficients should equal unity; this was in fact obtained and offers some assurance as to the accuracy of the numerical values.

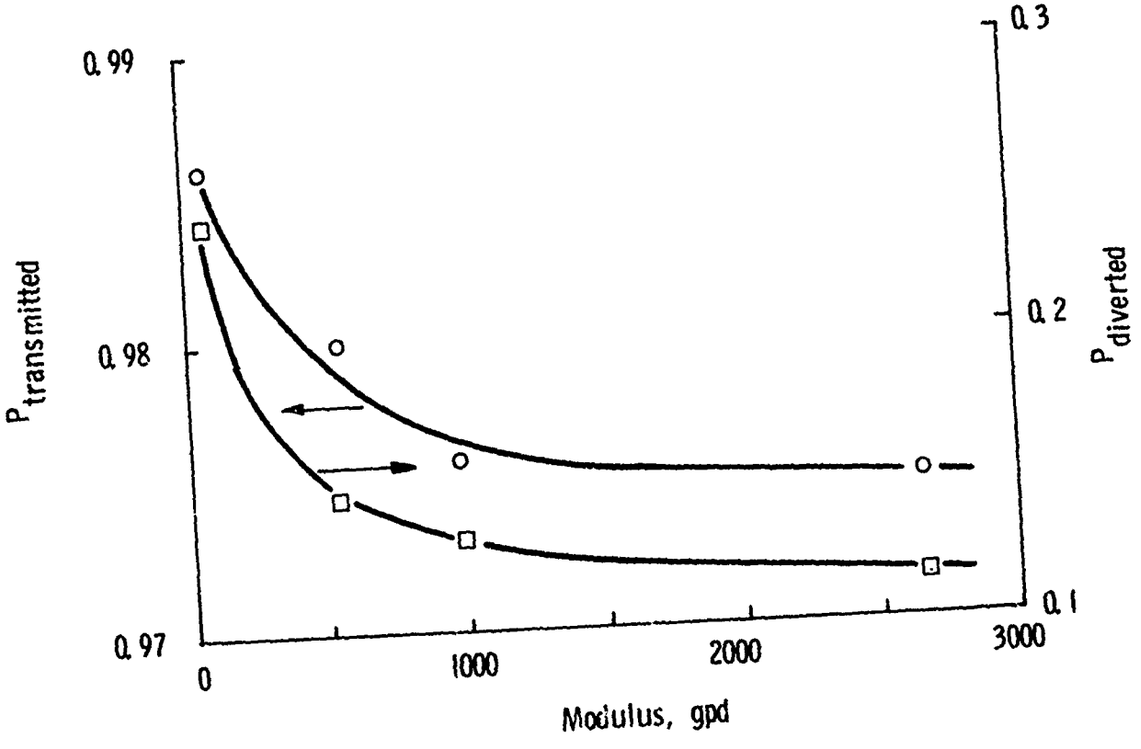

Figure 36. Influence of the fiber modulus on the fraction of stress wave intensity which is transmitted through a fiber crossover, in the absence of fiber-fiber sliding.

The variation in the transmission and diversion coefficients with fiber modulus is shown in Figure 36. The coefficient of reflection was near 1% over this range of moduli, but showed considerable scatter. It is seen that the diversion coefficient is of a much larger magnitude than the reflection coefficient, and that it varies more strongly with the fiber modulus. The major portion of the crossover influence on wave propagation is thus ascribed to diversion rather than reflection.

This observation is of significance, since an approximate treatment of fabric impact by Freeston and Claus [23] sought to predict the increase of strain at the impact point by considering wave propagation along a single fiber which reflects a certain portion of the outward-propagating wave at a series of discrete points along its length. The analysis is then reduced to a bookkeeping procedure in which one keeps track of inward and outward-propagating waves in each of the elements between these reflection points. This scheme leads to a very simple computer code and one would hope that it could provide at least approximate guidance in design.

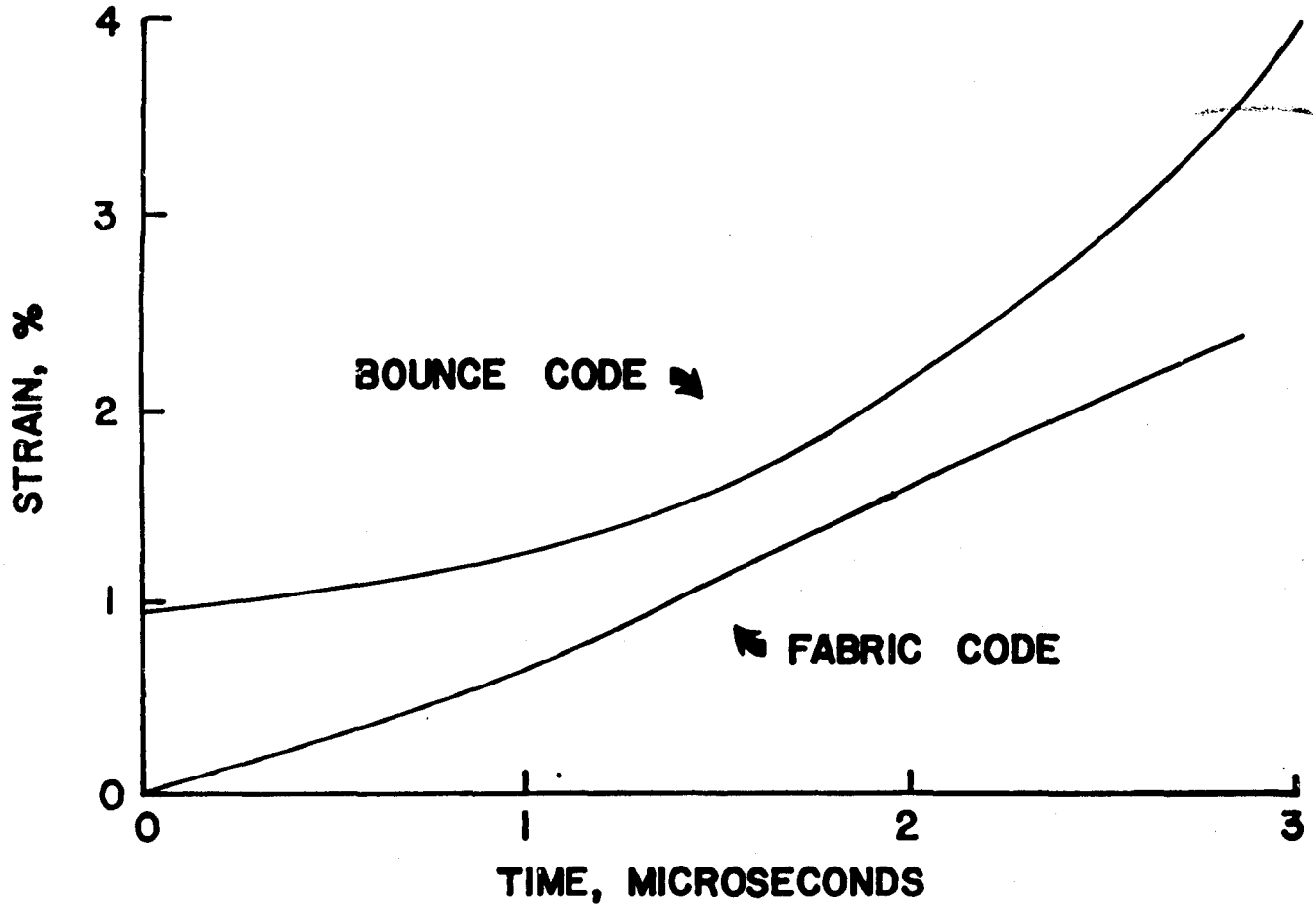

Figure 37. A comparison of the reflection-only bounce model for wave propagation in an impacted fabric, in comparison with the fabric model of this report.

Unfortunately, it appears that the reflection-only model predicts much too high a strain level, except at times very early in the ballistic event. Figure 37 shows the impact-point strain history as predicted by the reflection-only model for a 400 m/sec impact on a Kevlar 29 panel with 1575 yarns/m (the curve developed by the "BOUNCE" code). This prediction is compared

with that of the more general code described earlier (the curve labeled "FABRIC"). At very short times, the BOUNCE code results are likely superior, as they give strains equal to that developed in a single transversely-impacted fiber; the Fabric code shows a numerical lag in the development of strain. The two codes achieve similar values at near 1.5 microseconds, but after this the bounce code increases rapidly to unreasonably high values of strain and thus predicts penetration too early. It is interesting, however, that the value of the reflection coefficient chosen by Freeston and Claus in order to bring their model into line with experiment was very nearly that found explicitly in the crossover study (0.01).

As the slide factor α_s decreases from unity toward zero, representing less fiber-fiber friction at cross-over points, one would expect that the reflection and diversion coefficients would approach zero and that the transmission coefficient would approach unity. At $\alpha_s = 0$, there is no coupling between the two fibers (until the arrival of the transverse kink wave, which generally occurs later than the arrival of the longitudinal wave). As seen in Figures 38, 39 and 40, respectively, for Kevlar 29 fibers, this trend is quantified by the results of the crossover computations.

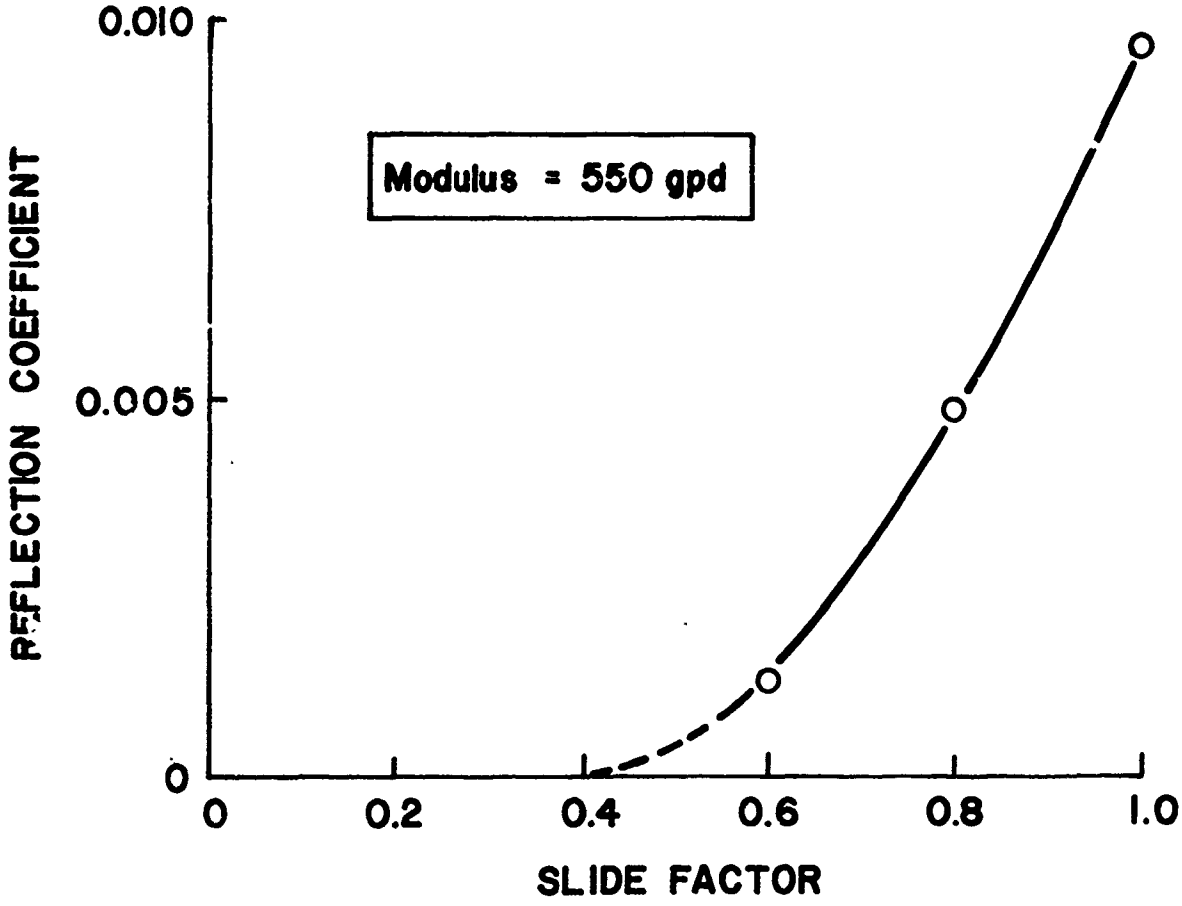

Figure 38. The influence of fiber-fiber sliding on the fraction of stress wave intensity which is reflected at fiber crossovers, as indicated by computer experiments on Kevlar 29 fibers.

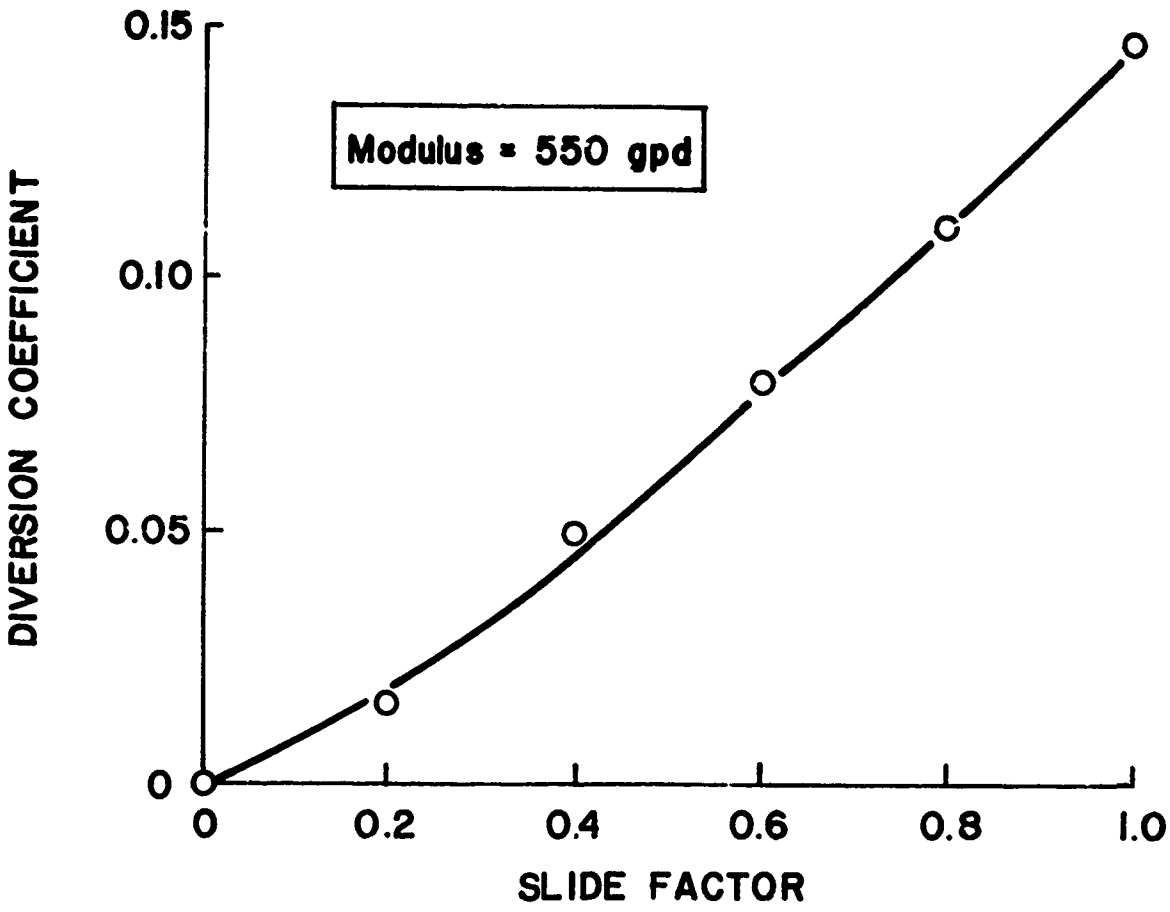

Figure 39. The influence of fiber-fiber sliding on the extent to which a portion of the propagating stress wave is diverted from the primary fiber to begin propagating along the transverse secondary fiber.

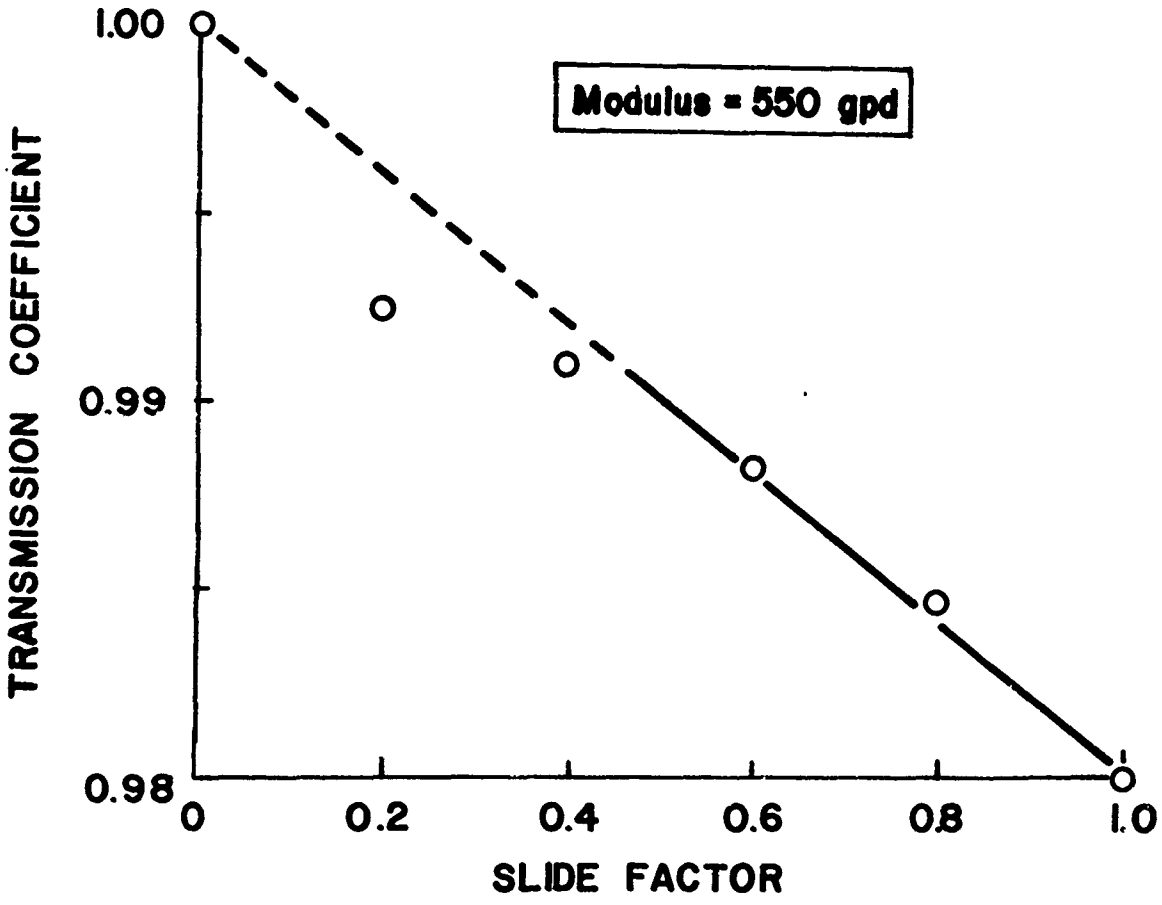

Figure 40. The influence of sliding on the extent of stress wave intensity propagated beyond fiber crossovers.

In principle, it would be possible to include the effects of fiber-fiber slippage in the two-dimensional fabric code by incorporating the formulae of this present chapter into the general code. Such an incorporation, however, would likely render the fabric code so much slower as to be uneconomic. In addition, one has at present no real means of assessing the slide parameter α_s needed for the computation. It might be possible, however, to adjust the viscosity of the

material model artificially in order to produce results similar to those caused by fiber slippage. This method would be similar to that employed during wave propagation calculations in geometrically dispersive composites [24]. If this approach is pursued in the future, the data of Figures 38-40 will be useful in providing guidance as to the desired effect. As a final comment on this work, it may be stated that the FABRIC impact code provides a simulation of impact on textile fabrics which is already of sufficient accuracy that inclusion of the fiber crossover effects would not be considered necessary, at least in the case of tightly woven panels which do not exhibit extensive fiber slippage during impact.

CONCLUSIONS

The numerical analyses described in this report offer a means whereby the designer of personnel armor may perform computer-aided design and analysis of what up until now has been an impossibly intractable problem. Perhaps as useful as the ability to perform such analyses, however, is the extent to which the armor designer's intuition of the mechanics of penetration is enhanced by this tool. These numerical codes

are easily implemented on any modern computer system, and run very economically. They are also extremely amenable to user modification in order to permit easy implementation of various constitutive laws, fracture models, etc.

Certain areas still exist, however, for significant improvement in this treatment. First, the codes are presently limited to zero-obliquity impact by a projectile whose lateral dimensions are small compared with the region of influence during impact. Relatively minor code modifications would be necessary to include oblique impacts by large and arbitrarily shaped projectiles. In this manner the influence of projectile geometry could be modeled. Second, and more important, is the necessity to incorporate more accurate models of material response. As was demonstrated within this report, rather sophisticated constitutive and fracture algorithms can be implemented within the codes with no serious difficulties. More work is needed, however, to determine the extent to which these or other models are applicable to fabric response in the ballistic time frame, and to determine the numerical parameters to be used in the models.

Two examples of this latter problem may be repeated here. First, recall that the treatment of nonlinear

viscoelastic effects was limited not by the code capability, but by the present lack of understanding as to which of several possible nonlinear constitutive laws would most accurately model ballistic response. Regardless of the model selected, work is required to obtain experimentally the numerical data required as input parameters.

Second, the otherwise very successful materials parametric study described in the report is deficient in that it predicts that Kevlar 29 should far outperform Kevlar 49. In fact, the two aramid fabrics perform almost equally well, and some evidence suggests that Kevlar 49 is actually superior. The authors have no doubt that this discrepancy lies not in the wave-propagation aspects of the code predictions, but in the dynamic failure criterion used. Micrographs of ballistically-fractured fibers show extensive fibrillation, and evidence exists which suggest that Kevlar 29 and 49 differ primarily in their extent of fibrillation during fracture. Experimental work aimed at elucidating the nature of the fracture mechanism is needed; incorporation of the resulting information into the penetration codes should follow without difficulty.

This document reports research undertaken in cooperation with the US Army Natick Research and Development Command under Contract No. DAAG 17-76-C-0013 and has been assigned No. NATICK/TR-80 /021 in the series of reports approved for publication.

REFERENCES

1. D.K. Roylance, Textile Res. J., 47 (1977) 679.

2. R.J. Coskren, N.J. Abbott, and J.H. Ross, AIAA Paper No. 75-1360, Nov. 1975.

3. H. Kolsky, Stress Waves in Solids (Dover Publications, New York, 1963).

4. D.K. Roylance, MIT Tech. Rept. R77-1, Dept. of Materials Sci. and Eng., Jan. 1977.

5. A.F. Wilde, J.J. Ricca, D.K. Roylance and G.C. Tocci, Tech. Rept. AMMRC TR72-12, Army Materials and Mechanics Research Center, Watertown, Mass. (1972).

6. G.I. Taylor, Scientific Papers of G.I. Taylor, (Cambridge University Press, 1958), paper no. 32.

7. T. von Karman and P. Duwez, J. Appl. Phys., 21 (1950) 987.

8. D.R. Petterson, G.M. Steward, F.A. Odell, and R.C. Maheux, Textile Res. J., 30 (1960) 411.

9. A.B. Schultz, P.A. Tuschak and A.A. Vicario, J. Appl. Mech. (1967) 392.

10. C.A. Fenstermaker and J.C. Smith, Appl. Polymer Symp., 1 (1965) 125.

11. S.N. Zhurkov, Intl. J. Fracture Mech., 1 (1965) 311.

12. K.L. DeVries and D.K. Roylance, Progress in Solid State Chem., 8 1973) 283.

13. A.F. Wilde, Textile Res. J., 44 (1974) 772.

14. S.J. Crandall, Engineering Analysis, (McGraw-Hill, New York, 1956) 396.

15. D.K. Roylance, A.F. Wilde and G.C. Tocci, Textile Res. J., 43 (1973) 34.

16. J.C. Smith, C.A. Fenstermaker, and P.J. Shouse, Textile Res. J., 35 (1965) 743.

17. N.G. McCrum, B.E. Read and G. Williams, Anelastic and Dielectric Effects in Polymeric Solids (Wiley, London, 1967).

18. D.K. Roylance, J. Appl. Mech., (1973) 143.

19. J.C. Smith and J.T. Fong, J. Res. Natl. Bur. Stan., 72-B (1968) 201.

20. J.C. Smith, J. Appl. Phys.- 37 (1966) 1697.

21. H. Eyring and G. Halsey, Textile Res. J., 15 (1945) 295.

22. B. Carnahan, Applied Numerical Methods, (Wiley, New York, 1969) 201.

23. W.D. Freeston and W.D. Claus, Textile Res. J., 43 (1973) 348.

24. W.L. Bade, Tech. Dept. AFWL-TR-72-8, Air Force Weapons Laboratory, Albuquerque (1972).

APPENDIX A - The FABRIC Code

General. FABRIC is a FORTRAN coding of the numerical analysis of fabric impact which was described in Chapter II. In its present form, the code is restricted to zero-obliquity impact on an orthogonal fabric mesh consisting of only one fiber type. These constraints could be relaxed through suitable code modifications. The code was developed and implemented on MIT's IBM 370/168 computer system, but was later implemented without difficulty on the NARADCOM computer. The code was run at MIT in a batch mode, but could easily be modified for interactive terminal operation: this would likely consist primarily of adding terminal queuing for data input and graphical display for output data.

Code input and output. The input data needed by FABRIC is detailed in a series of comment lines at the beginning of the code listing. Briefly, these include specification of the impact velocity and projectile mass, the fabric idealization (principally the number of fibers per unit length), the constitutive and fracture properties of the fibers, and such run paramaters as maximum alloted time and printing increment.

A typical data input set, for a 300-m/sec impact on a nylon panel is given below:

```
      LINEAR VISCOELASTIC FABRIC (BALLISTIC NYLON)
1.1          300.          19.533        10.16         5280
0.14         0.0           2.            1.4142        1.
   3
100.         0.2           5.
  36   1   1
```

Code output consists first of a series of values relative to the initial conditions which were read in and which the computer requires in order to begin the recursive calculations.

After each time increment (or less often, depending on the value used for the print skip increment INC), the code prints the current values of the field variables at each node in the fabric octant. Currently, these are simply dumped in order of the calculation scheme as defined by Figure 10. This presentation of data has been sufficient for the research studies discussed in this report, but for production design work, graphical or some other high-order output would likely be prefer-

able. The output for the first time increment of the above 300 m/sec nylon impact is given below for illustration. T10 and T01 are the tensions in the two orthogonal fibers passing through a node as shown in Figure 9, EPS10 and EPS01 are the corresponding strains, VZ is the transverse velocity and XCD and ZCD are the x- and z-coordinates of the i,j node. This print also presents the current time after impact, the current projectile velocity, the energy lost by the projectile and the partition of impact energy into a strain and kinetic components within the fabric. Clearly, a great deal of data is made available by the code, and the user should modify the output format so as to provide the most convenient display of results for his needs.

```
EXECUTION BEGINS...
1LINEAR VISCOELASTIC FABRIC (BALLISTIC NYLON)


 INPUT PARAMETERS:
 YARN DENIER, DENYRN (DEN)=    0.52800E+04
 INITIAL PROJECTILE VELOCITY,VPROJ (M/SEC)=    0.30000E+03
 PROJECTILE MASS, PMASS (GM)=    0.11000E+01
 FABRIC PANEL LENGTH XL (CM)=    0.10160E+02
 ELEMENT LENGTH DXL, (CM)=    0.29029E+00
 MAXIMUM IMPACT DURATION TMAX (MICROSEC)=    0.20000E+01
 STABILITY COEFFICIENT, CDTM=    0.14142E+01
 INCREMENTAL TIME  DTM (MICROSEC)=    0.69116E+00
 NUMBERS OF LAYERS, CLYR=    0.10000E+01


 STRAIN WAVE VELOCITY CWAVE(M/SEC)=    0.29698E+04
 INITIAL MODULUS OF YARN, EYRN(GR/DEN)=    0.10000E+03
 BACK UP ELASTIC SPRING CONSTANT XK (GR/CM/CM)=    0.0


 NUMBER OF NODES ALONG MODEL PANEL, JT= 36
 NUMBER OF TIME INCREMENT STEPS, NTINC=    2
 PRINTING FREQUENCY,INC=  1


 ACTUAL FABRIC MASS,FMASSA (GM)=    0.19533E+02
 MODEL FABRIC MASS, FMASSM (GM)=    0.16689E+02
 CRIMP=FMASSA/FMASSM=    0.11704E+01
 UNIT ELEMENT MASS *9.E05 (UNITM)=    0.35877E+04
 HALF UNIT ELEMENT MASS *9.E 05 (HUNITM)=    0.17938E+04


 INITIAL PROJECTILE KINETIC ENERGY, XKE (JOULE/GM)=    0.25342E+01

 MATERIALS PROPERTIES:
 OPTION--MATERIAL MODEL, IPT=     3
 INITIAL MODULUS, EYRN(GR/DEN)=    0.10000E+03


 VISCOELASTIC MODEL----STANDARD LINEAR SOLID PARAMETER
 MODEL GLASSY MODULUS (GPD)=    0.10000E+03
 MODEL VISCOUS FRACTION=    0.20000E+00
 MODEL RELAXATION TIME(MICROSECONDS)=    0.50000E+01


 RUPTURE STRAIN OF INDIVIDUAL FIBER,EPSB=    0.14000E+00
```

```
TIME=   0.69116E+00     WAVE FRONT AT=   1

          TIME          PROJ VEL    PROJ ENGY LOSS FABRC ENGY GAIN  BACK UP ENGY    STRAIN ENGY    K.E.--X,Y,Z
       0.69116E+00    0.30000E+03    0.46730E-04    0.91894E-02    0.0             0.56979E-05    0.0            0.0      0.91837E-02
T10(IX,IY)=
   0.24854E+00    0.0            0.0            0.0            0.0            0.0            0.0            0.0
   0.0            0.0            0.0            0.0            0.0            0.0            0.0            0.0
   0.0            0.0            0.0            0.0            0.0            0.0            0.0            0.0
   0.0            0.0            0.0            0.0            0.0            0.0            0.0            0.0
   0.0            0.0            0.0            0.0
T01(JX,JY)=
   0.24854E+00    0.0            0.0            0.0            0.0            0.0            0.0            0.0
   0.0            0.0            0.0            0.0            0.0            0.0            0.0            0.0
   0.0            0.0            0.0            0.0            0.0            0.0            0.0            0.0
   0.0            0.0            0.0            0.0            0.0            0.0            0.0            0.0
   0.0            0.0            0.0            0.0
 VZ(I,J)=
  0.30000E+03  0.0            0.0            0.0            0.0            0.0            0.0            0.0            0.0
  0.0          0.0            0.0            0.0            0.0            0.0            0.0            0.0            0.0
  0.0          0.0            0.0            0.0            0.0            0.0            0.0            0.0            0.0
  0.0          0.0            0.0            0.0            0.0            0.0            0.0            0.0            0.0
XCD(I,J)=
  0.0          0.29029E+00    0.58057E+00    0.87086E+00    0.11611E+01    0.14514E+01    0.17417E+01    0.20320E+01    0.23223E+01
  0.26126E+01  0.29029E+01    0.31931E+01    0.34834E+01    0.37737E+01    0.40640E+01    0.43543E+01    0.46446E+01    0.49349E+01
  0.52251E+01  0.55154E+01    0.58057E+01    0.60960E+01    0.63863E+01    0.66766E+01    0.69669E+01    0.72571E+01    0.75474E+01
  0.78377E+01  0.81280E+01    0.84183E+01    0.87086E+01    0.89989E+01    0.92891E+01    0.95794E+01    0.98697E+01    0.10160E+02
ZCD(I,J)=
  0.20735E-01  0.0            0.0            0.0            0.0            0.0            0.0            0.0            0.0
  0.0          0.0            0.0            0.0            0.0            0.0            0.0            0.0            0.0
  0.0          0.0            0.0            0.0            0.0            0.0            0.0            0.0            0.0
  0.0          0.0            0.0            0.0            0.0            0.0            0.0            0.0            0.0
EPS10(KX,KY)=
   0.25473E-02    0.0            0.0            0.0            0.0            0.0            0.0            0.0
   0.0            0.0            0.0            0.0            0.0            0.0            0.0            0.0
   0.0            0.0            0.0            0.0            0.0            0.0            0.0            0.0
   0.0            0.0            0.0            0.0            0.0            0.0            0.0            0.0
   0.0            0.0            0.0            0.0
EPS01(LX,LY)=
   0.25473E-02    0.0            0.0            0.0            0.0            0.0            0.0            0.0
   0.0            0.0            0.0            0.0            0.0            0.0            0.0            0.0
   0.0            0.0            0.0            0.0            0.0            0.0            0.0            0.0
   0.0            0.0            0.0            0.0            0.0            0.0            0.0            0.0
   0.0            0.0            0.0            0.0
```

Program Requirements. In its present form, the FABRIC code is self-contained, needing no external software support. All its subroutines, for instance, are contained within the listing given below. One qualification to this statement however, is the inclusion of a call to Subroutine UERTST within the nonlinear equation-solving subroutine ZNOLNR. UERTST is an error-handling routine available through the proprietary "International Mathematics and Statistics Library" (IMSL). If IMSL is not available at the user's location, the call to UERTST could be removed with little risk: no error-handling capability was needed during any of the computer experiments described in the body of this report.

FABRIC needs no tape or disk support; all computations are performed directly within core. Core requirements and run times are dependent both on problem specifications and on the computer system, but by way of illustration some parameters observed during a typical run on the IBM 370/168 system will be mentioned. During an impact simulation of a Kevlar 29 single layer at 300 m/sec, the computed time-to-penetration was

42.87 μsec. The panel was idealized as having a fiber spacing of 0.3175 cm, and the time step for optimum code stability was 0.32234 μsec. A total of 133 time increments was therefore necessary for the run, with each time increment involving an additional node relative to the previous step. The total run time for this job was 1.089 minutes ($12.92 at weekend rates), and a total of 182 kilobytes of CPU core was required. When this same problem was run at NARADCOM, 3 min 50 sec of CPU time was required, which illustrates the system dependency of such job parameters.

FLOW DIAGRAM AND LISTING

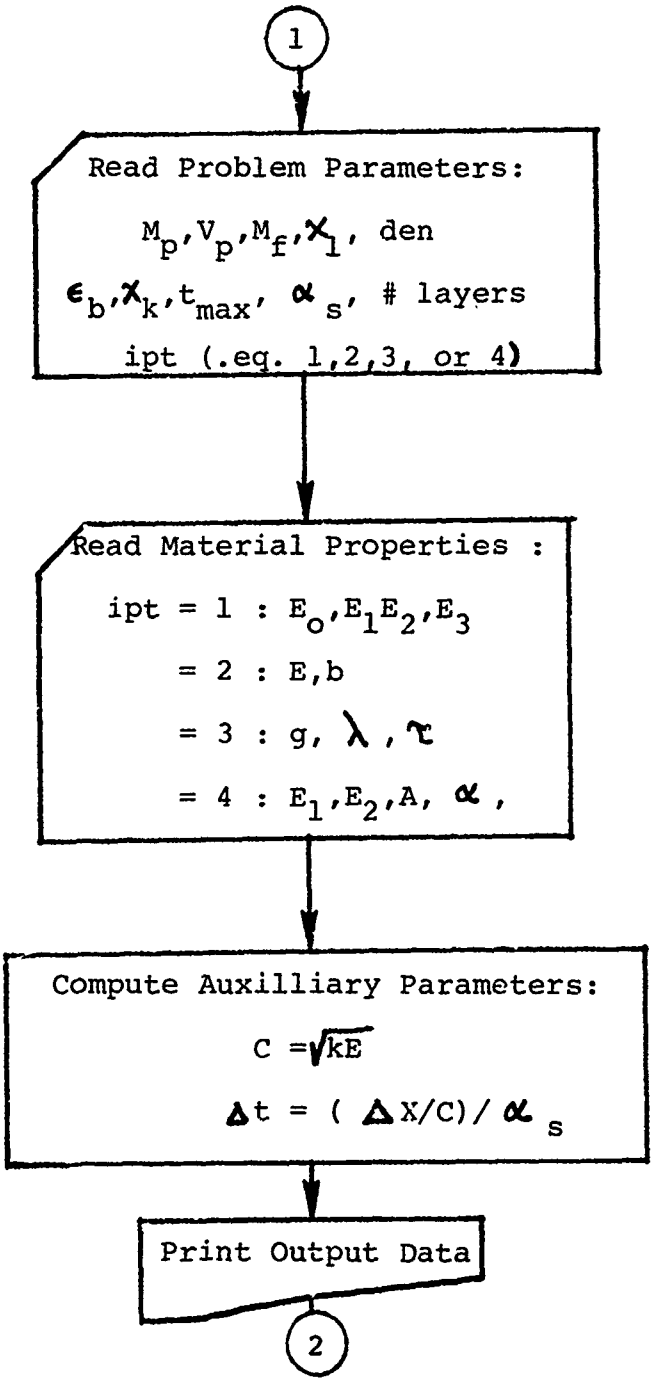

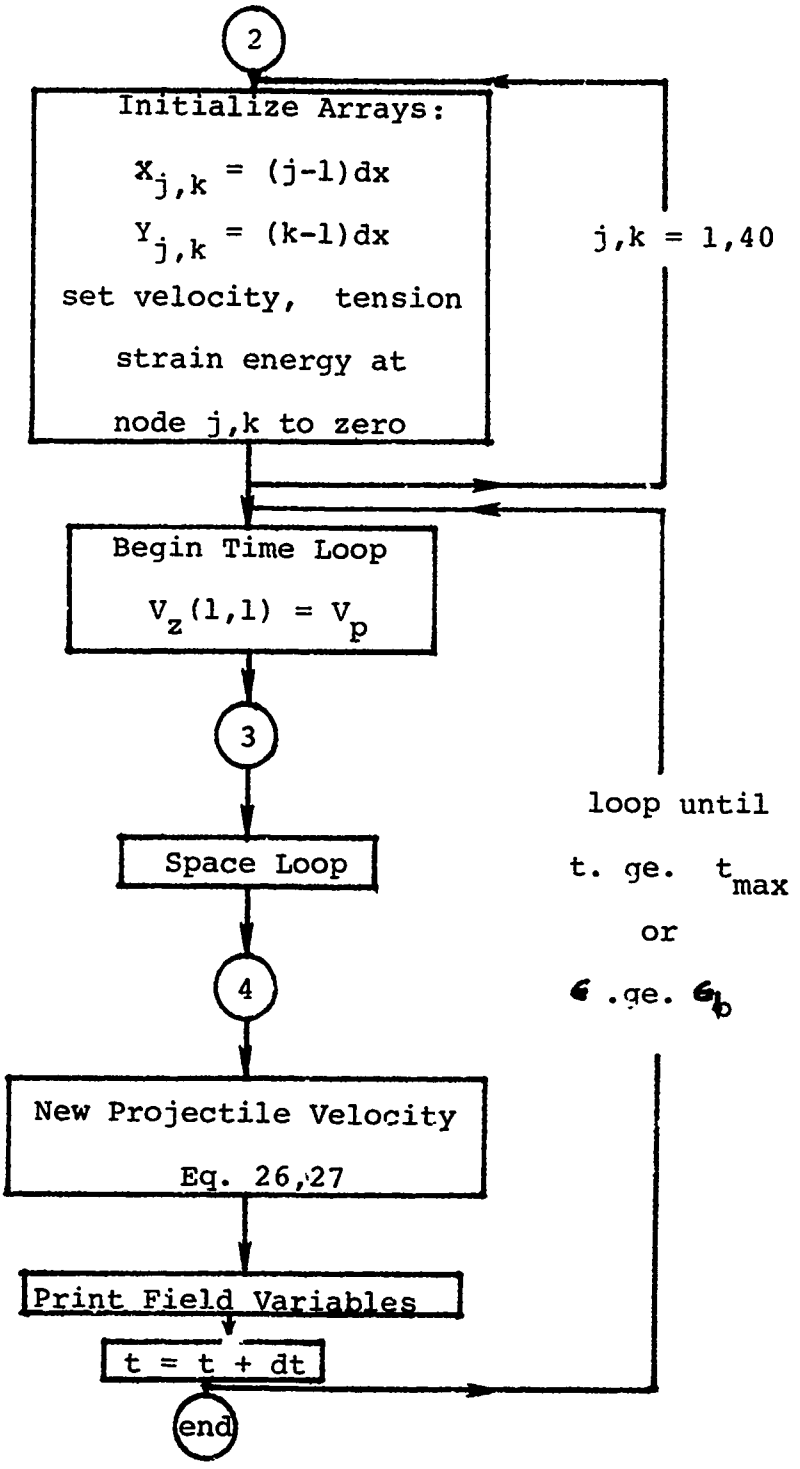
2
Initialize Arrays:
$X_{j,k}$ = (j-1)dx
$Y_{j,k}$ = (k-1)dx
set velocity, tension
strain energy at
node j,k to zero
j,k = 1,40
Begin Time Loop
$V_z(1,1) = V_p$
3
Space Loop
4
loop until
t. ge. t_{max}
or
ϵ .ge. ϵ_b
New Projectile Velocity
Eq. 26,27
Print Field Variables
t = t + dt
end

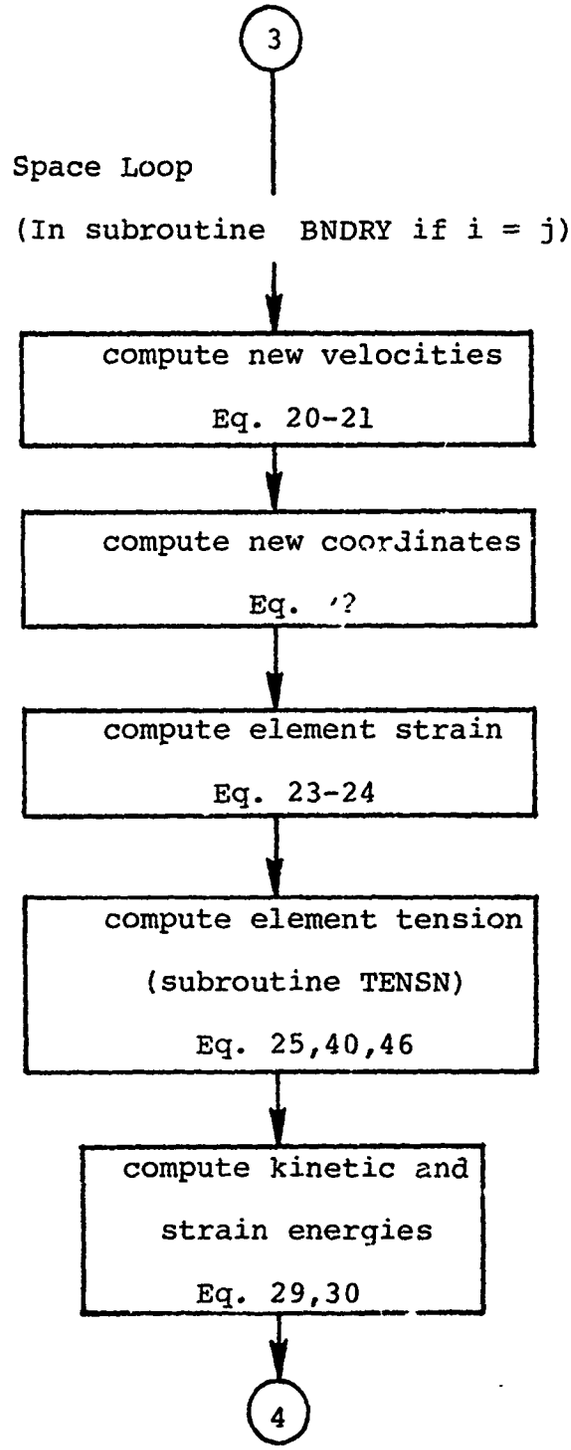
3
Space Loop
(In subroutine BNDRY if i = j)
compute new velocities
Eq. 20-21
compute new coordinates
Eq. '?
compute element strain
Eq. 23-24
compute element tension
(subroutine TENSN)
Eq. 25,40,46
compute kinetic and
strain energies
Eq. 29,30
4

```
C                                                                       FAB00010
C .....................................................................  FAB00020
C .                                                                     .  FAB00030
C .   F A B R I C                                                       .  FAB00040
C .                                                                     .  FAB00050
C .      A DIRECT NUMERICAL SOLUTION OF THE FIELD EQUATIONS             .  FAB00060
C .      FOR NORMAL-OBLIQUITY BALLISTIC IMPACT OF AN ORTHOGONAL         .  FAB00070
C .      FABRIC MESH                                                    .  FAB00080
C .                                                                     .  FAB00090
C .                                                                     .  FAB00100
C .      DEFINITION OF INPUT VARIABLES                                  .  FAB00110
C .                                                                     .  FAB00120
C .        1. PROBLEM HEADING (20A4)                                    .  FAB00130
C .                                                                     .  FAB00140
C .        2. RUN PARAMETERS (5E15.5)                                   .  FAB00150
C .                                                                     .  FAB00160
C .             PMASS   PROJECTILE MASS (GM)                            .  FAB00170
C .             VPROJ   INITIAL PROJECTILE VELOCITY (M/SEC)             .  FAB00180
C .             FMASSA  ACTUAL FABRIC MASS (GM)                         .  FAB00190
C .             XL      FABRIC PANEL LENGTH (CM)                        .  FAB00200
C .             DENYRN  YARN DENIER                                     .  FAB00210
C .                                                                     .  FAB00220
C .        3. RUN PARAMETERS (5E15.5)                                      FAB00230
C .                                                                     .  FAB00240
C .             EPSB    YARN BREAKING STRAIN                            .  FAB00250
C .             XK      ELASTIC SPRING CONSTANT (GMF/SQ CM)             .  FAB00260
C .             TMAX    MAXIMUM TIME (MICROSEC)                         .  FAB00270
C .             CDTM    STABILITY COEFFICIENT (.GE. 1)                  .  FAB00280
C .             CLYR    NUMBER OF FABRIC LAYERS IN PANEL                .  FAB00290
C .                                                                     .  FAB00300
C .        4. CONSTITUTIVE LAW OPTION (I5)                              .  FAB00310
C .                                                                     .  FAB00320
C .             IPT     .EQ. 1  NONLINEAR (CUBIC POLYNOMIAL)           .  FAB00330
C .                     .EQ. 2  NONLINEAR (EXPONENTIAL)                 .  FAB00340
C .                     .EQ. 3  STANDARD LINEAR SOLID                   .  FAB00350
C .                     .EQ. 4  EYRING VISCOELASTICITY                  .  FAB00360
C .                                                                     .  FAB00370
C .        5. STRAIN HARDENING PARAMETERS (2E15.5)                      .  FAB00380
C .             (IF IPT .EQ. 2)                                         .  FAB00390
C .                                                                     .  FAB00400
C .             EYRN    PREEXPONENTIAL FACTOR (GPD)                     .  FAB00410
C .             CHARD   STRAIN HARDENING EXPONENT                       .  FAB00420
C .                                                                     .  FAB00430
C .      OR 5 . NONLINEAR POLYNOMIAL COEFFICIENTS (4E15.5)              .  FAB00440
C .             (IF IPT .EQ. 1)                                         .  FAB00450
C .                                                                     .  FAB00460
C .             E0      FIRST TERM (GPD)                                .  FAB00470
C .             E1      SECOND TERM (GPD)                               .  FAB00480
C .             E2      THIRD TERM (GPD)                                .  FAB00490
C .             E3      FOURTH TERM (GPD)                               .  FAB00500
C .                                                                     .  FAB00510
C .      OR 5. STANDARD LINEAR SOLID PARAMETERS (3E15.5)                .  FAB00520
C .             (IF IPT .EQ. 3)                                         .  FAB00530
C .                                                                     .  FAB00540
C .             G       GLASSY MODULUS (GPD)                            .  FAB00550
```

```
C .              VLAMDA  VISCOUS FRACTION (.LE. 1.)                    . FAB00560
C .              TAU     RELAXATION TIME (MICROSEC)                    . FAB00570
C .                                                                    . FAB00580
C .     OR 5. EYRING NONLINEAR VISCOELASTICITY (5E15.5)                . FAB00590
C .              (IF IPT .EQ. 4)                                       . FAB00600
C .                                                                    . FAB00610
C .              EN1     EQUILIBRIUM SPRING CONSTANT (GPD)             . FAB00620
C .              EN2     SECOND SPRING CONSTANT (GPD)                  . FAB00630
C .              A       EYRING COEFFICIENT (1/SEC)                    . FAB00640
C .              ALP     EYRING EXPONENTIAL (1/GPD)                    . FAB00650
C .              VLBD    MODEL VISCOUS FRACTION (.LE. 1)               . FAB00660
C .                                                                    . FAB00670
C .        6 . MESH DENSITY AND PRINT INFORMATION (3I5)                . FAB00680
C .                                                                    . FAB00690
C .              JT      NUMBER OF NODES ALONG PANEL LENGTH            . FAB00700
C .              INC     PRINT SKIP INCREMENT                          . FAB00710
C .              MODE    .EQ. 0 DATA CHECK ONLY                        . FAB00720
C .                      .EQ. 1 EXECUTION                              . FAB00730
C .                                                                    . FAB00740
C . . . . . . . . . . . . . . . . . . . . . . . . . . . . . . . . . . . FAB00750
      REAL*8 EN1,EN2,A,ALP,VLBD                                        FAB00760
      COMMON/IXMATL/IPT                                                FAB00770
      COMMON/CMATL/EYRN,CHARD,E0,E1,E2,E3                              FAB00780
      COMMON/VISCO/G,VLAMDA,TAU                                        FAB00790
      COMMON/NONLR/EN1,EN2,A,ALP,VLBD                                  FAB00800
      COMMON/VARBL/JT,XL,DXL,DTM,DENYRN,     PMASS,CRIMP,FMASSA,FMASSM,FFAB00810
     &MASSF,UNITM,HUNITM                                               FAB00820
      COMMON/TSNOLD/T1OOLD(40,40),T01OLD(40,40),E1OOLD(40,40),E01OLD(40,FAB00830
     &40)                                                              FAB00840
      COMMON/BACKUP/XK                                                 FAB00850
      COMMON/CMESH/XCD(40,40),YCD(40,40),ZCD(40,40),XCDOLD,YCDOLD,ZCDOLDFAB00860
      COMMON/TEN/T10(40,40),T01(40,40),TX10(40,40),TX01(40,40),        FAB00870
     &TY10(40,40),TY01(40,40),TZ10(40,40),TZ01(40,40),                 FAB00880
     &EPS10(40,40),EPS01(40,40)                                        FAB00890
      COMMON/VELOC/VX(40,40),VY(40,40),VZ(40,40)                       FAB00900
      COMMON/ERGCUM/XKNRGY,YKNRGY,ZKNRGY,SNRGY                         FAB00910
      COMMON/ERGELM/ELKE(40,40),ELSE(40,40),TLELEN(40,40)              FAB00920
      DIMENSION HED (20)                                               FAB00930
C                                                                      FAB00940
C     READ AND PRINT INPUT PARAMETERS                                  FAB00950
C     AND COMPUTE INTERNAL CONTROL PARAMETERS                          FAB00960
C                                                                      FAB00970
      READ (5,120) HED                                                 FAB00980
  120 FORMAT (20A4)                                                    FAB00990
      READ(5,1) PMASS,VPROJ,FMASSA,XL,     DENYRN,EPSD,XK,TMAX,CDTM,CLYRFAB01000
    1 FORMAT(5E15.5)                                                   FAB01010
CC                                                                     FAB01020
      READ(5,3) IPT                                                    FAB01030
    3 FORMAT(16I5)                                                     FAB01040
      GO TO (31,32,33,34), IPT                                         FAB01050
   32 READ(5,4) EYRN,CHARD                                             FAB01060
      GO TO 39                                                         FAB01070
   31 READ(5,4) E0,E1,E2,E3                                            FAB01080
      GO TO 39                                                         FAB01090
    4 FORMAT(5E15.5)                                                   FAB01100
```

```
   33 READ(5,5) G,VLAMDA,TAU                                          FAB01110
      GO TO 39                                                        FAB01120
 5    FORMAT(5E15.5)                                                  FAB01130
   34 READ (5,6) EN1,EN2,A,ALP,VLBD                                   FAB01140
6     FORMAT(5D15.5)                                                  FAB01150
   39 CONTINUE                                                        FAB01160
      READ (5,2) JT,INC,MODE                                          FAB01170
 2    FORMAT(16I5)                                                    FAB01180
CC                                                                    FAB01190
      IF (IPT.EQ.1) EYRN = E1                                         FAB01200
      IF (IPT.EQ.3) EYRN = G                                          FAB01210
      IF (IPT.EQ.4) EYRN = EN1+EN2                                    FAB01220
      CWAVE=1.00E 02*SQRT(8.82E 00*EYRN)                              FAB01230
      JTM1=JT-1                                                       FAB01240
      DXL=XL/FLOAT(JTM1)                                              FAB01250
      DTM=1.00E 04*DXL/CWAVE                                          FAB01260
      DTM=DTM/CDTM                                                    FAB01270
      NTINC=IFIX(TMAX/DTM)                                            FAB01280
      IDIAG=0                                                         FAB01290
      JPRT=JT                                                         FAB01300
      JPRTY=1                                                         FAB01310
      IPLAST=0                                                        FAB01320
CC                                                                    FAB01330
CC                                                                    FAB01340
      DENYRN=DENYRN*CLYR                                              FAB01350
      FMASSA=FMASSA*CLYR                                              FAB01360
CC                                                                    FAB01370
      FMASSM=4.00E 00*FLOAT(JTM1)*(2.00E 00*DENYRN*XL)/9.0E 05        FAB01380
      FMASSF=4.00E 00*FLOAT(JTM1)*(2.00E 00*DENYRN*XL)                FAB01390
CC                                                                    FAB01400
      CRIMP=FMASSA/FMASSM                                             FAB01410
CC                                                                    FAB01420
      UNITM=CRIMP*2.00E 00*DENYRN*DXL                                 FAB01430
      HUNITM=0.50E 00*UNITM                                           FAB01440
      XKE=          0.50E-03*PMASS*VPROJ**2/(FMASSM*CRIMP)            FAB01450
CC                                                                    FAB01460
      WRITE (6,121) HED                                               FAB01470
  121 FORMAT (1H1,20A4)                                               FAB01480
      WRITE(6,61) DENYRN,VPROJ,PMASS,XL,DXL,TMAX,CDTM,DTM,CLYR        FAB01490
61    FORMAT(//1X,'INPUT PARAMETERS:'/                                FAB01500
     &1X,'YARN DENIER, DENYRN (DEN)=',E14.5/                          FAB01510
     &1X,'INITIAL PROJECTILE VELOCITY,VPROJ (M/SEC)=',E14.5/          FAB01520
     &1X,'PROJECTILE MASS, PMASS (GM)=',E14.5/                        FAB01530
     &1X,'FABRIC PANEL LENGTH XL (CM)=',E14.5/                        FAB01540
     &1X,'ELEMENT LENGTH DXL, (CM)=',E14.5/                           FAB01550
     &1X,'MAXIMUM IMPACT DURATION TMAX (MICROSEC)=',E14.5/            FAB01560
     &1X,'STABILITY COEFFICIENT, CDTM=',E14.5/                        FAB01570
     &1X,'INCREMENTAL TIME  DTM (MICROSEC)=',E14.5/                   FAB01580
     &1X,'NUMBERS OF LAYERS, CLYR=',E14.5)                            FAB01590
      WRITE(6,62) CWAVE,EYRN,XK                                       FAB01600
62    FORMAT(//1X,'STRAIN WAVE VELOCITY CWAVE(M/SEC)=',E14.5/         FAB01610
     &1X,'INITIAL MODULUS OF YARN, EYRN(GR/DEN)=',E14.5/              FAB01620
     &1X,'BACK UP ELASTIC SPRING CONSTANT XK (GR/CM/CM)=',E14.5)      FAB01630
      WRITE(6,63) JT, NTINC,INC                                       FAB01640
63    FORMAT(//1X,'NUMBER OF NODES ALONG MODEL PANEL, JT=',I3/         FAB01650
```

```
     &1X,'NUMBER OF TIME INCREMENT STEPS, NTINC=',I4/                    FAB01660
     &1X,'PRINTING FREQUENCY,INC=',I3)                                   FAB01670
      WRITE(6,64) FMASSA, FMASSM,CRIMP,UNITM,HUNITM                      FAB01680
64    FORMAT (//1X,'ACTUAL FABRIC MASS,FMASSA (GM)=',E14.5/              FAB01690
     &1X,'MODEL FABRIC MASS, FMASSM (GM)=',E14.5/                        FAB01700
     &1X,'CRIMP=FMASSA/FMASSM=', E14.5/                                  FAB01710
     &1X,'UNIT ELEMENT MASS *9.E05 (UNITM)=',E14.5/                      FAB01720
     &1X,'HALF UNIT ELEMENT MASS *9.E 05 (HUNITM)=',E14.5)               FAB01730
      WRITE(6,65) XKE                                                    FAB01740
65    FORMAT(//1X,'INITIAL PROJECTILE KINETIC ENERGY, XKE (JOULE/GM)=',EFAB01750
     &14.5)                                                              FAB01760
      WRITE(6,66) IPT,EYRN                                               FAB01770
66    FORMAT(/1X,'MATERIALS PROPERTIES:'/                                FAB01780
     &1X,'OPTION--MATERIAL MODEL, IPT=',I5/                              FAB01790
     &1X,'INITIAL MODULUS, EYRN(GR/DEN)=',E14.5/)                        FAB01800
      IF (IPT.EQ.2) WRITE (6,661) EYRN, CHARD                            FAB01810
  661 FORMAT (/1X,'EXPONENTIAL STRAIN HARDENING'/                        FAB01820
     &1X,'COEFFICIENT, EYRN (GR/DEN)=',E14.5/                            FAB01830
     &1X,'STRAIN HARDENING EXPONENT, CHARD=',E14.5/)                     FAB01840
      IF (IPT.EQ.1) WRITE (6,662) E0,E1,E2,E3                            FAB01850
  662 FORMAT (/1X,'NONLINEAR ELASTIC MODEL -- CUBIC POLYNOMIAL'/         FAB01860
     &1X,'E0 (GR/DEN)=',E14.5/                                           FAB01870
     &1X,'E1 (GR/DEN)=',E14.5/                                           FAB01880
     &1X,'E2 (GR/DEN)=',E14.5/                                           FAB01890
     &1X,'E3 (GR/DEN)=',E14.5)                                           FAB01900
      IF (IPT.EQ.3) WRITE(6,68) G,VLAMDA,TAU                             FAB01910
 68   FORMAT(/1X,'VISCOELASTIC MODEL---STANDARD LINEAR SOLID PARAMETER'/FAB01920
     &1X,'MODEL GLASSY MODULUS (GPD)=',E14.5/                            FAB01930
     &1X,'MODEL VISCOUS FRACTION=',E14.5/                                FAB01940
     &1X,'MODEL RELAXATION TIME(MICROSECONDS)=',E14.5)                   FAB01950
      IF (IPT.EQ.4) WRITE(6,69) EN1,EN2,A,ALP,VLBD                       FAB01960
69    FORMAT(//1X,'EYRING NONLINEAR MODEL, E1(GPD)=',D14.5/              FAB01970
     &1X,'EYRINGS NONLINEAR MODEL, E2(GPD)=',D14.5/                      FAB01980
     &1X,'NONLINEAR DASHPOT, A(1/SEC)=',D14.5/                           FAB01990
     &1X,'NONLINEAR DASHPOT, ALP(DEN/GF)=',D14.5/                        FAB02000
     &1X,'NONLINEAR ELASTIC ARM RATIO, VLBD=',D14.5)                     FAB02010
      WRITE(6,67) EPSB                                                   FAB02020
67    FORMAT(//1X,'RUPTURE STRAIN OF INDIVIDUAL FIBER,EPSB=',E14.5/)     FAB02030
      IF (MODE.EQ.0) STOP                                                FAB02040
C                                                                        FAB02050
C     INITIALIZE FIELD VARIABLES                                         FAB02060
C     ESTABLISH INITIAL NODAL COORDINATES                                FAB02070
C                                                                        FAB02080
      DO 11 K=1,40                                                       FAB02090
      DO 11 J=1,40                                                       FAB02100
      XCD(J,K)=(J-1)*DXL                                                 FAB02110
      YCD(J,K)=(K-1)*DXL                                                 FAB02120
      ZCD(J,K)=0.00E 00                                                  FAB02130
      VX(J,K)=0.00E 00                                                   FAB02140
      VY(J,K)=0.00E 00                                                   FAB02150
      VZ(J,K)=0.00E 00                                                   FAB02160
      ELSE(J,K)=0.00E 00                                                 FAB02170
      ELKE(J,K)=0.00E 00                                                 FAB02180
      TLELEN(J,K)=0.00E 00                                               FAB02190
      T10(J,K)=0.00E 00                                                  FAB02200
```

```
      TO1(J,K)=0.00E 00                                                 FAB02210
      TX10(J,K)=0.00E 00                                                FAB02220
      TY10(J,K)=0.00E 00                                                FAB02230
      TZ10(J,K)=0.00E 00                                                FAB02240
      TX01(J,K)=0.00E 00                                                FAB02250
      TY01(J,K)=0.00E 00                                                FAB02260
      TZ01(J,K)=0.00E 00                                                FAB02270
      EPS10(J,K)=0.00E 00                                               FAB02280
      EPS01(J,K)=0.00E 00                                               FAB02290
      T100LD(J,K)=0.00E 00                                              FAB02300
      T010LD(J,K)=0.00E 00                                              FAB02310
      E100LD(J,K)=0.00E 00                                              FAB02320
      E010LD(J,K)=0.00E 00                                              FAB02330
11    CONTINUE                                                          FAB02340
      INC1=0                                                            FAB02350
      NFRONT=JTM1*2                                                     FAB02360
C                                                                       FAB02370
C     BEGIN TIME LOOP                                                   FAB02380
C                                                                       FAB02390
      DO 12 IT=1,NTINC                                                  FAB02400
      VZ(1,1)=VPROJ                                                     FAB02410
      XKNRGY=0.00E 00                                                   FAB02420
      YKNRGY=0.00E 00                                                   FAB02430
      ZKNRGY=0.00E 00                                                   FAB02440
      SNRGY=0.00E 00                                                    FAB02450
      TIM=DTM*FLOAT(IT)                                                 FAB02460
      INC1=INC1+1                                                       FAB02470
C                                                                       FAB02480
C     COMPUTE BOUNDARY VALUES                                           FAB02490
C                                                                       FAB02500
      CALL BNDRY(IT,1,1)                                                FAB02510
      DO 14 IFRONT=2,NFRONT                                             FAB02520
      IF(IFRONT.LT.JT)  CALL BNDRY(IT,IFRONT,1)                         FAB02530
      IFLAG=0                                                           FAB02540
      NODES=IFRONT/2                                                    FAB02550
      IF(IFRONT-(JT+1)) 16,18,18                                        FAB02560
16    KSTART=1                                                          FAB02570
      GO TO 20                                                          FAB02580
18    KSTART =IFRONT-(JT-1)                                             FAB02590
C                                                                       FAB02600
C     BEGIN SPACE LOOP                                                  FAB02610
C                                                                       FAB02620
20    DO 22 K=KSTART,NODES                                              FAB02630
      J=IFRONT-K                                                        FAB02640
      IF(K.EQ.J) IDIAG=1                                                FAB02650
C                                                                       FAB02660
C     COMPUTE VELOCITY CHANGES FROM INPULSE-MOMENTUM BALANCE            FAB02670
C                                                                       FAB02680
      DVX=(TX10(J+1,K+1)-TX10(J,K+1)+TX01(J+1,K+1)-TX01(J+1,K))*DTM*8.82FAB02690
     &00E 00/(2.00E 00*DXL*CRIMP)                                       FAB02700
      DVY=(TY10(J+1,K+1)-TY10(J,K+1)+TY01(J+1,K+1)-TY01(J+1,K))*DTM*8.82FAB02710
     &00E 00/(2.00E 00*DXL*CRIMP)                                       FAB02720
      DVZ=(TZ10(J+1,K+1)-TZ10(J,K+1)+TZ01(J+1,K+1)-TZ01(J+1,K))*DTM*8.82FAB02730
     &00E 00/(2.00E 00*DXL*CRIMP)+XK*DXL*ZCD(J+1,K+1)*DTM*9.80E-06/(UNITFAB02740
     &M/9.00E 05)                                                       FAB02750
```

```
      DVZ=-DVZ                                                          FAB02760
      IF( ABS(DVX).GE.0.0001.OR.ABS(DVY).GE.0.0001.OR.ABS(DVZ).GE.0.0001FAB02770
     &) IFLAG=IFLAG+1                                                   FAB02780
C                                                                       FAB02790
C     COMPUTE NEW VELOCITIES                                            FAB02800
C                                                                       FAB02810
      VX(J+1,K+1)=VX(J+1,K+1)+DVX                                       FAB02820
      VY(J+1,K+1)=VY(J+1,K+1)+DVY                                       FAB02830
      VZ(J+1,K+1)=VZ(J+1,K+1)+DVZ                                       FAB02840
      VX(JT,K+1)=0.00E 00                                               FAB02850
      VY(JT,K+1)=0.00E 00                                               FAB02860
      VZ(JT,K+1)=0.00E 00                                               FAB02870
      VX(K+1,J+1)=VY(J+1,K+1)                                           FAB02880
      VY(K+1,J+1)=VX(J+1,K+1)                                           FAB02890
      VZ(K+1,J+1)=VZ(J+1,K+1)                                           FAB02900
      IF((IFRONT.GT.JTM1).AND.((J+1).EQ.JT)) GO TO 24                   FAB02910
C                                                                       FAB02920
COMPUTE CHANGE OF NODAL COORDINATES FROM VELOCITIES                     FAB02930
C                                                                       FAB02940
      XCD(J+1,K)=XCDOLD                                                 FAB02950
      YCD(J+1,K)=YCDOLD                                                 FAB02960
      ZCD(J+1,K)=ZCDOLD                                                 FAB02970
      XCD(K,J+1)=YCDOLD                                                 FAB02980
      YCD(K,J+1)=XCDOLD                                                 FAB02990
      ZCD(K,J+1)=ZCDOLD                                                 FAB03000
24    DSQ01=(XCD(J+1,K+1)-XCD(J+1,K))**2+(YCD(J+1,K+1)-YCD(J+1,K))**2+(ZFAB03010
     &CD(J+1,K+1)-ZCD(J+1,K))**2                                        FAB03020
      DIST01=SQRT(DSQ01)                                                FAB03030
      DSQX01=(XCD(J+1,K+1)+VX(J+1,K+1)*DTM/1.00E 04-XCD(J+1,K)-VX(J+1,K)FAB03040
     &*DTM/1.00E 04)**2                                                 FAB03050
      DSQY01=(YCD(J+1,K+1)+VY(J+1,K+1)*DTM/1.00E 04-YCD(J+1,K)-VY(J+1,K)FAB03060
     &*DTM/1.00E 04)**2                                                 FAB03070
      DSQZ01=(ZCD(J+1,K+1)+VZ(J+1,K+1)*DTM/1.00E 04-ZCD(J+1,K)-VZ(J+1,K)FAB03080
     &*DTM/1.00E 04)**2                                                 FAB03090
C                                                                       FAB03100
C     COMPUTE CHANGE IN ELEMENT STRAIN FROM NEW COORDINATES             FAB03110
C                                                                       FAB03120
      DDST01=SQRT(DSQX01+DSQY01+DSQZ01)                                 FAB03130
      DEPS=DDST01/DIST01-1.00E 00                                       FAB03140
      EPS01(J+1,K)=EPS01(J+1,K)+DEPS                                    FAB03150
      IF(IDIAG.EQ.1) GO TO 26                                           FAB03160
      EPS10(K,J+1)=EPS01(J+1,K)                                         FAB03170
 26   DSQ10=(XCD(J+1,K+1)-XCD(J,K+1))**2+(YCD(J+1,K+1)-YCD(J,K+1))**2+(ZFAB03180
     &CD(J+1,K+1)-ZCD(J,K+1))**2                                        FAB03190
      DIST10=SQRT(DSQ10)                                                FAB03200
      DSQX10=(XCD(J+1,K+1)+VX(J+1,K+1)*DTM/1.00E 04-XCD(J,K+1)-VX(J,K+1)FAB03210
     &*DTM/1.00E 04)**2                                                 FAB03220
      DSQY10=(YCD(J+1,K+1)+VY(J+1,K+1)*DTM/1.00E 04-YCD(J,K+1)-VY(J,K+1)FAB03230
     &*DTM/1.00E 04)**2                                                 FAB03240
      DSQZ10=(ZCD(J+1,K+1)+VZ(J+1,K+1)*DTM/1.00E 04-ZCD(J,K+1)-VZ(J,K+1)FAB03250
     &*DTM/1.00E 04)**2                                                 FAB03260
      DDST10=SQRT(DSQX10+DSQY10+DSQZ10)                                 FAB03270
      DEPS=DDST10/DIST10-1.00E 00                                       FAB03280
      EPS10(J,K+1)=EPS10(J,K+1)+DEPS                                    FAB03290
      EPS01(K+1,J)=EPS10(J,K+1)                                         FAB03300
```

```
      EPSLNY=EPS01(J+1,K)                                                FAB03310
      EPYOLD=E01OLD(J+1,K)                                               FAB03320
      TSYOLD=T01OLD(J+1,K)                                               FAB03330
      JP1=J+1                                                            FAB03340
C                                                                        FAB03350
C     CALL TENSN SUBROUTINE TO COMPUTE ELEMENTS                          FAB03360
C     TENSION FROM ELEMENT STRAIN OR STRAIN HISTORY                      FAB03370
C                                                                        FAB03380
      CALL TENSN(IT,JP1,K,EPSLNY,TSLY,EPYOLD,TSYOLD,DSNRGY)             FAB03390
      T01(J+1,K)=TSLY                                                    FAB03400
      T01OLD(J+1,K)=TSYOLD                                               FAB03410
      T10OLD(K,J+1)=T01OLD(J+1,K)                                        FAB03420
      E01OLD(J+1,K)=EPYOLD                                               FAB03430
      E10OLD(K,J+1)=E01OLD(J+1,K)                                        FAB03440
C                                                                        FAB03450
C     COMPUTE KINETIC AND STRAIN ENERGIES                                FAB03460
C                                                                        FAB03470
      BSEM=1.00E 00                                                      FAB03480
      IF(J.GT.1.AND.K.EQ.1) BSEM=0.500E 00                               FAB03490
      SNRGY=SNRGY+DSNRGY*(2-IDIAG)*BSEM                                  FAB03500
      ELSE(J+1,K)=ELSE(J+1,K)+DSNRGY/4.00E 00                            FAB03510
      EPSLNX=EPS10(J,K+1)                                                FAB03520
      EPXOLD=E10OLD(J,K+1)                                               FAB03530
      TSXOLD=T10OLD(J,K+1)                                               FAB03540
      KP1=K+1                                                            FAB03550
      CALL TENSN(IT,J,KP1,EPSLNX,TSLX,EPXOLD,TSXOLD,DSNRGY)             FAB03560
      T10(J,K+1)=TSLX                                                    FAB03570
      T10OLD(J,K+1)=TSXOLD                                               FAB03580
      T01OLD(K+1,J)=T10OLD(J,K+1)                                        FAB03590
      E10OLD(J,K+1)=EPXOLD                                               FAB03600
      E01OLD(K+1,J)=E10OLD(J,K+1)                                        FAB03610
      IF(J.EQ.1.AND.K.EQ.1) GO TO 51                                     FAB03620
      SNRGY=SNRGY+DSNRGY*(2-IDIAG)                                       FAB03630
      ELSE(J,K+1)=ELSE(J,K+1)+DSNRGY/4.00E 00                            FAB03640
51    ELSE(K+1,J)=ELSE(J,K+1)                                            FAB03650
      ELSE(K,J+1)=ELSE(J+1,K)                                            FAB03660
      T10(K,J+1)=T01(J+1,K)                                              FAB03670
      T01(K+1,J)=T10(J,K+1)                                              FAB03680
      XCDOLD=XCD(J,K+1)                                                  FAB03690
      YCDOLD=YCD(J,K+1)                                                  FAB03700
      ZCDOLD=ZCD(J,K+1)                                                  FAB03710
      ELKE(J,K+1)=ELKE(J,K+1)+0.50E-03*HUNITM*          (VX(J,K+1)**2+VYFAB03720
     &(J,K+1)**2+VZ(J,K+1)**2)/(FMASSF*CRIMP)                            FAB03730
      ELKE(J+1,K)=ELKE(J+1,K)+0.500E-03*HUNITM*          (VX(J+1,K)**2+VFAB03740
     &Y(J+1,K)**2+VZ(J+1,K)**2)/(FMASSF*CRIMP)                           FAB03750
      ELKE(K+1,J)=ELKE(J,K+1)                                            FAB03760
      ELKE(K,J+1)=ELKE(J+1,K)                                            FAB03770
      TLELEN(J,K+1)=ELSE(J,K+1)+ELKE(J,K+1)                              FAB03780
      TLELEN(J+1,K)=ELSE(J+1,K)+ELKE(J+1,K)                              FAB03790
      TLELEN(K,J+1)=TLELEN(J+1,K)                                        FAB03800
      TLELEN(K+1,J)=TLELEN(J,K+1)                                        FAB03810
      BKEXYK=1.00E 00                                                    FAB03820
      BKEXYJ=1.00E 00                                                    FAB03830
      IF(K.EQ.1.AND.J.LT.JT) BKEXYK=0.50E 00                             FAB03840
      IF(J.EQ.1.AND.K.LT.JT) BKEXYJ=0.50E 00                             FAB03850
```

```
      XKNRGY=XKNRGY+4.0CE 00*0.50E-03*HUNITM*(BKEXYK*VX(J+1,K)**2+BKEXYJFAB03860
     &*VX(J,K+1)**2)/(FMASSF*CRIMP)                                     FAB03870
      YKNRGY=YKNRGY+4.00E 00*0.50E-03*HUNITM*(BKEXYK*VY(J+1,K)**2+BKEXYJFAB03880
     &*VY(J,K+1)**2)/(FMASSF*CRIMP)                                     FAB03890
      ZKNRGY=ZKNRGY+(2.0E 00-IDIAG)*4.00E 00*0.50E-03*HUNITM*(BKEXYK*VZ(FAB03900
     &J+1,K)**2+BKEXYJ*VZ(J,K+1)**2)/(FMASSF*CRIMP)                     FAB03910
      IF(IDIAG.EQ.1) GO TO 28                                           FAB03920
      XKNRGY=XKNRGY+4.00E 00*0.50E-03*HUNITM*(BKEXYK*VX(K,J+1)**2+BKEXYJFAB03930
     &*VX(K+1,J)**2)/(FMASSF*CRIMP)                                     FAB03940
      YKNRGY=YKNRGY+4.00E 00*0.50E-03*HUNITM*(BKEXYK*VY(K,J+1)**2+BKEXYJFAB03950
     &*VY(K+1,J)**2)/(FMASSF*CRIMP)                                     FAB03960
C                                                                       FAB03970
C     STORE NEW NODAL COORDINATES                                       FAB03980
C                                                                       FAB03990
28    XCD(J+1,K)=XCD(J+1,K)+VX(J+1,K)*DTM/1.00E 04                      FAB04000
      YCD(J+1,K)=YCD(J+1,K)+VY(J+1,K)*DTM/1.00E 04                      FAB04010
      ZCD(J+1,K)=ZCD(J+1,K)+VZ(J+1,K)*DTM/1.00E 04                      FAB04020
      XCD(J,K+1)=XCD(J,K+1)+VX(J,K+1)*DTM/1.00E 04                      FAB04030
      YCD(J,K+1)=YCD(J,K+1)+VY(J,K+1)*DTM/1.00E 04                      FAB04040
      ZCD(J,K+1)=ZCD(J,K+1)+VZ(J,K+1)*DTM/1.00E 04                      FAB04050
      IF(J.EQ.K) GO TO 40                                               FAB04060
      XCD(K,J+1)=XCD(K,J+1)+VX(K,J+1)*DTM/1.00E 04                      FAB04070
      YCD(K,J+1)=YCD(K,J+1)+VY(K,J+1)*DTM/1.00E 04                      FAB04080
      ZCD(K,J+1)=ZCD(K,J+1)+VZ(K,J+1)*DTM/1.00E 04                      FAB04090
      IF(J.EQ.(K+1)) GO TO 40                                           FAB04100
      XCD(K+1,J)=XCD(K+1,J)+VX(K+1,J)*DTM/1.00E 04                      FAB04110
      YCD(K+1,J)=YCD(K+1,J)+VY(K+1,J)*DTM/1.00E 04                      FAB04120
      ZCD(K+1,J)=ZCD(K+1,J)+VZ(K+1,J)*DTM/1.00E 04                      FAB04130
C                                                                       FAB04140
C     OBTAIN VECTOR COMPONENTS OF ELEMENT TENSIONS                      FAB04150
C                                                                       FAB04160
40    A1=ATAN((YCD(J+1,K+1)-YCD(J,K+1))/(XCD(J+1,K+1)-XCD(J,K+1)))      FAB04170
      COSA1=COS(A1)                                                     FAB04180
      SINA1=SIN(A1)                                                     FAB04190
      IF(ABS(ZCD(J+1,K+1)-ZCD(J,K+1))- 0.0001) 90,90,91                 FAB04200
90    COSB1=0.00E 00                                                    FAB04210
      SINB1=1.00E 00                                                    FAB04220
      GO TO 92                                                          FAB04230
91    B1=ATAN(((XCD(J+1,K+1)-XCD(J,K+1))**2+(YCD(J+1,K+1)-YCD(J,K+1))**2FAB04240
     &)**0.50/(ZCD(J,K+1)-ZCD(J+1,K+1)))                                FAB04250
      COSB1=COS(B1)                                                     FAB04260
      SINB1=SIN(B1)                                                     FAB04270
92    IF(ABS(XCD(J+1,K+1)-XCD(J+1,K))- 0.0001) 96,96,97                 FAB04280
96    COSA2=0.00E 00                                                    FAB04290
      SINA2=1.00E 00                                                    FAB04300
      GO TO 98                                                          FAB04310
97    A2=ATAN((YCD(J+1,K+1)-YCD(J+1,K))/(XCD(J+1,K+1)-XCD(J+1,K)))      FAB04320
      COSA2=COS(A2)                                                     FAB04330
      SINA2=SIN(A2)                                                     FAB04340
98    IF(ABS(ZCD(J+1,K+1)-ZCD(J+1,K))- 0.0001) 93,93,94                 FAB04350
93    COSB2=0.00E 00                                                    FAB04360
      SINB2=1.00E 00                                                    FAB04370
      GO TO 95                                                          FAB04380
94    B2=ATAN(((XCD(J+1,K+1)-XCD(J+1,K))**2+(YCD(J+1,K+1)-YCD(J+1,K))**2FAB04390
     &)**0.50/(ZCD(J+1,K)-ZCD(J+1,K+1)))                                FAB04400
```

```
      COSB2=COS(B2)                                                     FAB04410
      SINB2=SIN(B2)                                                     FAB04420
95    TX10(J,K+1)=T10(J,K+1)*SINB1*COSA1                                FAB04430
      TY10(J,K+1)=T10(J,K+1)*SINB1*SINA1                                FAB04440
      TZ10(J,K+1)=T10(J,K+1)*COSB1                                      FAB04450
      TX01(J+1,K)=T01(J+1,K)*SINB2*COSA2                                FAB04460
      TY01(J+1,K)=T01(J+1,K)*SINB2*SINA2                                FAB04470
      TZ01(J+1,K)=T01(J+1,K)*COSB2                                      FAB04480
      T10(K,J+1)=T01(J+1,K)                                             FAB04490
      T01(K+1,J)=T10(J,K+1)                                             FAB04500
      T10OLD(K,J+1)=T01OLD(J+1,K)                                       FAB04510
      T01OLD(K+1,J)=T10OLD(J,K+1)                                       FAB04520
      TX10(K,J+1)=TY01(J+1,K)                                           FAB04530
      TY10(K,J+1)=TX01(J+1,K)                                           FAB04540
      TZ10(K,J+1)=TZ01(J+1,K)                                           FAB04550
      TX01(K+1,J)=TY10(J,K+1)                                           FAB04560
      TY01(K+1,J)=TX10(J,K+1)                                           FAB04570
      TZ01(K+1,J)=TZ10(J,K+1)                                           FAB04580
      IDIAG=0                                                           FAB04590
C                                                                       FAB04600
C     RECYCLE ON SPACE LOOP                                             FAB04610
C                                                                       FAB04620
22    CONTINUE                                                          FAB04630
C                                                                       FAB04640
C     IF SPACE LOOP COMPLETED, COMPUTE NEW PROJECTILE VELOCITY          FAB04650
C     FROM MOMENTUM BALANCE                                             FAB04660
C                                                                       FAB04670
      IF(IFLAG.EQ.0) GO TO 44                                           FAB04680
14    CONTINUE                                                          FAB04690
      GO TO 49                                                          FAB04700
44    IFRTM1=IFRONT-1                                                   FAB04710
      WRITE (6,48) TIM,IFRTM1                                           FAB04720
48    FORMAT(/1X,'TIME=',E14.5,4X,'WAVE FRONT AT=',I4)                  FAB04730
49    APROJ=ATAN((ZCD(2,1)-ZCD(1,1))/(XCD(2,1)-XCD(1,1)))              FAB04740
      TCTR=4.00E 00*T10(1,1)*SIN(APROJ)                                 FAB04750
      VPROJ=VPROJ+TCTR*DTM*DENYRN*9.80E-06*CRIMP/PMASS-XK*DXL*ZCD(1,1)*DFAB04760
     &TM*9.80E-06/PMASS                                                 FAB04770
      DKE=XKE-0.50E-03*PMASS*VPROJ**2/(FMASSM*CRIMP)                    FAB04780
      TLEGFR=SNRGY+XKNRGY+YKNRGY+ZKNRGY                                 FAB04790
      ENGYBK=DKE-TLEGFR                                                 FAB04800
      IF(XK.LT.0.001) ENGYBK=0.00E 00                                   FAB04810
      IF(VPROJ.LE.0.00E 00.OR.EPS10(1,1).GT.EPSB)  GO TO 42             FAB04820
      IF(INC1.NE.INC) GO TO 12                                          FAB04830
C                                                                       FAB04840
C     PRINT CURRENT FIELD VARIABLES                                     FAB04850
C                                                                       FAB04860
      WRITE(6,80)                                                       FAB04870
80    FORMAT( /1X,11X,'TIME',7X,'PROJ VEL',3X,'PROJ ENGY LOSS',1X,'FABRCFAB04880
     & ENGY GAIN',2X,'BACK UP ENGY',3X,'STRAIN ENGY',3X,'K.E.--X,Y,Z')  FAB04890
      WRITE(6,81) TIM,VPROJ,DKE,TLEGFR,ENGYBK,SNRGY,XKNRGY,YKNRGY,ZKNRGYFAB04900
81    FORMAT( 4X,9E14.5)                                                FAB04910
802   WRITE(6,72) ((T10(IX,IY),IX=1,JPRT),IY=1,JPRTY)                   FAB04920
72    FORMAT(1X,'T10(IX,IY)='/8(E15.5))                                 FAB04930
      WRITE(6,74)((T01(JX,JY),JX=1,JPRT),JY=1,JPRTY)                    FAB04940
74    FORMAT(1X,'T01(JX,JY)='/8(E15.5))                                 FAB04950
```

```
      WRITE (6,702) (( VZ(NX,NY),NX=1,JPRT),NY=1,JPRTY)                  FAB04960
702   FORMAT(1X,' VZ(I,J)='/9(E14.5))                                    FAB04970
      WRITE(6,701) ((XCD(MX,MY),MX=1,JPRT),MY=1,JPRTY)                   FAB04980
701   FORMAT(1X,'XCD(I,J)='/9(E14.5))                                    FAB04990
      WRITE(6,703) ((ZCD(ICX,ICY),ICX=1,JPRT),ICY=1,JPRTY)               FAB05000
703   FORMAT(1X,'ZCD(I,J)='/9(E14.5))                                    FAB05010
      WRITE(6,76) ((EPS10(KX,KY),KX=1,JPRT),KY=1,JPRTY)                  FAB05020
76    FORMAT(1X,'EPS10(KX,KY)='/8(E15.5))                                FAB05030
      WRITE(6,78) ((EPS01(LX,LY),LX=1,JPRT),LY=1,JPRTY)                  FAB05040
70    FORMAT(1X,'EPS01(LX,LY)='/8(E15.5))                                FAB05050
      IF(IPLAST.GT.0) GO TO 101                                          FAB05060
      INC1=0                                                             FAB05070
C                                                                        FAB05080
C     RECYCLE ON TIME LOOP                                               FAB05090
C                                                                        FAB05100
12    CONTINUE                                                           FAB05110
      WRITE(6,102) TMAX                                                  FAB05120
102   FORMAT(//1X,1X,'FABRIC DOES NOT FRACTURE AT TMAX', 2X,E14.5)       FAB05130
      GO TO 101                                                          FAB05140
42    WRITE(6,80)                                                        FAB05150
      WRITE(6,82) TIM,VPROJ,DKE,TLEGFR,ENGYBK,SNRGY,XKNRGY,YKNRGY,ZKNRGYFAB05160
82    FORMAT(//1X,'AT FAILURE:'/1X,4X,9E14.5)                            FAB05170
      IPLAST=1                                                           FAB05180
      GO TO 802                                                          FAB05190
101   IEND=1                                                             FAB05200
      STOP                                                               FAB05210
      END                                                                FAB05220
      SUBROUTINE BNDRY(IT,J,K)                                           FAB05230
      COMMON/IXMATL/IPT                                                  FAB05240
      COMMON/CMATL/EYRN,CHARD,EO,E1,E2,E3                                FAB05250
      COMMON/VISCO/G,VLAMDA,TAU                                          FAB05260
      COMMON/VARBL/JT,XL,DXL,DTM,DENYRN,     PMASS,CRIMP,FMASSA,FMASSM,FFAB05270
     &MASSF,UNITM,HUNITM                                                 FAB05280
      COMMON/TSNOLD/T10OLD(40,40),T01OLD(40,40),E10OLD(40,40),E01OLD(40,FAB05290
     &40)                                                                FAB05300
      COMMON/BACKUP/XK                                                   FAB05310
      COMMON/CMESH/XCD(40,40),YCD(40,40),ZCD(40,40),XCDOLD,YCDOLD,ZCDOLDFAB05320
      COMMON/TEN/T10(40,40),T01(40,40),TX10(40,40),TX01(40,40),          FAB05330
     &TY10(40,40),TY01(40,40),TZ10(40,40),TZ01(40,40),                   FAB05340
     &EPS10(40,40),EPS01(40,40)                                          FAB05350
      COMMON/VELOC/VX(40,40),VY(40,40),VZ(40,40)                         FAB05360
      COMMON/ERGCUM/XKNRGY,YKNRGY,ZKNRGY,SNRGY                           FAB05370
      COMMON/ERGELM/ELXE(40,40),ELSE(40,40),TLELEN(40,40)                FAB05380
      DVX=(TX10(J+1,K)-TX10(J,K)+2.00E 00*TX01(J+1,K))*DTM*8.8200E 00/(2FAB05390
     &.00E 00*DXL*CRIMP)                                                 FAB05400
      DVZ=(TZ10(J+1,K)-TZ10(J,K)+2.00E 00*TZ01(J+1,K))*DTM*8.8200E 00/(2FAB05410
     &.00E 00*DXL*CRIMP)+XK*DXL*ZCD(J+1,K)*DTM*9.80E-06/(UNITM/9.0E 05) FAB05420
      DVZ=-DVZ                                                           FAB05430
      VX(J+1,K)=VX(J+1,K)+DVX                                            FAB05440
      VY(J+1,K)=0.00E 00                                                 FAB05450
      VZ(J+1,K)=VZ(J+1,K)+DVZ                                            FAB05460
      VX(JT,K)=0.00E 00                                                  FAB05470
      VY(JT,K)=0.00E 00                                                  FAB05480
      VZ(JT,K)=0.00E 00                                                  FAB05490
      VX(K,J+1)=VY(J+1,K)                                                FAB05500
```

```
      VY(K,J+1)=VX(J+1,K)                                                    FAB05510
      VZ(K,J+1)=VZ(J+1,K)                                                    FAB05520
      DSQX=(XCD(J+1,K)+VX(J+1,K)*DTM/1.00E 04-XCD(J,K)-VX(J,K)*DTM/1.00EFAB05530
     & 04)**2                                                               FAB05540
      DSQY=(YCD(J+1,K)+VY(J+1,K)*DTM/1.00E 04-YCD(J,K)-VY(J,K)*DTM/1.00EFAB05550
     & 04)**2                                                               FAB05560
      DSQZ=(ZCD(J+1,K)+VZ(J+1,K)*DTM/1.00E 04-ZCD(J,K)-VZ(J,K)*DTM/1.00EFAB05570
     & 04)**2                                                               FAB05580
      DDL= SQRT(DSQX+DSQY+DSQZ)                                             FAB05590
      DSQ=(XCD(J+1,K)-XCD(J,K))**2+(YCD(J+1,K)-YCD(J,K))**2+(ZCD(J+1,K)-FAB05600
     &ZCD(J,K))**2                                                          FAB05610
      DIST= SQRT(DSQ)                                                       FAB05620
      DEPS=DDL/DIST-1.00E 00                                                FAB05630
      EPS10(J,K)=EPS10(J,K)+DEPS                                            FAB05640
      EPS01(K,J)=EPS10(J,K)                                                 FAB05650
      TSLOLD=T100LD(J,K)                                                    FAB05660
      EPSOLD=E100LD(J,K)                                                    FAB05670
      EPSLN=EPS10(J,K)                                                      FAB05680
      CALL TENSN(IT,J,K,EPSLN,TSL,EPSOLD,TSLOLD,DSNRGY)                     FAB05690
      T10(J,K)=TSL                                                          FAB05700
      T01(K,J)=T10(J,K)                                                     FAB05710
      T100LD(J,K)=TSLOLD                                                    FAB05720
      T010LD(K,J)=T100LD(J,K)                                               FAB05730
      E100LD(J,K)=EPSOLD                                                    FAB05740
      E010LD(K,J)=E100LD(J,K)                                               FAB05750
      BKEXY=2.00E 00                                                        FAB05760
      IF(J.EQ.1.AND.K.EQ.1) BKEXY=1.00E 00                                  FAB05770
      XKNRGY=XKNRGY+          BKEXY*0.50E-03*HUNITM*VX(J,K)**2/(FMASSF*CRFAB05780
     &IMP)+      BKEXY*0.50E-03*HUNITM*     VX(K,J)**2/(FMASSF*CRIMP)      FAB05790
      YKNRGY=YKNRGY+          BKEXY*0.50E-03*HUNITM*VY(J,K)**2/(FMASSF*CRFAB05800
     &IMP)+      BKEXY*0.50E-03*HUNITM*     VY(K,J)**2/(FMASSF*CRIMP)      FAB05810
      BKEZZ=4.00E 00                                                        FAB05820
      IF(J.EQ.1.AND.K.EQ.1) BKEZZ=2.00E 00                                  FAB05830
      ZKNRGY=ZKNRGY+          BKEZZ*0.50E-03*HUNITM*     VZ(J,K)**2/(FMASSFAB05840
     &F*CRIMP)                                                              FAB05850
      SNRGY=SNRGY+DSNRGY                                                    FAB05860
      CTRSE=4.00E 00                                                        FAB05870
      IF(J.EQ.1.AND.K.EQ.1) CTRSE=1.00E 00                                  FAB05880
      ELSE(J,K)=ELSE(J,K)+DSNRGY/CTRSE                                      FAB05890
      ELSE(K,J)=ELSE(J,K)                                                   FAB05900
      CTRKE=1.00E 00                                                        FAB05910
      IF(J.EQ.1.AND.K.EQ.1) CTRKE=2.00E 00                                  FAB05920
      ELKE(J,K)=ELKE(J,K)+CTRKE*0.50E-03*HUNITM*     (VX(J,K)**2+VY(J,K)*FAB05930
     &*2+VZ(J,K)**2)/(FMASSF*CRIMP)                                         FAB05940
      ELKE(K,J)=ELKE(J,K)                                                   FAB05950
      TLELEN(J,K)=ELSE(J,K)+ELKE(J,K)                                       FAB05960
      TLELEN(K,J)=TLELEN(J,K)                                               FAB05970
      XCDOLD=XCD(J,K)                                                       FAB05980
      YCDOLD=YCD(J,K)                                                       FAB05990
      ZCDOLD=ZCD(J,K)                                                       FAB06000
      XCD(J,K)=XCD(J,K)+VX(J,K)*DTM/1.00E 04                                FAB06010
      YCD(J,K)=YCD(J,K)+VY(J,K)*DTM/1.00E 04                                FAB06020
      ZCD(J,K)=ZCD(J,K)+VZ(J,K)*DTM/1.00E 04                                FAB06030
      IF(J.EQ.K) GO TO 20                                                   FAB06040
      XCD(K,J)=XCD(K,J)+VX(K,J)*DTM/1.00E 04                                FAB06050
```

```
      YCD(K,J)=YCD(K,J)+VY(K,J)*DTM/1.00E 04                                FAB06060
      ZCD(K,J)=ZCD(K,J)+VZ(K,J)*DTM/1.00E 04                                FAB06070
20    A=ATAN((YCD(J+1,K)-YCD(J,K))/(XCD(J+1,K)-XCD(J,K)))                   FAB06080
      COSA=COS(A)                                                           FAB06090
      SINA=SIN(A)                                                           FAB06100
      IF(ABS(ZCD(J+1,K)-ZCD(J,K))-0.0001) 10,10,11                          FAB06110
10    COSB=0.00E 00                                                         FAB06120
      SINB=1.00E 00                                                         FAB06130
      GO TO 12                                                              FAB06140
11    B=ATAN((XCD(J+1,K)-XCD(J,K))/(ZCD(J,K)-ZCD(J+1,K)))                   FAB06150
      COSB=COS(B)                                                           FAB06160
      SINB=SIN(B)                                                           FAB06170
12    TX10(J,K)=T10(J,K)*SINB*COSA                                          FAB06180
      TY10(J,K)=T10(J,K)*SINB*SINA                                          FAB06190
      TZ10(J,K)=T10(J,K)*COSB                                               FAB06200
      TX01(K,J)=TY10(J,K)                                                   FAB06210
      TY01(K,J)=TX10(J,K)                                                   FAB06220
      TZ01(K,J)=TZ10(J,K)                                                   FAB06230
      RETURN                                                                FAB06240
      END                                                                   FAB06250
      SUBROUTINE TENSN(IT,J,K,EPSS,TS,EPSOLD,TSLOLD,DSEN)                   FAB06260
C . . . . . . . . . . . . . . . . . . . . . . . . . . . . . . . . . . . . . FAB06270
C .                                                                       . FAB06280
C .   T E N S N                                                           . FAB06290
C .                                                                       . FAB06300
C .       A SUBROUTINE TO CALL APPROPRIATE CONSTITUTIVE MODEL             . FAB06310
C .       FOR COMPUTATION OF ELEMENT TENSION FROM STRAIN                  . FAB06320
C .       OR STRAIN HISTORY                                               . FAB06330
C .                                                                       . FAB06340
C . . . . . . . . . . . . . . . . . . . . . . . . . . . . . . . . . . . . . FAB06350
C                                                                         FAB06360
      EXTERNAL F                                                          FAB06370
      REAL*8 EN1,EN2,A,ALP,VLBD,F,X(1),EPS,EPS2,ETA,B1,B2,B3,B4,A1,A2,A3FAB06380
      REAL*8 DSINH,DCOSH                                                  FAB06390
      COMMON/IXMATL/IPT                                                   FAB06400
      COMMON/CMATL/EYRN,CHARD,E0,E1,E2,E3                                 FAB06410
      COMMON/VISCO/G,VLAMDA,TAU                                           FAB06420
      COMMON/NONLR/EN1,EN2,A,ALP,VLBD                                     FAB06430
      COMMON/NONEC/A1,A2,A3                                               FAB06440
      COMMON/VARBL/JT,XL,DXL,DTM,DENYRN,     PMASS,CRIMP,FMASSA,FMASSM,FFAB06450
     &MASSF,UNITM,HUNITM                                                  FAB06460
      COMMON/TSNOLD/T10OLD(40,40),T01OLD(40,40),E10OLD(40,40),E01OLD(40,FAB06470
     &40)                                                                 FAB06480
      COMMON/BACKUP/XK                                                    FAB06490
      IF(EPSS.LE.0.00E 00) GO TO 1                                        FAB06500
      SYMCTR=1.00E 00                                                     FAB06510
      IF(J.EQ.1.AND.K.EQ.1) SYMCTR=0.500E 00                              FAB06520
      IF(IPT.EQ.2) GO TO 12                                               FAB06530
      IF(IPT.EQ.3) GO TO 14                                               FAB06540
      IF(IPT.EQ.4) GO TO 18                                               FAB06550
C                                                                         FAB06560
C     NONLINEAR (CUBIC POLYNOMIAL) ELASTIC MODEL                          FAB06570
C                                                                         FAB06580
      TS=E0+E1*EPSS+E2*EPSS**2+E3*EPSS**3                                 FAB06590
      DSEN=4.00E 00*(E0*EPSS+0.50E 00*EPSS**2+0.33333E 00*EPSS**3+0.2500FAB06600
```

```
     &E 00*EPSS**4)*DENYRN*DXL*CRIMP*9.80E-05*SYMCTR/(FMASSM*CRIMP)      FAB06610
      GO TO 2                                                            FAB06620
C                                                                        FAB06630
C     NONLINEAR (EXPONENTIAL STRAIN HARDENING) ELASTIC MODEL             FAB06640
C                                                                        FAB06650
12    TS=EYRN*EPSS**CHARD                                                FAB06660
      DSEN=4.0E 00*(1.00E 00/(1.00E 00+CHARD))*EYRN*EPSS**(1.00E 00+CHARFAB06670
     &D)*DENYRN*DXL*CRIMP*9.80E-05*SYMCTR/(FMASSM*CRIMP)                 FAB06680
      GO TO 2                                                            FAB06690
C                                                                        FAB06700
C     LINEAR (STANDARD LINEAR SOLID) VISCOELASTIC MODEL                  FAB06710
C                                                                        FAB06720
14    B=G*(1.00E 00-VLAMDA)/TAU                                          FAB06730
      D=1.00E 00+DTM/TAU                                                 FAB06740
      IF(IT.GT.1) GO TO 16                                               FAB06750
      EPSOLD=0.00E 00                                                    FAB06760
      TSLOLD=0.00E 00                                                    FAB06770
16    TS=(G*(EPSS-EPSOLD)+B*EPSS*DTM+TSLOLD)/D                           FAB06780
      DSEN=(4.00E 00*0.50E 00*(TS+TSLOLD)*(EPSS-EPSOLD)*DXL*DENYRN*CRIMPFAB06790
     &*9.80E-05*SYMCTR)/(FMASSM*CRIMP)                                   FAB06800
      EPSOLD=EPSS                                                        FAB06810
      TSLOLD=TS                                                          FAB06820
      GO TO 2                                                            FAB06830
C                                                                        FAB06840
C     NONLINEAR (EYRING) VISCOELASTIC MODEL                              FAB06850
C                                                                        FAB06860
18    IF(IT.GT.1) GO TO 20                                               FAB06870
      EPSOLD=0.00E 00                                                    FAB06880
      TSLOLD=0.00E 00                                                    FAB06890
20    B1=EN2*A*DTM                                                       FAB06900
      B2=EN2*(1.00D 00+VLBD)                                             FAB06910
      B3=ALP*EN1*EPSS                                                    FAB06920
      B4=EPSS-EPSOLD                                                     FAB06930
      A1=B1*DCOSH(B3)                                                    FAB06940
      A2=-B1*DSINH(B3)                                                   FAB06950
      A3=-B2*B4-TSLOLD                                                   FAB06960
      EPS=1.00D-06                                                       FAB06970
      EPS2=1.00D-06                                                      FAB06980
      ETA=1.00D-02                                                       FAB06990
      NSIG=6                                                             FAB07000
      N=1                                                                FAB07010
      X(1)=TSLOLD                                                        FAB07020
      ITMAX=100                                                          FAB07030
      CALL ZNONLR(F,EPS,EPS2,ETA,NSIG,N,X,ITMAX,IER)                     FAB07040
      TS=X(1)                                                            FAB07050
      DSEN=(4.00E 00*0.50E 00*(TS+TSLOLD)*(EPSS-EPSOLD)*DXL*DENYRN*CRIMPFAB07060
     &*9.80E-05*SYMCTR)/(FMASSM*CRIMP)                                   FAB07070
      EPSOLD=EPSS                                                        FAB07080
      TSLOLD=TS                                                          FAB07090
      GO TO 2                                                            FAB07100
1     TS=0.00E 00                                                        FAB07110
      DSEN=0.00E 00                                                      FAB07120
2     RETURN                                                             FAB07130
      END                                                                FAB07140
      REAL FUNCTION F*8(S)                                               FAB07150
```

```
      REAL*8 DSINH,DCOSH                                                FAB07160
      REAL*8 EN1,EN2,A,ALP,VLBD,S,A1,A2,A3                              FAB07170
      COMMON/NONLR/EN1,EN2,A,ALP,VLBD                                   FAB07180
      COMMON/NONEQ/A1,A2,A3                                             FAB07190
      F=S+A1*DSINH(ALP*S)+A2*DCOSH(ALP*S)+A3                            FAB07200
      RETURN                                                            FAB07210
      END                                                               FAB07220
      SUBROUTINE ZNONLR(F,EPS,EPS2,ETA,NSIG,N,X,ITMAX,IER)              FAB07230
C                                                                       FAB07240
C     MULLER ALGORITHM FOR ITERATIVE SOLUTION OF NONLINEAR              FAB07250
C     EQUATION - - USED FOR EYRING CONSTITUTIVE MODEL                   FAB07260
C                                                                       FAB07270
      DIMENSION          X(1)                                           FAB07280
      DOUBLE PRECISION   X,XI,AXI,EPS,EPS2,ETA,FXI,AFXI,DI,HI,FXIPHI,  FAB07290
     *                   DER,XIPI,ERR,ERR1,CRIT1,P1,P001,ZERO,ONE,TEN   FAB07300
      DATA               P1,P001,ZERO,ONE,TEN/.1D0,.001D0,0.D0,1.D0,    FAB07310
     *                   10.D0/                                         FAB07320
      IER = 0                                                           FAB07330
      IR=0                                                              FAB07340
      CRIT1 = TEN**(-NSIG)                                              FAB07350
      DO 30 I=1,N                                                       FAB07360
         IC = 1                                                         FAB07370
         XI = X(I)                                                      FAB07380
 5       AXI = DABS(XI)                                                 FAB07390
         IF (I .EQ. 1) GO TO 15                                         FAB07400
         NM1=I-1                                                        FAB07410
         DO 10 J= 1,NM1                                                 FAB07420
            IF (DABS(XI - X(J)) .LT. EPS2) XI = XI + ETA                FAB07430
10       CONTINUE                                                       FAB07440
15       FXI = F(XI)                                                    FAB07450
         AFXI = DABS(FXI)                                               FAB07460
         IF (AFXI .LE. EPS) GO TO 25                                    FAB07470
         DI = 10.D-9                                                    FAB07480
         IF (AXI .GE. P1) DI = P001*AXI                                 FAB07490
         HI=DMIN1(AFXI,DI)                                              FAB07500
         FXIPHI = F(XI + HI)                                            FAB07510
         DER = (FXIPHI - FXI)/HI                                        FAB07520
         IF (DER .EQ. ZERO) GO TO 20                                    FAB07530
         XIPI=FXI/DER                                                   FAB07540
         CALL OVERFL (J)                                                FAB07550
         IF (J .EQ. 1) GO TO 20                                         FAB07560
         XIPI=XI-XIPI                                                   FAB07570
         ERR = DABS(XIPI - XI)                                          FAB07580
         XI = XIPI                                                      FAB07590
         IF(AXI.EQ.ZERO) AXI=ONE                                        FAB07600
         ERR1=ERR/AXI                                                   FAB07610
         CALL OVERFL(J)                                                 FAB07620
         IF(J.EQ.1) ERR1=ERR                                            FAB07630
         IF(ERR1.LE.CRIT1) GO TO 25                                     FAB07640
         IC = IC + 1                                                    FAB07650
         IF (IC .LE. ITMAX)  GO TO 5                                    FAB07660
         X(I) = 111111.D0                                               FAB07670
         IR=IR+1                                                        FAB07680
         IER=33                                                         FAB07690
         GO TO 30                                                       FAB07700
```

```
20        X(I) = 222222.D0                                        FAB07710
          IR=IR+1                                                 FAB07720
          IER=34                                                  FAB07730
          GO TO 30                                                FAB07740
25        X(I)=XI                                                 FAB07750
30      CONTINUE                                                  FAB07760
        ITMAX = IC                                                FAB07770
        IF(IER.EQ.0) GO TO 9005                                   FAB07780
        IF(IR.LE.1) GO TO 9000                                    FAB07790
        IER=35                                                    FAB07800
9000    CONTINUE                                                  FAB07810
        CALL UERTST(IER,6HZREAL2)                                 FAB07820
9005    RETURN                                                    FAB07830
        END                                                       FAB07840
```

APPENDIX B - The XOVER Code

General. XOVER is the FORTRAN program written to carry out the calculations described in Chapter IV of this report. It is identical in concept to the FABRIC code, differing primarily in the dimensionality of the problem. XOVER is essentially a treatment of transverse ballistic impact on a single fiber as described earlier by Roylance [18], but it has been modified to include a second fiber, transverse to the first, which receives its loading from the motion of the first (primary) fiber. The code is made more complicated than the single-fiber case by the necessity of allowing motion in all three directions for the secondary fiber, and in computing the initial values of the secondary fiber in terms of the primary fiber motion. As described in the text, allowance is made for slippage of the secondary fiber along the primary.

Code requirements. As was true for the FABRIC code, XOVER requires little hardware or software support. At present, the code includes a call to an MIT library subroutine PRTPLT for the purpose of obtaining a rough plot of the nodal variable values on the system line printer. This subroutine call could

be removed without affecting the performance of other parts of the code. For a typical run, in which two crossed Kevlar fibers were impacted at 300 m/sec, the job run time was 0.305 minutes and 170 kilobytes of core was reserved.

Definition of program variables. XOVER is conveniently described by means of a listing of the principal program variables: (* denotes input data)

A	8.826×10^6 (dt/dl)
CROSS*	Initial crossover position (fraction of XL1)
CZ	Wavespeed (m/sec)
DEN*	Fiber denier
DL	Length increment (cm)
DT	Time increment (sec)
E1(J), E2(J)	Strain at jth node in primary and secondary fiber
E1OLD(J), E2OLD(J)	Strain at previous time increment
EMAX*	Maximum strain permitted
EEMAX	Maximum strain in fibers
G*	Instantaneous modulus (gm/den)
IPLOT*	.EQ. 0 if no printer plot is desired
I1,I2,I3*	Node numbers at which plot desired (I3 on secondary)

JX	Crossover node on primary fiber
JJX	Initial crossover node
KMAX	Maximum number of time increments
LPSKIP*	Length print skip
LTSKIP*	Time print skip
NLINC*	Number of length increments on primary fiber
PMASS*	Projectile mass (gm)
PVELOC*	Projectile velocity (m/sec)
SLIDE*	Slip factor (1-no slip, 0-no friction)
TAU*	Viscous relaxation time (sec)
TITLE*	Alphanumeric title (80 characters max.)
T1(J), T2(J)	Tension in primary and secondary fibers (gm/den)
T1OLD(J), T2)LD(J)	Previous tension (gm/den)
TMAX*	Maximum time (sec)
U1(J), U2(J)	X-component of velocity in primary and secondary fibers (m/sec)
V1(J), V2(J)	Y-component of velocity
VLAMDA*	Viscous fraction (0-elastic, 1-purely viscous)

W1(J), W2(J)	Z-component of velocity
XL1, XL2	Half-length of primary and secondary fibers (cm)
X1(J), X2(J)	X-coordinate of jth node on primary and secondary fibers
Y1(J), Y2(J)	Y-coordinate
Z1(J), Z2(J)	Z-coordinate

Note that in its present form, XOVER is written explicitly for viscoelastic material response of the standard linear solid type. For elastic fibers, the user should set VLAMDA to zero and G to the Young's modulus; TAU could be any nonzero value. The variables required by the code are indicated as input information and are specified in the above list by an asterisk; an example of a typical input data set is given below.

EXAMPLE:

```
VELOCITY STUDY, V = 300 m/sec  KEVLAR 29
1.0E+06   300     20.          10.      0.5      1.0
1500      550   0.14-0.4        0.
   100      5        5         287E     0.05
     1     25       75         25
```

1) 204A TITLE

2) 6E10.3 PMASS, PVELØC, XL1, XL2, CRØSS, SLIDE

3) 4E10. DEN, G. TAU, VLAMPA

4) 3I 10, 2E 10.3 NLINC, LPSKIP, LTSKIP, TMAX, EMAX

5) 4I 10 IPLØT, I1, I2, I3

Typical Output. Typical output from the XOVER code for impact on two crossed Kevlar 29 fibers at 300 m/sec is given below:

VELOCITY STUDY, V =300 M/SEC KEVLAR 29

PROJECTILE MASS = 0.100E+07 GRAMS
PROJECTILE VELOCITY = 300.0 M/SEC
HALF-LENGTH OF PRIMARY FIBER = 20.00 CM
HALF-LENGTH OF SECONDARY FIBER = 10.00 CM
CROSSOVER POINT = 0.500 (FRACTION OF PRIMARY)
SLIDE FACTOR = 1.000

FIBER DENIER = 1500.0
INSTANTANEOUS MODULUS = 550.0 GM/DEN
RELAXATION TIME = 0.143E-01 SEC
VISCOUS FRACTION = 0.0

NUMBER LENGTH INCREMENTS = 100
PRINT SKIP FACTOR = 5
TIME SKIP FACTOR = 10
MAXIMUM TIME = 0.287E-04 SEC
MAXIMUM STRAIN = 0.050

LENGTH INCREMENT = 0.200E+00 CM
NUMBER NODES IN PRIMARY = 101
NUMBER NODES IN SECONDARY = 51
WAVESPEED = 6967.3 M/SEC
TIME INCREMENT = 0.287E-06 SEC
CROSSOVER NODE = 51
MAXIMUM NUMBER TIME INCREMENTS = 99

PLOT OPTIONS = 1 25 75 25

VELOCITY STUDY, V =300 M/SEC KEVLAR 29

OUTPUT FOR TIME = 0.258E-04 SEC
CURRENT PROJECTILE VELOCITY = 300.0 M/SEC

FIELD VARIABLES FOR PRIMARY FIBER

J	X1(J)	Y1(J)	U1(J)	V1(J)	T1(J)	P1(J)
1	0.0	0.775	0.0	300.0	5.42	0.00985
6	0.912	0.343	-13.7	269.8	5.38	0.00979
11	1.848	0.095	-67.7	25.8	5.36	0.00974
16	2.852	0.000	-68.9	0.0	5.43	0.00987
21	3.867	0.000	-67.3	0.0	5.36	0.00974
26	4.877	0.000	-67.9	0.0	5.48	0.00996
31	5.887	0.000	-67.1	0.0	5.51	0.01002
36	6.897	0.000	-66.2	0.0	5.54	0.01007
41	7.908	0.000	-64.8	0.0	5.49	0.00997
46	8.918	0.000	-66.6	0.0	5.60	0.01019
51	9.928	0.000	-66.7	0.0	5.24	0.00952
56	10.937	0.0	-64.1	0.0	5.06	0.00920
61	11.947	0.0	-66.1	0.0	5.20	0.00946
66	12.956	0.0	-68.7	0.0	5.40	0.00982
71	13.966	0.0	-63.5	0.0	5.00	0.00908
76	14.975	0.0	-66.3	0.0	5.23	0.00951
81	15.985	0.0	-77.7	0.0	6.11	0.01111
86	16.996	0.0	-52.0	0.0	4.10	0.00745
91	18.000	0.0	0.0	0.0	0.0	0.0

CROSSOVER NODE = 51

FIELD VARIABLES FOR SECONDARY FIBER

J	X2(J)	Y2(J)	Z2(J)	U2(J)	V2(J)	W2(J)	T2(J)	P2(J)
1	9.928	0.000	0.0	-66.7	0.0	0.0	0.70	0.00128
6	10.000	0.0	0.993	-0.0	0.0	-8.8	0.69	0.00125
11	10.000	0.0	1.994	0.0	0.0	-10.0	0.78	0.00142
16	10.000	0.0	2.996	0.0	0.0	-10.6	0.83	0.00150
21	10.000	0.0	3.997	0.0	0.0	-8.8	0.69	0.00126
26	10.000	0.0	4.999	0.0	0.0	-7.2	0.56	0.00102
31	10.000	0.0	5.999	0.0	0.0	-5.8	0.46	0.00083
36	10.000	0.0	7.000	0.0	0.0	-1.0	0.08	0.00014
41	10.000	0.0	8.000	0.0	0.0	0.0	0.0	0.0

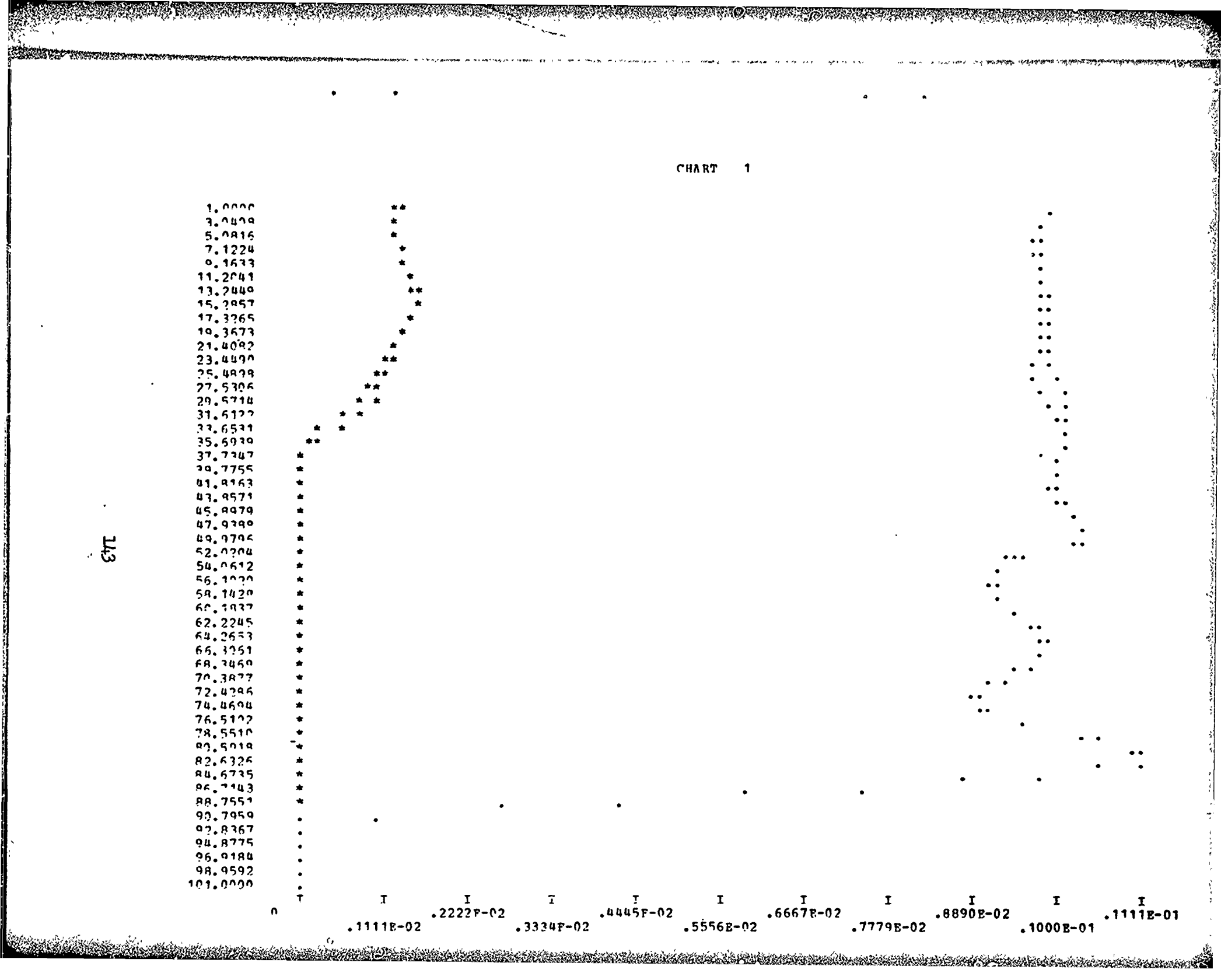
CHART 1
1.0000
3.0409
5.0816
7.1224
9.1633
11.2041
13.2449
15.2857
17.3265
19.3673
21.4082
23.4490
25.4898
27.5306
29.5714
31.6122
33.6531
35.6939
37.7347
39.7755
41.8163
43.8571
45.8979
47.9388
49.9796
52.0204
54.0612
56.1020
58.1429
60.1837
62.2245
64.2653
66.3061
68.3469
70.3877
72.4286
74.4694
76.5102
78.5510
80.5918
82.6326
84.6735
86.7143
88.7551
90.7959
92.8367
94.8775
96.9184
98.9592
101.0000
0
.1111E-02
.2222E-02
.3334E-02
.4445E-02
.5556E-02
.6667E-02
.7779E-02
.8890E-02
.1000E-01
.1111E-01

CHART 2

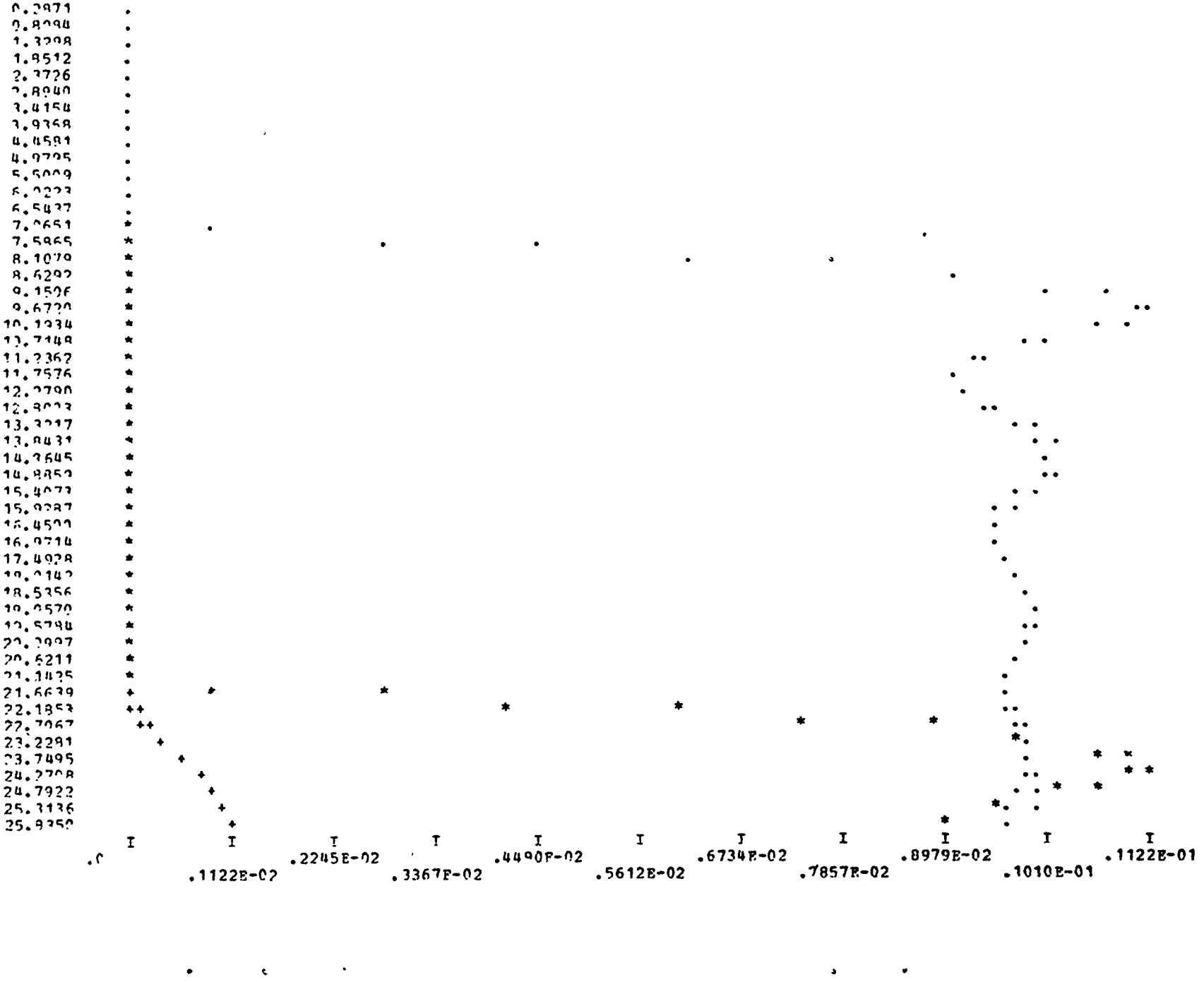
0.0
.1122E-02
.2245E-02
.3367E-02
.4490E-02
.5612E-02
.6734E-02
.7857E-02
.8979E-02
.1010E-01
.1122E-01

```
                C
                C   XOVER - A DIRECT-ANALYSIS CODE FOR TWO CROSSED FIBERS
                C   AUTHOR  DAVID BOYLANCE  MIT   WRITTEN 1976
                C
0001                  DIMENSION  TITLE(200),X1(200),X2(200),Y1(200),Z2(200),U1(200),
                     1      U2(200),V1(200),V2(200),W2(200),T1(200),T2(200),E1(200),
                     2      E2(200),T1OLD(200),T2OLD(200),E1OLD(200),E2OLD(200),Y2(200),
                     3      APPAY(200,4),APPAZ(200,3)
                C
                C   READ AND PRINT PROBLEM INPUT PARAMETERS
                C
0002               10  READ(5,1000,END=110) (TITLE(J),J=1,20)
0003                   READ(5,1010) PMASS,PVELOC,XL1,XL2,CROSS,SLIDE
0004                   READ(5,1020) DEN,G,TAU,VLAMDA
0005                   READ(5,1030) NLINC,LPSKIP,LTSKIP,TMAX,EMAX
0006                   READ(5,1035) IPLOT,I1,I2,I3
                C
0007                   WRITE(6,1040) (TITLE(J),J=1,20)
0008                   WRITE(6,1050) PMASS,PVELOC,XL1,XL2,CROSS,SLIDE
0009                   WRITE(6,1060) DEN,G,TAU,VLAMDA
0010                   WRITE(6,1070) NLINC,LPSKIP,LTSKIP,TMAX,EMAX
                C
                C   COMPUTE AND PRINT INTERNAL PROBLEM PARAMETERS
                C
0011                   DL=XL1/NLINC
0012                   NL1=NLINC+1
0013                   NL2=(XL2/DL)+1.5
0014                   NMAX=NL1
0015                   IF(NL1.LT.NL2) NMAX=NL2
0016                   CZ=SQRT(88260.*G)
0017                   DT=DL/(100.*CZ)
0018                   JX=(XL1*CROSS/DL)+1.5
0019                   JJX=JX
0020                   KMAX=TMAX/DT
0021                   A=8.826E+06*DT/DL
0022                   WRITE(6,1080) DL,NL1,NL2,CZ,DT,JX,KMAX
0023                   WRITE(6,1085) IPLOT,I1,I2,I3
                C
                C   INITIALIZE ARRAYS
                C
0024                   DO 20 J=1,200
0025                      X1(J)=DL*FLOAT(J-1)
0026                      Y1(J)=0.
0027                      U1(J)=0.
0028                      V1(J)=0.
0029                      T1(J)=0.
0030                      T1OLD(J)=0.
0031                      E1(J)=0.
0032                      E1OLD(J)=0.
0033                      APPAZ(J,1)=FLOAT(J)
0034                      APPAZ(J,2)=0.
0035                      APPAZ(J,3)=0.
0036               20  CONTINUE
```

```
                C
0037                  DO 30 J=1,200
0038                     X2(J)=X1(JX)
0039                     Z2(J)=DL*FLOAT(J-1)
0040                     Y2(J)=0.
0041                     U2(J)=0.
0042                     V2(J)=0.
0043                     W2(J)=0.
0044                     T2(J)=0.
0045                     T2OLD(J)=0.
0046                     P2(J)=0.
0047                     E2OLD(J)=0.
0048               30    CONTINUE
0049                     ITSKIP=0
                C
                C    BEGIN TIME LOOP - IMPOSE PROJECTILE VELOCITY ON PRIMARY FIBER
                C
0050                  DO 90 K=1,KMAX
0051                     V1(1)=PVELOC
0052                     U1(1)=0.
0053                     T=FLOAT(K)*DT
                C
                C       BEGIN PRIMARY LENGTH LOOP
                C
0054                     DO 50 J=1,VL1
                C
                C          BRANCH IF AHEAD OF WAVEFRONT
                C
0055                     KK=K+2
0056                     IF(J.GE.KK) GO TO 55
                C
                C          MOMENTUM BALANCE
                C
0057                     THETA1=ATAN((Y1(J+1)-Y1(J))/(X1(J+1)-X1(J)))
0058                     THETA2=ATAN((Y1(J+2)-Y1(J+1))/(X1(J+2)-X1(J+1)))
0059                     U1(J+1)=U1(J+1)+(T1(J+1)*COS(THETA2)-T1(J)*COS(THETA1))*A
0060                     V1(J+1)=V1(J+1)+(T1(J+1)*SIN(THETA2)-T1(J)*SIN(THETA1))*A
                C
                C          ADD EFFECT OF SECONDARY FIBER IF AT J = JX - 1
                C
0061                     KK2=JX-1
0062                     IF(J.NE.KK2) GO TO 40
                C
0063                        D2=((X2(2)-X2(1))**2+(Y2(2)-Y2(1))**2
                1              +(Z2(2)-Z2(1))**2)**0.5
0064                        D1=((X1(JX)-X1(JX-1))**2+(Y1(JX)-Y1(JX-1))**2)**0.5
0065                        PHI1=ATAN((Y1(JX)-Y1(JX-1))/(X1(JX)-X1(JX-1)))
0066                        T2PARA=(T2(1)/(D2*D1))*((X2(2)-X2(1))*(X1(JX)-X1(JX-1))
                1              +(Y2(2)-Y2(1))*(Y1(JX)-Y1(JX-1)))
0067                        T2PERP=(T2(1)/(D2*D1))*((X2(2)-X2(1))*(Y1(JX-1)-Y1(JX))
                1              +(Y2(2)-Y2(1))*(X1(JX)-X1(JX-1)))
0069                        U1(J+1)=U1(J+1)+2.*(SLIDE*T2PARA*COS(PHI1)
                1              +T2PERP*SIN(PHI1))*A
```

```
0069                        V1(J+1)=V1(J+1)+2.*(SLIDE*T2PARA*SIN(PHI1)
                       1       +T2PERP*COS(PHI1))*A
                    C
0070                   40   CONTINUE
                    C
                    C       IMPOSE CLAMP BOUNDARY CONDITION
                    C
0071                        U1(NL1)=0.
0072                        V1(NL1)=0.
                    C
                    C       STRAIN-DISPLACEMENT RELATION
                    C
0073                        ALOLD=SQRT((Y1(J)-Y1(J+1))**2+(X1(J)-X1(J+1))**2)
0074                        ALNEW=SQRT(
                       1        ((Y1(J)+V1(J)*DT*100.)-(Y1(J+1)+V1(J+1)*DT*100.))**2
                       2      +((X1(J)+U1(J)*DT*100.)-(X1(J+1)+U1(J+1)*DT*100.))**2)
0075                        E1(J)=E1(J)+(ALNEW/ALOLD)-1.
0076                        AREAZ(J,2)=E1(J)
                    C
                    C       CONSTITUTIVE RELATION (STANDARD LINEAR SOLID)
                    C
0077                        T1(J)=(G*(E1(J)-E1OLD(J))+((1.-VLAMDA)*G/TAU)*E1(J)*DT
                       1       +T1OLD(J))/(1.+DT/TAU)
0078                        E1OLD(J)=E1(J)
0079                        T1OLD(J)=T1(J)
                    C
                    C       COMPUTE NEW COORDINATES
                    C
0080                        X1(J)=X1(J)+U1(J)*100.*DT
0081                        Y1(J)=Y1(J)+V1(J)*100.*DT
                    C
                    C     END OF PRIMARY LENGTH LOOP
                    C
0082                   50   CONTINUE
                    C
                    C     IMPOSE SLIP CONDITION ON SECONDARY FIBER, IF REACHED BY WAVEFRONT
                    C
0083                   55   CONTINUE
0084                        KK3=JJY-2
0085                        IF (K.LT.KK3) GO TO 82
0086                        THETA=ATAN((Y1(JX)-Y1(JX-1))/(X1(JX)-X1(JX-1)))
0087                        VPARA=U1(JX)*COS(THETA)+V1(JX)*SIN(THETA)
0088                        VPERP=V1(JX)*COS(THETA)-U1(JX)*SIN(THETA)
                    C
0089                        U2(1)=SLIDE*VPARA*COS(THETA)-VPERP*SIN(THETA
0090                        V2(1)=SLIDE*VPARA*SIN(THETA)+VPERP*COS(THETA)
0091                        W2(1)=0.
                    C
                    C     BEGIN SECONDARY LENGTH LOO
                    C
0092                        DO 60 J=1,NL2
                    C
                    C       BRANCH IF AHEAD OF WAVEFRONT
```

```
                      C
0093                          KK2=K-JJX+2
0094                          IF(J.GE.KK2) GO TO 65
                      C
                      C       MOMENTUM BALANCE
                      C
0095                          ALJ=SQRT((X2(J+1)-X2(J))**2+(Y2(J+1)-Y2(J))**2
                         1       +(Z2(J+1)-Z2(J))**2)
0096                          ALJP1=SQRT((X2(J+2)-X2(J+1))**2+(Y2(J+2)-Y2(J+1))**2
                         1       +(Z2(J+2)-Z2(J+1))**2)
0097                          SUMFX=T2(J+1)*((X2(J+2)-X2(J+1))/ALJP1)
                         1       -T2(J)*((X2(J+1)-X2(J))/ALJ)
0098                          SUMFY=T2(J+1)*((Y2(J+2)-Y2(J+1))/ALJP1)
                         1       -T2(J)*((Y2(J+1)-Y2(J))/ALJ)
0099                          SUMFZ=T2(J+1)*((Z2(J+2)-Z2(J+1))/ALJP1)
                         1       -T2(J)*((Z2(J+1)-Z2(J))/ALJ)
                      C
0100                          U2(J+1)=U2(J+1)+SUMFX*A
0101                          V2(J+1)=V2(J+1)+SUMFY*A
0102                          W2(J+1)=W2(J+1)+SUMFZ*A
                      C
                      C       IMPOSE CLAMP BOUNDARY CONDITION
                      C
0103                          U2(NL2)=0.
0104                          V2(NL2)=0.
0105                          W2(NL2)=0.
                      C
                      C       STRAIN-DISPLACEMENT RELATION
                      C
0106                          ALOLD=SQRT((X2(J)-X2(J+1))**2+(Y2(J)-Y2(J+1))**2
                         1       +(Z2(J)-Z2(J+1))**2)
0107                          ALNEW=SQRT(((X2(J)+U2(J)*100.*DT)-(X2(J+1)+U2(J+1)*100.
                         1       *DT))**2    +((Y2(J)+V2(J)*100.*DT)-(Y2(J+1)+V2(J+1)
                         2       *100.*DT))**2 +((Z2(J)+W2(J)*100.*DT)
                         3       -(Z2(J+1)+W2(J+1)*100.*DT))**2)
0108                          F2(J)=F2(J)+(ALNEW/ALOLD)-1.
0109                          ARRAZ(J,3)=E2(J)
                      C
                      C       CONSTITUTIVE RELATION (STANDARD LINEAR SOLID)
                      C
0110                          T2(J)=(G*(E2(J)-E2OLD(J))+((1.-VLAMDA)*G/TAU)*E2(J)*DT
                         1       +T2OLD(J))/(1.+DT/TAU)
0111                          F2OLD(J)=F2(J)
0112                          T2OLD(J)=T2(J)
                      C
                      C       COMPUTE NEW COORDINATES
                      C
0113                          X2(J)=X2(J)+U2(J)*100.*DT
0114                          Y2(J)=Y2(J)+V2(J)*100.*DT
0115                          Z2(J)=Z2(J)+W2(J)*100.*DT
                      C
                      C     END OF SECONDARY LENGTH LOOP
                      C
```

```
0116                60      CONTINUE
                    C
                    C       LOCATE NEW CROSSOVER NODE
                    C
0117                65      CONTINUE
0118                        CHECK=(X2(1)-X1(JX))/(X1(JX+1)-X1(JX))
0119                        MOVE=1
0120                        IF (CHECK.LT.0.) MOVE=-1
0121                        CHECK=CHECK*MOVE
0122                        IF (CHECK.LT.0.5) GO TO 80
0123                        JX=JX+MOVE
0124                        GO TO 65
0125                80  CONTINUE
                    C
                    C       CALCULATE NEW PROJECTILE VELOCITY
                    C
0126                82      PVELOC=PVELOC-2.*T1(1)*SIN(ATAN((Y1(1)-Y1(2))/(X1(2)-X1(1))))
                      1        *9.80665*DEN*DT/PMASS
                    C
                    C       STORE SELECTED STRAIN VALUES IN PLOT ARRAY
                    C
0127                        IF(IPLOT.EQ.0) GO TO 84
0128                           ARRAY(K,1)=T*1.0E+06
0129                           ARRAY(K,2)=P1(I1)
0130                           ARRAY(K,3)=P1(I2)
0131                           ARRAY(K,4)=P2(I3)
0132                84      CONTINUE
                    C
                    C       PRINT FIELD VARIABLES AT TIME T
                    C
0133                        ITSKIP=ITSKIP+1
0134                        IF(ITSKIP.NE.LTSKIP) GO TO 90
0135                        WRITE(6,1090) (TITLE(J),J=1,20),T,PVELOC
0136                        WRITE(6,1100)
0137                        IF(KK.GT.NL1) KK=NL1
0138                        WRITE(6,1110) (J,X1(J),Y1(J),U1(J),V1(J),T1(J),P1(J),
                      1        J=1,KK,LPSKIP)
0139                        WRITE(6,1115) JX
0140                        IF(K.LT.KK2) GO TO 85
0141                        WRITE(6,1120)
0142                        IF(KK2.GT.NL2) KK2=NL2
0143                        WRITE(6,1130) (J,X2(J),Y2(J),Z2(J),U2(J),V2(J),W2(J),
                      1        T2(J),P2(J),J=1,KK2,LPSKIP)
0144                85      ITSKIP=0
0145                        IF(IPLOT.EQ.0) GO TO 88
0146                        CALL PRTPLT(1,ARRAY,NMAX,3,0,0,200,3)
0147                88      CONTINUE
                    C
                    C       RECYCLE FOR NEW TIME INCREMENT
                    C
0148                        KK4=K
0149                90  CONTINUE
0150                91  CONTINUE
```

```
0151                    IF(TPLOT.EQ.0) GO TO 10
0152                    CALL PRTPIT(2,ARRAY,KK4,4,0,0,200,4)
                      C*******************
                      C   AVERAGE STRAIN CALCULATION
                      C
0153                    AN=0.
0154                    AVG1=0.
0155                    AVG2=0.
0156                    AVG3=0.
0157                    DO 92 J=10,40
0158                       AVG1=AVG1+E1(J)
0159                       AN=AN+1.
0160                 92 CONTINUE
0161                    AVG1=AVG1/AN
0162                    AN=0.
0163                    DO 94 J=55,85
0164                      AVG2=AVG2+E1(J)
0165                      AN=AN+1.
0166                 94 CONTINUE
0167                    AVG2=AVG2/AN
0168                    AN=0.
0169                    DO 96 J=5,20
0170                       AVG3=AVG3+E2(J)
0171                       AN=AN+1.
0172                 96 CONTINUE
0173                    AVG3=AVG3/AN
0174                    WRITE(6,1500) T,AVG1,AVG2,AVG3
0175               1500 FORMAT('1',//10X,'STRAIN AVERAGES AT TIME',E15.4,/15X,3E15.4)
                      C*******************
0176                    GO TO 10
                      C
                      C       PRINT FOR MAXIMUM STRAIN EXCEEDED
                      C
0177                  100 WRITE(6,1140) T
0178                    GO TO 91
                      C
0179                  110 STOP
                      C
                      C    FORMAT STATEMENTS
                      C
                      C       INPUT OF TITLE AND PROBLEM PARAMETERS
                      C
0180                 1000 FORMAT (20A4)
0181                 1010 FORMAT (6F10.2)
0182                 1020 FORMAT (4E10.2)
0183                 1030 FORMAT (3I10,2F10.2)
0184                 1035 FORMAT (4I10)
                      C
                      C       OUTPUT OF TITLE AND PROBLEM PARAMETERS
                      C
0185                 1040 FORMAT ('1',//10X,20A4//)
0186                 1050 FORMAT (15X,'PROJECTILE MASS =',F10.3,' GRAMS',/15X,
                         1    'PROJECTILE VELOCITY =',F6.1,' M/SEC',/15X,
```

```
                2    'HALF-LENGTH OF PRIMARY FIBER =',F6.2,' CM',/15X,
                3    'HALF-LENGTH OF SECONDARY FIBER =',F6.2,' CM',/15X,
                4    'CROSSOVER POINT =',F6.3,' (FRACTION OF PRIMARY)',/15X,
                5    'SLIDE FACTOR =',F6.3,//)
0187          1060  FORMAT (15X,'FIBER DENIER =',F8.1,/15X,
                1    'INSTANTANEOUS MODULUS =',F7.1,' GM/DEN',/15X,
                2    'RELAXATION TIME =',E10.3,' SEC',/15X,
                3    'VISCOUS FRACTION =',F6.3,//)
0188          1070  FORMAT (15X,'NUMBER LENGTH INCREMENTS =',I5,/15X,
                1    'PRINT SKIP FACTOR =',I3,/15X,
                2    'TIME SKIP FACTOR =',I3,/15X,
                3    'MAXIMUM TIME =',E10.3,' SEC',/15X,
                4    'MAXIMUM STRAIN =',F6.3,//)
0189          1080  FORMAT (15X,'LENGTH INCREMENT =',E10.3,' CM',/15X,
                1    'NUMBER NODES IN PRIMARY =',I4,/15X,
                2    'NUMBER NODES IN SECONDARY =',I4,/15X,
                3    'WAVESPEED =',F8.1,' M/SEC',/15X,
                4    'TIME INCREMENT =',E10.3,' SEC',/15X,
                5    'CROSSOVER NODE =',I4,/15X,
                6    'MAXIMUM NUMBER TIME INCREMENTS =',I6)
0190          1085  FORMAT (//15X,'PLOT OPTIONS =',8I5)
              C
              C       OUTPUT FOR EACH TIME INCREMENT
              C
0191          1090  FORMAT ('1',//10X,20A4,//10X,
                1    'OUTPUT FOR TIME =',E10.3,' SEC',/10X,
                2    'CURRENT PROJECTILE VELOCITY =',F6.1,' M/SEC')
0192          1100  FORMAT (//10X,'FIELD VARIABLES FOR PRIMARY FIBER',//9X,
                1    'J',8X,'X1(J)',5X,'Y1(J)',5X,'U1(J)',5X,'V1(J)',
                2    5X,'T1(J)',5X,'F1(J)',//)
0193          1110  FORMAT (7X,I3,6X,F7.3,3X,F7.3,3X,F7.1,3X,F7.1,5X,F5.2,5X,F7.5)
0194          1115  FORMAT (//15X,'CROSSOVER NODE =',I4)
0195          1120  FORMAT (//10X,'FIELD VARIABLES FOR SECONDARY FIBER',//9X,
                1    'J',8X,'X2(J)',5X,'Y2(J)',5X,'Z2(J)',5X,'U2(J)',5X,
                2    'V2(J)',5X,'W2(J)',5X,'T2(J)',5X,'E2(J)',//)
0196          1130  FORMAT (7X,I3,6X,F7.3,3X,F7.3,3X,F7.3,3X,F7.1,3X,F7.1,3X,F7.1,
                1    5X,F5.2,4X,F7.5)
              C
              C       MAX STRAIN MESSAGE
              C
0197          1140  FORMAT (//20X,'MAXIMUM STRAIN EXCEEDED AT ',E10.3,' SEC')
0198                END
```